UNIVERSIDADE FEDERAL DO CEARÁ

CENTRO DE TECNOLOGIA

DEPARTAMENTO DE ENGENHARIA ELÉTRICA

PROGRAMA DE PÓS-GRADUAÇÃO EM ENGENHARIA ELÉTRICA

DOUTORADO EM ENGENHARIA ELÉTRICA

THIAGO ALVES LIMA

CONTRIBUTIONS TO THE CONTROL OF INPUT-SATURATED SYSTEMS: TIME DELAY AND ALLOCATION FUNCTION CASES

FORTALEZA

2021

THIAGO ALVES LIMA

CONTRIBUTIONS TO THE CONTROL OF INPUT-SATURATED SYSTEMS: TIME DELAY AND ALLOCATION FUNCTION CASES

Tese apresentada ao Curso de Doutorado em Engenharia Elétrica do Programa de Pós-graduação em Engenharia Elétrica do Centro de Tecnologia da Universidade Federal do Ceará, como requisito parcial à obtenção do título de doutor em Engenharia Engenharia Elétrica. Área de Concentração: Controle e Automação.

Orientador: Prof. Dr. Fabrício G. Nogueira

Coorientador: Prof. Dr. Bismark C. Torrico

FORTALEZA

2021

Dados Internacionais de Catalogação na Publicação
Universidade Federal do Ceará
Biblioteca Universitária
Gerada automaticamente pelo módulo Catalog, mediante os dados fornecidos pelo(a) autor(a)

A482c Alves Lima, Thiago.
Contributions to the control of input-saturated systems: time delay and allocation function cases / Thiago Alves Lima. – 2021.
150 f. : il. color.

Tese (doutorado) – Universidade Federal do Ceará, Centro de Tecnologia, Programa de Pós-Graduação em Engenharia Elétrica, Fortaleza, 2021.
Orientação: Prof. Dr. Fabrício Gonzalez Nogueira.
Coorientação: Prof. Dr. Bismark Claure Torrico.

1. Actuator Saturation. 2. Dead-time Compensators. 3. Time-varying delays. 4. Allocation Functions. 5. Linear matrix inequalities (LMIs). I. Título.

CDD 621.3

THIAGO ALVES LIMA

CONTRIBUTIONS TO THE CONTROL OF INPUT-SATURATED SYSTEMS: TIME DELAY AND ALLOCATION FUNCTION CASES

Tese apresentada ao Curso de Doutorado em Engenharia Elétrica do Programa de Pós-graduação em Engenharia Elétrica do Centro de Tecnologia da Universidade Federal do Ceará, como requisito parcial à obtenção do título de doutor em Engenharia Engenharia Elétrica. Área de Concentração: Controle e Automação.

Aprovada em: 31 de Maio de 2021.

BANCA EXAMINADORA

Prof. Dr. Fabrício G. Nogueira (Orientador)
Universidade Federal do Ceará (UFC)

Prof. Dr. Bismark C. Torrico (Coorientador)
Universidade Federal do Ceará (UFC)

Prof. Dr. Valter Júnior de Souza Leite
Centro Federal de Educação Tecnológica (CEFET-MG)

Prof. Dr. Diego de Sousa Madeira
Universidade Federal do Ceará (UFC)

Prof. Dr. Guilherme de Alencar Barreto
Universidade Federal do Ceará (UFC)

À minha mãe, Antonia. Ao meu pai, Antonio, e às minhas irmãs, Glau e Carla. À minha avó, Maria.

ACKNOWLEDGEMENTS

Thanks to my advisors Dr. Fabrício Nogueira and Dr. Bismark Torrico, who introduced me to the fascinating field of control systems, and also were very supportive of my research and always made me feel free to investigate new subjects.

Je voudrais exprimée ma reconnaissance et gratitude à Sophie Tarbouriech, chargée de recherche au LAAS-CNRS, d'avoir accepté me recevoir pour mon mobilité doctorale à Toulouse. Je n'aurais pas pu faire cette thèse sans ses conseils, enseignements et encouragements. Je remercie aussi Frédéric Gouaisbaut, de m'avoir aidé à atteindre mes objectifs de recherche pendant ma période de mobilité.

Merci à toute l'equipe MAC du LAAS, qui m'a beaucoup appris sur les systèmes de contrôle (et le ping pong) et qui m'a inspiré par leur curiosité infinie. Vous m'avez vraiment fait sentir faire partie de ce groupe spectaculaire.

Merci à mes amis à Toulouse. Matteo, Vinícius, Larbi, Carla, Maria, Guilherme, Jordão et Cássio, vous avez rendu mes 15 mois en France encore plus fantastiques.

Thanks to my colleague and friend Magno, who greatly helped me in the development of this research. Also thanks to all my dear colleagues in my Brazilian lab GPAR-UFC.

Um agradecimento especial à minha mãe, Antonia, por seu amor e apoio sem fim. Obrigado ao meu pai, e às minhas irmãs Glau e Carla, por estarem sempre presentes. Obrigado à minha avó, Maria, grande matriarca da nossa família. Esse trabalho é dedicado a vocês.

I am grateful to Valessa, who helped me immensely through the moments of uncertainty and pressure of writing a doctoral thesis. Her love and friendship have been one of a kind.

Lastly, thanks to the Brazilian people and CAPES for providing me financial support during this journey, both in Brazil and during my research stay in France.

“An old friend once told me something that gave me great comfort. Something he read. He said Mozart, Beethoven and Chopin never died. They simply became music.”

(Dr. Robert Ford, in *Westworld*)

RESUMO

Atuadores saturantes estão presentes em todos os processos do mundo real. As correntes e tensões em circuitos elétricos, a velocidade dos motores em sistemas robóticos, a concentração de agentes em reações químicas, e assim por diante, são todas variáveis limitadas em amplitude. A consideração dessas limitações em sistemas representados por modelos lineares em malha aberta introduz alguns desafios para os engenheiros e matemáticos da área de controle. Desde a década de 80 até os dias atuais, pesquisadores de controle vêm desenvolvendo estratégias matemáticas baseadas na teoria de Lyapunov para a análise e síntese de controles estabilizantes desses sistemas. Embora seja possível afirmar que esse seja um assunto já maduro na literatura, ainda existem alguns problemas interessantes relacionados ao controle de sistemas com saturação na entrada, principalmente quando considerado juntamente a outras questões desafiadoras.

A consideração dos atrasos de transporte é outro assunto interessante em sistemas de controle. Nesta tese, trata-se principalmente do controle preditivo desses sistemas. Para esse fim, utilizam-se os chamados compensadores de tempo morto, que são uma classe de controladores derivados do preditor de Smith, desenvolvido na década de 50. As contribuições desta parte estão divididas em dois capítulos: ii) Primeiramente, é desenvolvida uma proposta de estrutura compensadora de tempo morto para sistemas com saturação na entrada através da adição de uma estratégia *anti-windup*. Os fatos interessante sobre a estratégia consistem na demonstração que devido à compensação do atraso no caso nominal, a estratégia pode ser aplicada de uma maneira simples (com regras de ajustes fáceis a se seguir) e também pode ser aplicada em sistemas sem atraso de maneira unificada. ii) Além disso, no caso de atrasos variantes no tempo, é apresentada uma nova estratégia para a caracterização e análise da região de atração do sistema na presença de saturação na entrada. Por meio de problemas de otimização convexa, são estabelecidas relações entre as variáveis de ajuste do controlador, os limites do atraso variante no tempo e o tamanho da região de atração estimada. Ambos os capítulos desta parte foram desenvolvidos no domínio do tempo discreto.

O problema dos sistemas sobre-atuados/ com entradas redundantes também é abordado na parte final desta tese. Esse assunto está intimamente relacionado a aplicações aeroespaciais e robóticas, onde a redundância dos atuadores é frequentemente necessária. Além das estruturas do controlador e do *anti-windup*, um terceiro subsistema, denominado 'função de alocação', necessita ser projetado com o objetivo de distribuir o esforço de controle desejado entre os múltiplos atuadores. A contribuição nesta parte está relacionada ao desenvolvimento

de condições convexas para o projeto simultâneo de um alocador dinâmico e um *anti-windup* estático. Além disso, é mostrado que as condições desenvolvidas são sempre factíveis sob certas premissas. O desenvolvimento desta parte é feito no domínio do tempo contínuo.

As contribuições nesta tese são, portanto, relacionadas à análise, controle e estratégias *anti-windup* para sistemas com saturação na entrada em conjunto com atrasos de transporte ou funções de alocação. Deste modo, não pretende-se de alguma forma argumentar que foram desenvolvidas novas metodologias gerais para o estudo do maduro campo da não-linearidade de saturação. No entanto, as contribuições reportadas são importantes para os casos especiais considerados.

Palavras-chave: Saturação do atuador. Compensadores de tempo morto. Atraso variante no tempo. Funções de alocação. Desigualdades matriciais lineares.

ABSTRACT

Saturating actuators are ubiquitous to real-world processes. Currents and voltages in circuits, motors speed in robotics systems, the concentration of agents in chemical reactions, and so on, are all variables limited in amplitude. The consideration of such limitations in otherwise open-loop linear systems introduces some special challenges to the control engineer/ mathematician. From the ’80s to the early years of the new millennium, control researchers have spent efforts in developing mathematical tools based on the Lyapunov theory for the stability analysis and stabilization of such systems. Although one could say that a mature stage of the subject has been achieved, some interesting problems still arise for the control of input saturated systems, especially when considered in conjunction with other challenging issues.

Time delays are another subject of main interest in control systems. In this thesis, we are mainly interested in the predictor/ model-based control of such systems. Specially, we address dead-time compensators (DTCs), which are a class of controllers derived from Smith’s idea developed in the ’50s. The contributions in this part are split throughout two chapters: i) First, we develop a DTC structure for systems with saturating inputs through the addition of an anti-windup strategy. The interesting facts about the proposed strategy are that we show that due to the *compensation* of the delay in the nominal case, the strategy can be used in a very practical manner (with easy to follow tuning rules) and can also be applied in a unified way to delay-free systems. ii) Secondly, in the case of time-varying delays, a new strategy for the characterization and analysis of the system region of attraction in the presence of saturating inputs is presented. By means of convex optimization problems, we establish relations between the controller tuning variables, bounds on the time-varying delay and sizes of the estimated region of attraction. Both chapters in this part are developed in the discrete-time domain.

The problem of over-actuated/ input-redundant systems is also approached in the final part of the thesis. This subject is closely related to aerospace and robotics applications, where redundancy of actuators is often necessary. Besides the controller and anti-windup subsystems, a third subsystem, designated “allocation function", needs to be designed in order to distribute the desired control effort among the multiple actuators. The contribution in this part is related to the development of convex conditions for the co-design of a dynamic allocator subsystem along with static anti-windup. Furthermore, we show that the developed conditions are always feasible under certain assumptions. The development in this part is made in the continuous-time domain.

The contributions in this thesis are, therefore, related to the analysis, control and

anti-windup strategies for input saturated systems in conjunction with either time delays or allocation functions. Thus, we intend by no means to argue that we have developed novel general methodologies to the study of the mature field of the saturation nonlinearity. However, the contributions reported here are of importance for the special covered cases.

Keywords: Actuator Saturation. Dead-time Compensators. Time-varying delays. Allocation Functions. Linear matrix inequalities (LMIs).

LIST OF FIGURES

LIST OF TABLES

LIST OF ABBREVIATIONS AND ACRONYMS

FIR	Finite Impulse Response
FSP	Filtered Smith Predictor
ISE	Integral Square Error
LMI	Linear Matrix Inequality
MIMO	Multiple-Input Multiple-Output
NCSs	Networked Control Systems
PI	Proportional Integral
PID	Proportional Integral Derivative
SISO	Single-Input Single-Output
SP	Smith Predictor
TCP	Transmission Control Protocol

NOTATION

$\star$	Denotes symmetric blocks in the expression of a matrix.
$\mathbb{Z}$	Stands for the set of integer numbers.
$\mathbb{Z}^+$	Stands for the set of nonnegative integer numbers.
$\mathbb{N}$	Stands for the set of natural numbers.
$\mathbb{R}$	Stands for the set of real numbers.
$\mathbb{R}^+$	Stands for the set of nonnegative real numbers.
$\mathbb{S}_n^+$	Stands for the set of $n \times n$ positive definite matrices.
t	Stands for continuous time.
k	Stands for discrete-time sample.
I	Denotes the identity matrix of appropriate dimensions. I_n is used if we want explicitly present its dimension.
0	Denotes the null matrix of appropriate dimensions. $0_{n\times m}$ represents the $n \times m$ null matrix.
$\mathrm{Y}_{(i)}$	Denotes the ith row of a matrix $\mathrm{Y} \in \mathbb{R}^{n\times m}$.
$v_{(i)}$	Denotes the ith component of a vector $v \in \mathbb{R}^m$.
$\mathrm{A}^\top$	Means the transpose of matrix A.
$\mathrm{He}\{\mathrm{A}\}$	Denotes the operator $\mathrm{He}\{\mathrm{A}\} = \mathrm{A} + \mathrm{A}^\top$.
A^{-1}	Denotes the inverse of matrix A.
$\mathrm{A} \succ 0$	Means that matrix A is positive definite.
$\mathrm{A} \succeq 0$	Means that matrix A is positive semidefinite.
$\mathrm{A} \prec 0$	Means that matrix A is negative definite.
$\mathrm{A} \preceq 0$	Means that matrix A is negative semidefinite.
$diag(\mathrm{A}_1, \mathrm{A}_2, ..., \mathrm{A}_m)$	Denotes the block-diagonal matrix formed with matrices $\mathrm{A}_i, i = 1, ..., m$.

CONTENTS

Part I

General Introduction

1 INTRODUCTION

Actuator saturation is a major topic of research in control systems. Although most control systems projects do not consider boundaries in the amplitude or rate of the process control input, all real actuators present such limitations. For instance, electrical actuators have voltage and current limits, whereas there exist bounds on both volume and rate of flow in hydraulic actuators. This can be a cause of instability in the closed-loop system, due to a phenomenon popularly known as windup. Instability is, however, only one of the possible outcomes due to this condition, which might include the occurrence of limit cycles, multiple equilibria and performance degradation (TARBOURIECH *et al.*, 2011; ZACCARIAN; TEEL, 2011). Therefore, it is necessary to consider strategies which avoid windup and its undesirable effects in the control loop. Moreover, in the historical perspective, saturated actuators have had implications in many tragedies such as aircraft crashes and the Chernobyl nuclear power station disaster (TARBOURIECH; TURNER, 2009). Thus, it is mandatory to guarantee stability of control structures operating at such conditions. However, this is not an easy task and the necessary mathematical rigor to make such guarantees was mainly developed in the 1990s along with the spread of the Linear Matrix Inequality (LMI) theory.

Windup occurs when the model of the saturation to the plant input is unknown, thus leading the states of the controller to be wrongly updated (KOTHARE *et al.*, 1994). Especially, this can make the output of the plant oscillatory or unstable. In other cases, the set-point tracking response can become painfully slow. The origin of the term windup comes from the cases of Proportional Integral (PI) and Proportional Integral Derivative (PID) controllers, in which the integral state "winds up" to large values during saturation events; the associated energy is later dissipated, causing the problems described above. It is import to note that although early practice control engineers associated this phenomenon to integral action, the view of this problem has evolved and windup in the sense of modern multivariable control theory is more linked to the instability problems caused by the reduction on the closed-loop region of attraction, what is not necessarily linked with the presence of integral action. To put it into words, the region of attraction of a system is defined as the region of the state space for which given any initial conditions within this region, the evolution of the system states over time will remain inside this region and will converge asymptotically to the origin. In the presence of saturating inputs, the open-loop linear system becomes nonlinear in closed loop, and global stability can only be achieved under some strict conditions (SONTAG, 1984; LASSERRE, 1993). Therefore, the

anti-windup problem becomes that of enlarging the estimation on regions of safe operation, that is, regions in the state space for which the initial conditions are guaranteed to be contained within the region of attraction.

Regarding systems with time delays, the definition of a set of initial conditions for which stability is guaranteed in the presence of the saturation nonlinearity is non-trivial. In the continuous-time case, time-delay systems fall within the larger class of infinite-dimensional systems, which are not easily handled (KRSTIC, 2009; FRIDMAN, 2014). The stability of time-delay systems is studied through augmented functionals which take into account not only the current state but also a function describing the evolution of the states in the previous interval, i.e. an interval ranging from $(t_0 - d)$ to t_0, where d is the delay and t_0 the current time. In case saturation is present, it is often necessary to characterize a set of such functions for which asymptotic stability still holds. In this work, we deal with time-delay systems in the discrete-time domain, which benefits of being finite-dimensional as opposed to its continuous-time counterpart. However, discrete-time delay systems contain their own challenging issues. We will go through details about the available strategies in the literature and the proposed ones in the later specific chapters dealing with time delays.

In addition to avoiding windup consequences, research effort on saturated systems is of interest because considering limitations on the control signal can lead to the synthesis of more economic control laws. Consider the case of overactuation, which is a situation present in many systems. For example, satellites possess redundant actuators which are combined to generate the forces that drive them to the desired position and orientation. To a given desired set of forces, there might exist infinitely many combinations of the multiple actuators that generate the aimed control effort. Some law must then be implemented to distribute effort among actuators in an optimized manner. This is realized by another subsystem besides the controller and the anti-windup, which is commonly called an allocation function or control allocator (DURHAM *et al.*, 2016; DUCARD, 2009). In the case that the multiple actuators are individually saturated, the problem becomes even more evolved as not all virtual control inputs (as the forces acting in the satellites) are achievable by the set of available actuators. Then, the study of allocation functions along with anti-windup strategies is necessary to properly take the saturation condition into account, which could degrade overall system performance and stability properties.

The objective of this introduction is not to provide a fully detailed review of the area of control saturation, which can be found in the survey works of the area (GALEANI *et*

al., 2009; TARBOURIECH; TURNER, 2009), but rather to give a flat overview of traditional and modern aspects of saturation and also to connect the subject to the problems of time delays and allocation functions. For more specific reviews on the literature of time delays, allocation functions, and their joint problem with saturation, the reader is referred to the later chapters of this text, as detailed in the thesis outline (Section 1.1).

The classes of systems considered throughout the thesis are mathematically specified within each chapter. For the sake of simplicity of notation, repeated symbols in different chapters do not represent the same variable, unless explicitly said so.

1.1 Thesis outline

This thesis is divided into three parts, as detailed below:

- Part I is composed of the first two chapters and is dedicated to presenting the general introduction and organization of this thesis. Besides that, the main theoretical preliminaries necessary to establish stability of input-saturated systems are reviewed in Chapter 2.
- Part II is composed of chapters 3-6 and is dedicated to time-delay systems. Chapter 3 serves as the introductory chapter to time-delay systems and also reviews some preliminaries on their stability concepts. Chapter 4 aims at discussing some of the classical strategies for the control of linear input-delayed systems. Some parts of the chapter are loosely based on the following articles:
  - TORRICO, B. C.; FILHO, M. P. de A.; **ALVES LIMA, T.**; SANTOS, T. L.; NOGUEIRA, F. G. *New simple approach for enhanced rejection of unknown disturbances in LTI systems with input delay*. ISA Transactions, 2019.
  - TORRICO, B. C.; FILHO, M. P. de A.; **ALVES LIMA, T.**; FORTE, M. D. do N.; Sá, R. C.; NOGUEIRA, F. G. *Tuning of a dead-time compensator focusing on industrial processes*. ISA Transactions, v. 83, p. 189 – 198, 2018.
  - **ALVES LIMA, T.**; FILHO, M. P. de A.; TORRICO, B. C.; FORTE, M. D. do N.; PEREIRA, R. D. O.; NOGUEIRA, F. G. *First-order Dead-time Compensation with Feedforward Action*. European Control Conference, 2019.

  Chapters 5 and 6 then present the main contributions of Part II, where some problems related to input saturation in time-delay systems are investigated and are based, respectively, on the following articles:
  - **ALVES LIMA, T.**; FILHO, M. P. de A.; TORRICO, B. C.; NOGUEIRA, F. G.;

CORREIA, W. B. *A practical solution for the control of time-delayed and delay-free systems with saturating actuators*. European Journal of Control, v. 51, p. 53 – 64, 2020.

  - **ALVES LIMA, T.**; TARBOURIECH, S.; GOUAISBAUT, F.; F.; FILHO, M. P. de A.; GARCÍA, P; TORRICO, B. C. NOGUEIRA, F. G. *Analysis and experimental application of a dead-time compensator for input saturated processes with output time-varying delays*. IET Control Theory Appl. 2021; 1–14.

- Part III is composed of the last chapter of this thesis and is dedicated to the subject of control allocation. To ease the comprehension of the contributions in this part, some introductory aspects about allocation functions are initially given in Chapter 7. Then, the rest of the chapter presents a new strategy for the design of allocation functions in the presence of saturating actuators, which is based on the following article:
  - **ALVES LIMA, T.**; TARBOURIECH, S.; NOGUEIRA, F. G.; TORRICO, B. C. *Co-design of dynamic allocation functions and anti-windup*, IEEE Control Systems Letters, 2021.

The thesis then ends with general conclusions, whilst possible future works are enlisted. Whenever relevant, detailed discussion about the main contributions is drawn by the end of each chapter.

2 THEORETICAL PRELIMINARIES

In this chapter, preliminary contents regarding stability are presented. Initially, the concept of LMIs, which is a powerful tool for synthesis and analysis of robust control laws is presented in Section 2.1. The main notions regarding Lyapunov theory and stability of systems with saturating actuators are latter presented.

2.1 Linear Matrix Inequalities

A wide variety of control problems can be described in the format of LMIs. These are matrix inequalities which have an affine relationship with a set of matrix variables. While most of the earlier works on Lyapunov stability were formulated using algebraic Riccati equations, the use of LMIs became popular in the 1990s due to the development of efficient interior-point method algorithms (BOYD *et al.*, 1994). LMIs soon became a powerful tool in robust control synthesis in the presence of structured uncertainties (CHILALI; GAHINET, 1996), and later in the presence of actuator saturation (WESTON; POSTLETHWAITE, 2000). There exist many software packages which provide implementation and solution to LMIs by using convex optimization, such as the Yalmip toolbox (LÖFBERG, 2004).

The main attractions for the use of LMIs are listed as (SKOGESTAD; POSTLETHWAITE, 2005)

- LMIs can be used to solve problems which involve several matrix variables.
- Their manipulation is flexible, thus a wide variety of problems can be posed as LMIs in a very straightforward manner.
- Restrictions that cause traditional formulations to either fail or struggle to find a solution can often be removed by using LMIs. Furthermore, LMIs can aid their extension to more general scenarios.
- Multiple control objectives can be gathered into a single LMI.

Consider the following definition borrowed from Boyd *et al.* (1994).

Definition 2.1

A linear matrix inequality (LMI) is described by the following expression

$$\mathrm{F}(x) \triangleq \mathrm{F}_0 + \sum_{i=1}^{m} x_i \mathrm{F}_i \succ 0. \tag{2.1}$$

Where

- $\mathrm{F}_i = \mathrm{F}_i^\top \in \mathbb{R}^{nxn}$ are real given symmetric matrices.
- $x = [x_1, ..., x_m] \in \mathbb{R}^m$ is the decision vector.
- The inequality $\succ 0$ denotes that $\mathrm{F}(x)$ is positive definite, i.e. all eigenvalues are positive. Thus, $u^\top \mathrm{F}(x)u > 0$ for all $u \in \mathbb{R}^n, u \neq 0$. Non-strict LMIs are defined by using the symbol $\succeq$.

The LMI problem in Equation (2.1) is to find x such that $\mathrm{F}(x)$ holds. This is a convex constraint on x, i.e., the set $\{x|\mathrm{F}(x) \succ 0\}$ is convex. Multiple LMIs $\mathrm{F}_1(x) \succ 0, \mathrm{F}_2(x) \succ 0, ..., \mathrm{F}_m(x) \succ 0$, can be expressed as a single LMI of the form:

$$\mathrm{F}(x) = \begin{bmatrix} \mathrm{F}_1(x) & \cdots & 0 \\ \vdots & \ddots & \vdots \\ 0 & \cdots & \mathrm{F}_m(x) \end{bmatrix} \succ 0, \tag{2.2}$$

which is also a convex set. Convex optimization may be arranged into two main problems to be solved under the LMI framework. The first one is called a feasibility problem and consists of either finding any x such that $\mathrm{F}(x) \succ 0$ holds or determining that the problem is infeasible. The second is called an optimization problem (also called eigenvalue problem) and consists of minimizing (or maximizing) some convex cost function of the unknown variable x subject to LMI constraints as

$$\min \mathit{criterion}(x) \text{ such that } \mathrm{F}(x) \succ 0. \tag{2.3}$$

Standard tricks used in the manipulation of LMIs such as the Schur complement and the S-procedure can be found in Boyd *et al.* (1994), Duan and Yu (2013).

2.2 Lyapunov Stability

This subsection aims at reviewing some fundamental concepts regarding stability. There are different forms of stability, being input-output stability and stability of equilibrium points the most used. The latter, which heavily is employed in this work, is characterized in the sense of Lyapunov functionals. Consider the following autonomous dynamical system

$$\dot{x} = f(x), \tag{2.4}$$

where $x(t)$ is called the state variable and $f(x)$ is a Lipschitz continuous map, which guarantees existence and uniqueness of the solutions of (2.4). The equilibrium points x^* of (2.4) are the

solutions to $f(x^*) = 0$. For convenience, let us consider $x^* = 0$. There is no loss of generality in doing so because any equilibrium point of the autonomous system (2.4) can be shifted to the origin via a change of variables. Now consider the following definition (KHALIL, 2002).

Definition 2.2

The equilibrium point $x^* = 0$ of system (2.4) is

(i) Stable if, for each $\varepsilon > 0$, there exists $\delta(\varepsilon) > 0$ such that

$$\|x(t_0)\| < \delta(\varepsilon) \implies \|x(t)\| < \varepsilon, \forall t \geq t_0.$$

(ii) Asymptotically stable if it is stable and $\delta(\varepsilon)$ can be chosen such that

$$\|x(t_0)\| < \delta(\varepsilon) \implies \lim_{t\to\infty} x(t) = 0.$$

(iii) Unstable if it is not stable.

Technically, from Definition 2.2, we can conclude that if all states starting in a neighborhood nearby an equilibrium point remain nearby, then this equilibrium point is stable. An asymptotically stable equilibrium point is a point for which the trajectories of states with different initial conditions converge to the origin as time approaches infinity. The region of attraction of an equilibrium point x^* is the set of all initial conditions x_0 for which $x(x_0,t) \to x^*$ as t goes to infinity. Furthermore, an equilibrium point is said to be globally stable if its region of attraction is the whole space, e.g. $\mathbb{R}^n$ (KHALIL, 2002).

Once we establish the notions of stability, it is necessary to find ways to determine the stability of equilibrium points. In this sense, it is well known that such a task might be very difficult (or even impossible) to realize in analytically manner. The celebrated Lyapunov theorem is thus stated as follows (KHALIL, 2002).

Theorem 2.1

Let $x^* = 0$ be an equilibrium point of (2.4) in a domain $\mathcal{D} \subset \mathbb{R}^n$ around $x^* = 0$. Let $\mathrm{V} : \mathcal{D} \mapsto \mathbb{R}$ be a continuously differentiable function such that

$$\mathrm{V}(0) = 0 \text{ and } \mathrm{V}(x) > 0, \forall x \in \mathcal{D} - \{0\},$$

and

$$\dot{\mathrm{V}}(x) \leq 0, \forall x \in \mathcal{D},$$

then $x^* = 0$ is stable. Moreover, if

$$\dot{\mathrm{V}}(x) < 0, \forall x \in \mathcal{D} - \{0\},$$

then $x^* = 0$ is asymptotically stable.

Slightly modified conditions are used to establish global stability and are given in the following theorem (KHALIL, 2002).

Theorem 2.2

Let $x^* = 0$ be an equilibrium point of (2.4) and let $\mathrm{V} : \mathbb{R}^n \mapsto \mathbb{R}$ be a continuously differentiable function such that

$$\mathrm{V}(0) = 0 \text{ and } \mathrm{V}(x) > 0, \forall x \neq 0,$$

$$\|x\| \to \infty \implies \mathrm{V}(x) \to \infty,$$

$$\dot{\mathrm{V}}(x) < 0, \forall x \neq 0,$$

then $x^* = 0$ is said to be globally asymptotically stable.

In the global case, the extra necessary condition $\|x\| \to \infty \implies \mathrm{V}(x) \to \infty$ means that $\mathrm{V}(x)$ is *radially unbounded*. One can look at Khalil (2002) for the proofs of Theorems 2.1 and 2.2 to see that these conditions are sufficient to establish stability since $f(x)$ in (2.4) is, by definition, a Lipschitz continuous map.

In the discrete-time domain, the time t dependence is usually replaced by the sample k. Consider the discrete-time dynamical system

$$x(k+1) = f(x(k)).$$

Similarly to the continuous-time case, the origin of the above system is locally asymptotically stable if there exists a positive definite function $\mathrm{V}(x(k))$ such that

$$\Delta\mathrm{V}(x(k)) := \mathrm{V}(x(k+1)) - \mathrm{V}(x(k)) < 0, \forall x(k) \in \mathcal{D} - \{0\},$$

where $\mathcal{D}$ is a region of the state-space. Furthermore, if $\mathcal{D}$ is the whole state-space and $\mathrm{V}(x(k))$ is radially unbounded, the system is globally asymptotically stable.

2.3 Absolute Stability of Lure Systems

Many practical systems can be represented by the interconnection between a linear system and a memoryless nonlinearity. Consider the unforced system given by

$$\begin{cases} \dot{x}(t) = \mathrm{A}x(t) + \mathrm{B}u(t) \\ y(t) = \mathrm{C}x(t) + \mathrm{D}u(t) \\ u(t) = \psi(t,y) \end{cases} \tag{2.5}$$

where $x \in \mathbb{R}^n$, u and $y \in \mathbb{R}^m$, the pairs (A,B) and (A,C) are controllable and observable, respectively, and $\psi(\cdot)$ is a memoryless, possibly time-varying, nonlinearity. System (2.5) is represented in Figure 1, where the transfer function $G(s) = \mathrm{C}(s\mathrm{I} - \mathrm{A})^{-1}\mathrm{B} + \mathrm{D}$ is square and proper.

Figure 1 – Feedback interconnection between linear system and memoryless nonlinearity.

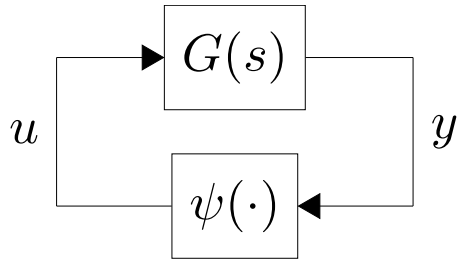

Source: The author.

The nonlinearity $\psi(\cdot)$ is assumed to be piecewise continuos in t, locally Lipschitz in y, and is required to satisfy a sector condition as follows (TARBOURIECH *et al.*, 2011).

Definition 2.3

A memoryless nonlinearity $\psi(t,y)$ is said to satisfy a sector condition if

$$[\psi(t,y) - \Omega_{min}y]^\top [\psi(t,y) - \Omega_{max}y] \leq 0, \quad \forall t \geq 0, \quad \forall y \in \mathcal{D} \subseteq \mathbb{R}^m \tag{2.6}$$

for real matrices Ω_{min} and Ω_{max} where $\Omega = \Omega_{max} - \Omega_{min}$ is symmetric positive definite and the origin is contained in the subset $\mathcal{D}$. Furthermore, if $\mathcal{D} = \mathbb{R}^m$, then the nonlinearity $\psi(t,y)$ globally satisties the sector condition.

When $\psi(t,y)$ satisfies (2.6) for $\mathcal{D} \subseteq \mathbb{R}^m$, the nonlinearity $\psi(t,y)$ is said to belong locally to sector (Ω_{min},Ω_{max}). If $\mathcal{D} = \mathbb{R}^m$, the nonlinearity $\psi(t,y)$ is said to belong globally to sector (Ω_{min},Ω_{max}). Figure 2 illustrates these two cases.

Figure 2 – Sector conditions.

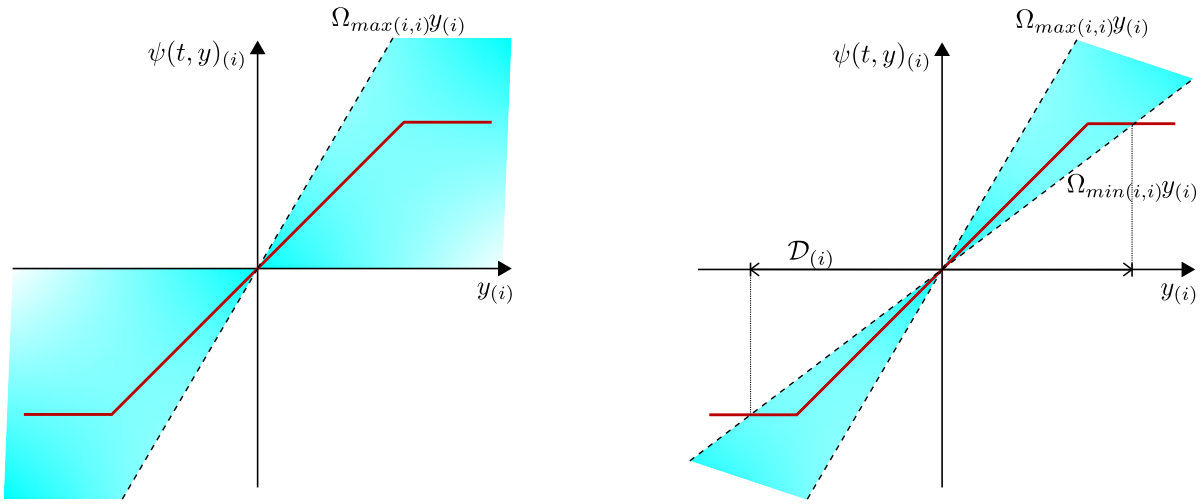

(a) Global case (with $\Omega_{min(i,i)} = 0$).

(b) Local case.

Source: The author.

The problem of stability of system (2.5) is often called the Lure problem in literature. From definition 2.3 the absolute stability of system (2.5) can be defined (KHALIL, 2002).

Definition 2.4

Consider system (2.5), where the nonlinearity $\psi(\cdot)$ satisfies a sector condition as presented in Definition 2.3. Then, (2.5) is absolutely stable if the origin is globally uniformly asymptotically stable for any nonlinearity in the given sector. It is absolutely stable with a finite domain if the origin is uniformly asymptotically stable.

2.4 Sector Nonlinearity Models

Systems with saturating actuators are on the boundary between linearity and nonlinearity. Even if an open-loop process is linear, the saturation of the actuator will turn the closed loop into a nonlinear system. The presence of the saturation nonlinearity can induce some unexpected behaviour to closed-loop systems. Thus, it is important to find a model for the saturation in order to propose strategies to avoid its undesirable effects, or at least analyze the stability of the closed-loop system under its presence. There are different ways to model the saturation nonlinearity. In this work, we follow the sector nonlinearity model approach, which allows solving the stability analysis problem of a system with saturating actuators by fitting it into the general framework of stability of lure systems, i.e. a linear system interconnected with a decentralized memoryless nonlinearity. To ease comprehension, the modelling, as well as

the sector conditions, are presented for the special case of Single-Input Single-Output (SISO) systems, which is the case approached in Part II and represents the biggest part of this thesis. Extensions for the Multiple-Input Multiple-Output (MIMO) case are only needed for the last chapter when dealing with the allocation problem and therefore will be presented therein.

Consider τ_{sat} as the following linear system subject to input saturation

$$\tau_{sat} \triangleq \begin{cases} \dot{x}(t) = \mathrm{A}x(t) + \mathrm{B}u(t) & (2.7) \\ u(t) = sat(v(t)) & (2.8) \\ v(t) = \mathrm{K}x(t) & (2.9) \end{cases}$$

where $x(t) \in \mathbb{R}^n$ is the state vector, $v(t),\ u(t) \in \mathbb{R}$ are the computed control effort and the system saturating input, respectively. Matrices A, B, and K are of appropriate dimensions. Let us formally define the saturation nonlinearity for SISO systems as

$$sat(v) = \begin{cases} u_{max} & \text{if } v > u_{max} \\ v & \text{if } u_{min} \leq v \leq u_{max} \\ -u_{min} & \text{if } v < -u_{min} \end{cases} \tag{2.10}$$

where u_{min} and u_{max} define lower and upper bounds on the control signal, respectively. Such function is graphically illustrated in Figure 3a.

Figure 3 – Nonlinearities.

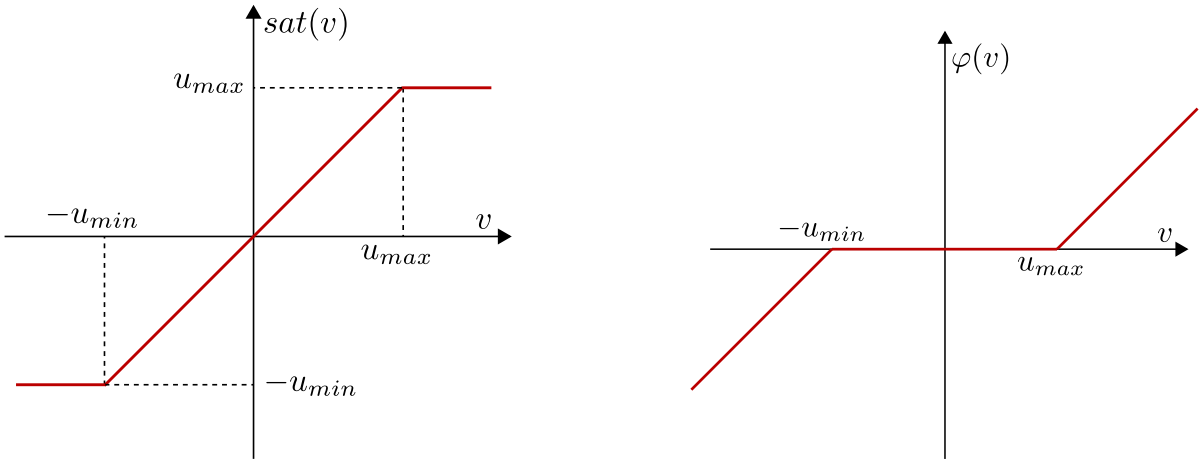

(a) The saturation function.

(b) The deadzone function.

Source: The author.

Note that τ_{sat} clearly presents a connection between a linear system and the $sat(\cdot)$ nonlinearity. However, such representation might not be interesting since the linear system (2.7)

may be unstable (due to system matrix A). In order to overcome this problem, the following deadzone nonlinearity is defined

$$\varphi(v(t)) = v(t) - sat(v(t)), \tag{2.11}$$

which is graphically shown in Figure 3b. System τ_{sat} can then be equivalently rewritten as

$$\tau_{\varphi} \triangleq \begin{cases} \dot{x}(t) = (\mathrm{A}+\mathrm{BK})x(t) - \mathrm{B}\varphi(v(k)), & (2.12) \\ v(t) = \mathrm{K}x(t). & (2.13) \end{cases}$$

Note that τ_{φ} also clearly presents a connection between a linear system and the memoryless nonlinearity $\varphi(\cdot)$. However, in this case, the linear system (2.12) is stable if $(\mathrm{A}+\mathrm{BK})$ is Hurwitz, that is, if $v(t) = \mathrm{K}x(t)$ is a stabilizing control law. Thus, stability can be conveniently analyzed under Lure's framework. The following two sector conditions are employed throughout this work.

2.4.1 Classical sector condition

Consider the following set

$$\mathscr{L}(v,\bar{u}_{min},\bar{u}_{max}) = \{v \in \mathbb{R}; -\bar{u}_{min} \leq v \leq \bar{u}_{max}\}, \tag{2.14}$$

where $\bar{u}_{min} = \dfrac{u_{min}}{1-\Lambda}$ and $\bar{u}_{max} = \dfrac{u_{max}}{1-\Lambda}$, $0 \leq \Lambda < 1 \ \in \mathbb{R}$. We state the following lemma (TARBOURIECH *et al.*, 2011; TURNER; POSTLETHWAITE, 2007).

Lemma 2.1

If v belongs to set $\mathscr{L}(v,\bar{u}_{min},\bar{u}_{max})$, then the deadzone nonlinearity $\varphi(v)$ satisfies the following inequality, which is true for any positive definite (one-by-one) matrix $\mathrm{W} \in \mathbb{R}$

$$\varphi^{\top}(v)\mathrm{W}[\varphi(v) - \Lambda v] \leq 0. \tag{2.15}$$

Proof. The following holds for $0 \leq \Lambda < 1$.

$$0 \leq v \leq \bar{u}_{max} \implies \varphi(v) \geq 0 \text{ and } \varphi(v) \leq \Lambda v$$

$$-\bar{u}_{min} \leq v \leq 0 \implies \varphi(v) \leq 0 \text{ and } \varphi(v) \geq \Lambda v$$

Thus, $\varphi^{\top}(v)\mathrm{W}[\varphi(v) - \Lambda v] \leq 0$ provided that $\mathrm{W} > 0$. In this case, $\mathscr{L}(v,\bar{u}_{min},\bar{u}_{max}) \subset \mathbb{R}$ and $\varphi(v)$ is said to belong locally to the sector $(0,\Lambda)$. □

For the global case, the following lemma can be stated (TARBOURIECH *et al.*, 2011; TURNER; POSTLETHWAITE, 2007).

Lemma 2.2

For all $v \in \mathbb{R}$, the deadzone nonlinearity $\varphi(v)$ satisfies the following inequality, which is true for any positive definite (one-by-one) matrix $\mathrm{W} \in \mathbb{R}$

$$\varphi^{\top}(v)\mathrm{W}[\varphi(v) - v] \leq 0. \tag{2.16}$$

Proof. Following statements hold.

$$v \geq 0 \implies \varphi(v) \geq 0 \text{ and } \varphi(v) \leq v$$
$$v \leq 0 \implies \varphi(v) \leq 0 \text{ and } \varphi(v) \geq v$$

Thus, $\varphi^{\top}(v)\mathrm{W}[\varphi(v) - v] \leq 0$ provided that $\mathrm{W} > 0$. In this case, $\varphi(v)$ is said to belong globally to the sector $(0, 1)$. □

Figure 4 illustrates the $\varphi(v)$ nonlinearity in the global and local cases. Note that when $\Lambda = 0, \bar{u}_{min} = u_{min}, \bar{u}_{max} = u_{max}$ and $\mathscr{L}(v, \bar{u}_{min}, \bar{u}_{max})$ corresponds to the region of linearity of the system, that is the region for which $\varphi(v) = v$. As Λ increases, the set $\mathscr{L}(v, \bar{u}_{min}, \bar{u}_{max})$ increases, and when $\Lambda \to 1$, $\mathscr{L}(v, \bar{u}_{min}, \bar{u}_{max})$ tends to cover the whole space.

Figure 4 – Deadzone nonlinearity in sectors.

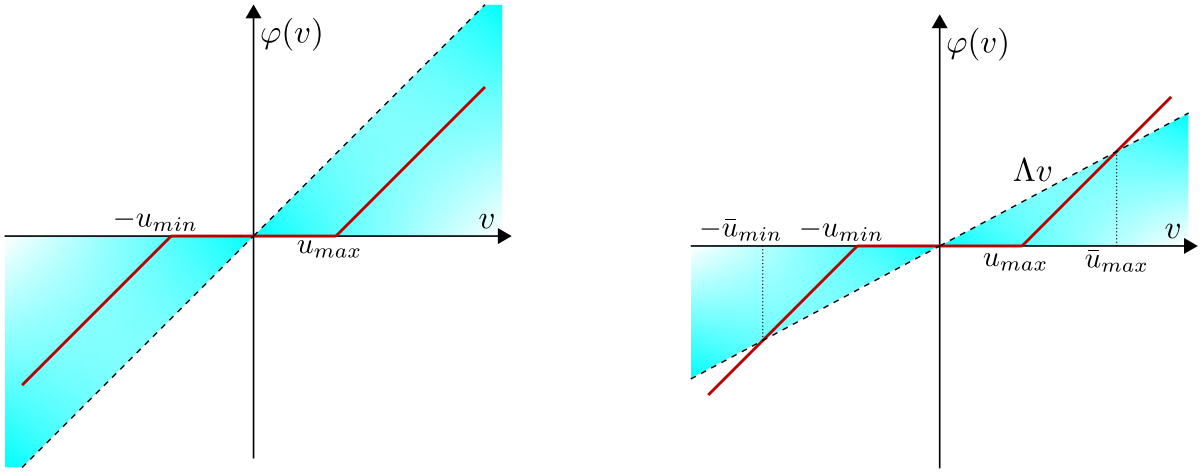

(a) Global sector.

(b) Local sector ($0 \leq \Lambda < 1$).

Source: The author.

2.4.2 Generalized sector condition

The classical sector condition presented in subsection 2.4.1 not only applies to the deadzone nonlinearity, but also for a wider family of nonlinearities. This is a hint that it may

yield conservative results. In order to solve this problem, the generalized sector condition, which applies specifically for deadzone nonlinearities (as highlight in the last paragraph of page 42 in Tarbouriech *et al.* (2011)), was introduced in Gomes da Silva Jr. and Tarbouriech (2005). Therefore, conditions derived with this sector condition tend to be less conservative and are useful in order to enlarge estimations[1] on the region of attraction of closed-loop saturated systems. Consider the following set (GOMES DA SILVA JR.; TARBOURIECH, 2005; TARBOURIECH *et al.*, 2011)

$$\mathscr{L}(v-\theta,u_{min},u_{max})=\{v\in\mathbb{R};\theta\in\mathbb{R};-u_{min}\leq v-\theta\leq u_{max}\}. \tag{2.17}$$

We then state the following result (GOMES DA SILVA JR.; TARBOURIECH, 2005; TARBOURIECH *et al.*, 2011).

Lemma 2.3

If v and θ belong to set $\mathscr{L}(v-\theta,u_{min},u_{max})$, then the deadzone nonlinearity $\varphi(v)$ satisfies the following inequality, which is true for any positive definite (one-by-one) matrix $\mathrm{W}\in\mathbb{R}$

$$\varphi^{\top}(v)\mathrm{W}[\varphi(v)-\theta]\leq 0. \tag{2.18}$$

Proof. Assume that v and θ are elements of $\mathscr{L}(v-\theta,u_{min},u_{max})$. Then, it follows that $v-u_{max}-\theta\leq 0$ and $v+u_{min}-\theta\geq 0$. Consider now the three cases below.

- Case 1: $v>u_{max}$. It follows that $\varphi(v)=v-u_{max}>0$. Also, $\varphi^{\top}(v)\mathrm{W}[\varphi(v)-\theta]=\varphi^{\top}(v)\mathrm{W}[v-u_{max}-\theta]<0$ provided that $\mathrm{W}>0$.
- Case 2: $-u_{min}\leq v\leq -u_{max}$. In this situation, $\varphi(v)=0$ and $\varphi^{\top}(v)\mathrm{W}[\varphi(v)-\theta]=0$.
- Case 3: $v<-u_{min}$. It follows that $\varphi(v)=u_{min}+v<0$. Also, $\varphi^{\top}(v)\mathrm{W}[\varphi(v)-\theta]=\varphi^{\top}(v)\mathrm{W}[v+u_{min}-\theta]<0$ provided that $\mathrm{W}>0$.

Thus, if v and θ are elements of $\mathscr{L}(v-\theta,u_{min},u_{max})$, we can conclude that (2.18) holds. □

Note that (2.15) is a special case of (2.18) when $\theta=\Lambda v$. Consider, for example, the case when the control law is given by $v=\mathrm{K}x$. The free term θ helps to yield less conservative results in the estimation of regions of guaranteed stability since one can define, for example, $\theta=\mathrm{G}x$, where G is an auxiliary variable allowing the set $\mathscr{L}(v-\theta,u_{min},u_{max})$ in (2.17) to grow while avoiding nonlinear terms when developing LMIs. This allows maximizing estimates on the

[1] Sometimes, in this text, we call such estimations on the region of attraction a region of asymptotic stability (RAS).

region of attraction. The derivation with the classical condition, however, would include the term $\Lambda \mathrm{K}x$, which impairs the gathering of convex conditions for the design of K unless Λ is fixed, thus prejudicing the elaboration of more efficient optimization problems for the maximization of $\mathscr{L}(v,\bar{u}_{min},\bar{u}_{max})$ in (2.14).

Remark 2.1: About the sector conditions

Both the classical and the generalized sector conditions were presented for the case where the deadzone nonlinearity is defined by relation (2.11). Such definition was applied, for example, in Turner and Postlethwaite (2007) and Gomes da Silva Jr. and Tarbouriech (2005) and is used for Chapters 5 and 6 in this thesis. Alternatively, some references define the deadzone nonlinearity as

$$\varphi(v(t)) = sat(v(t)) - v(t). \tag{2.19}$$

This is the case, for example, in Tarbouriech *et al.* (2011), and is the identity that will be used in Chapter 7 of this thesis. In this situation, conditions (2.15) and (2.18) need to be appropriately changed to

$$\varphi^{\top}(v)\mathrm{W}[\varphi(v) + \Lambda v] \leq 0, \tag{2.20}$$

and

$$\varphi^{\top}(v)\mathrm{W}[\varphi(v) + \theta] \leq 0, \tag{2.21}$$

respectively. The definitions of the sets $\mathscr{L}(v,\bar{u}_{min},\bar{u}_{max})$ in (2.14) and $\mathscr{L}(v-\theta,u_{min},u_{max})$ in (2.17) remain, however, unaltered. See Tarbouriech *et al.* (2011) for the proofs in this case. It is important to remark that there is no difference in terms of conservatism in using either of the two definitions for the deadzone.

2.5 Application of sector conditions to stability analysis

In order to analyse the stability of linear systems interconnected with a isolated nonlinearity, one can use a combination of the Lyapunov theorem and some sector condition. Particularly, the quadratic Lyapunov function $V(x) = x^{\top}\mathrm{P}x$, with P in $\mathbb{S}_n^+$, is often used to this end. We will not go through all the details for the gathering of convex conditions for the stability analysis of system τ_{φ}, given by (2.12)-(2.13), since the LMIs for this type of analysis can be readily found in Tarbouriech *et al.* (2011), among others. However, it is interesting to comment

that the proof is based on the application of the following inequality

$$\dot{\mathrm{V}}(x) - \boldsymbol{\varphi}^{\top}(v)\mathrm{W}[\boldsymbol{\varphi}(v) - \boldsymbol{\theta}] < 0,$$

with $\boldsymbol{\theta} = \mathrm{G}x$, which implies that $\dot{\mathrm{V}}(x) < 0$ for any x belonging to the ellipsoidal region $\boldsymbol{\varepsilon} = \{x \in \mathbb{R}^n : x\mathrm{P}x \leq 1\}$ as longs as we use a second inequality to ensure inclusion of $\boldsymbol{\varepsilon}$ in the resulting set $\mathscr{L}(\bar{u}) = \{x \in \mathbb{R}^n; |\mathrm{K}x - \mathrm{G}x| \leq \bar{u}\}$, where $\bar{u}$ is a symmetric saturation level. Applications of the generalized sector condition with other choices for $\boldsymbol{\theta}$ can also be found in the literature, as $\boldsymbol{\theta} = \mathrm{K}x - \mathrm{G}x$ or $\boldsymbol{\theta} = \mathrm{K}x + \mathrm{G}x$.

Part II

Time-delay systems

3 INTRODUCTION TO TIME DELAYS

Time delays appear in a wide variety of real processes from biology to economics and communication systems. The source of delay can be related to many causes such as mass or energy transportation in the process. For instance, in the case of economics, time delay looks quite natural since there exist time intervals between information acquisition, decision making and their effects in the market. Time delay is a rather challenging issue in the process control area because the transport delay can lead the system to undesired oscillatory closed-loop response or even instability. According to Fridman (2014), the stability analysis and the robust control of time-delay systems are, therefore, of theoretical and practical importance. Despite being historically related to degrading effects in the closed loop and imposing difficulties for the control engineer, some techniques have also purposefully introduced delays in control laws to generate a stabilizing effect or improve other aspects of the closed loop. As an illustration of this, one can look, for instance, at Example 5.3.5 presented on page 177 of Briat (2015).

Stability and control of systems with constant delays have received most of the attention in the last decades, whereas the problem of time-varying delays has gained more importance in recent years due to the rise of Networked Control Systems (NCSs) (ZHANG *et al.*, 2017; GUPTA; CHOW, 2010). Time-varying delays can be more harmful to control systems than constant ones since the rate of variation of the delay has a non-negligible effect on stability. For illustration, consider the example taken from Louisell (2001), re-enunciated on page 178 of Briat (2015). The example demonstrates that the time-delay system described by

$$\dot{x} = -x(t) - 1.5x(t-d)$$

is exponentially stable for any constant delay $d \in [0,\bar{d})$, where $\bar{d} = \frac{2}{\sqrt{5}}\arccos\left(\frac{-2}{3}\right) \approx 2.05765$. Nonetheless, the example also demonstrates that for a certain class of sawtooth time-varying delays $d(t)$, the system is stable for $d(t) < log(5) \approx 1.6094 < \bar{d}$, which shows that the system can become unstable even though the time-varying delay takes values inside the interval for which stability is assured in the case of constant delays. This situation is commonly known in the literature as the *quenching phenomenon* (BRIAT, 2015; PAPACHRISTODOULOU *et al.*, 2007). Moreover, another difficulty when dealing with time-varying delays is that, due to the fact that the delay can change at each sampling time, the use of classical analysis tools such as state augmentation (in the discrete-time case) becomes involved (FRIDMAN, 2014).

Time-varying delays naturally appear in networked control systems since they are dis-

tributed systems in which data is transmitted between actuators, sensors, and controllers through communication networks, often relying on protocols such as Transmission Control Protocol (TCP). This research area is identified as a key for the future of control systems (LAMNABHI-LAGARRIGUE *et al.*, 2017; HESPANHA *et al.*, 2007) due to its diverse application; networks of mobile vehicles, smart grids and the healthcare industry are a few examples. A general structure of a networked output-feedback control system is depicted in Figure 5, where $y(k)$ is the process measured output, $v(k)$ is the decoded computed control signal and d_k is a time-varying delay due to the communication network.

Figure 5 – General networked output-feedback control system.

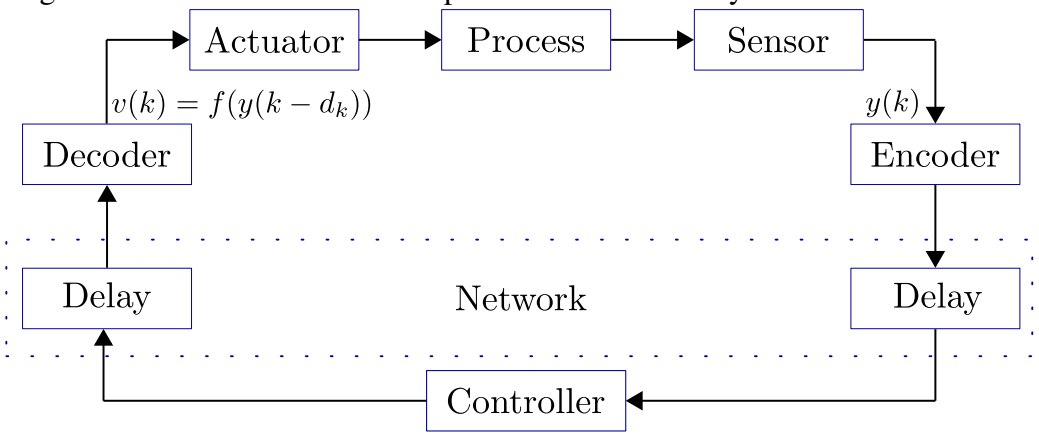

Source: The author.

Time delays affect dynamical systems in different manners, thus classification according to the type of delay is necessary. Three popular sub-classes which are widely recovered in the literature are those of systems with output, input, and state delays. Remarkably, the first two are, in many situations, treated as a unique problem, mainly when the delay is constant and the system is modelled using frequency-domain representations as in Normey-Rico and Camacho (2007). This might not be interesting, however, when distinguishing the problem of time-varying measurement delays from the case of input delays in time-domain models. In a theoretical point of view, the case of state delays has gained a lot of attention in recent years due to the application of Lyapunov-Krasoviskii methods for its stability analysis and also stabilization, mainly with feedback gain techniques (SEURET; GOUAISBAUT, 2015; ZHANG *et al.*, 2017; SEURET; GOUAISBAUT, 2018; LIU *et al.*, 2017; HE *et al.*, 2008; DE SOUZA *et al.*, 2019; CASTRO *et al.*, 2020). It is worth to remind that systems with input or output delays become state-delayed systems in closed loop, thus justifying the attention given to this last case in the literature.

In the next sections, we will go through some important aspects of time-delay

systems, starting by their solution concept and finishing with some remarks about their stability analysis in the presence of saturating inputs. We then end by giving out some clues on the content of the subsequent chapters of Part II.

3.1 Systems with input and output delays

Input and output delays normally occur due to actuator and sensor dynamics. A discrete-time system with constant input delay can be represented by the following state-space model

$$\begin{cases} x(k+1) = \mathrm{A}x(k) + \mathrm{B}u(k-d), \\ y(k) = \mathrm{C}x(k), \\ u(k) = \phi(k),\ k \in [-d,-1], \end{cases} \tag{3.1}$$

where $d > 0$ is the delay, $x \in \mathbb{R}^n$ is the state, $u \in \mathbb{R}^m$ is the input, $y \in \mathbb{R}^q$ is the output, and matrices A, B, C are of appropriate dimensions. Furthermore, $x(0)$ and $\phi(k)$ define the initial condition. Similarly, in case of measurement (output) delays, the following model takes place

$$\begin{cases} x(k+1) = \mathrm{A}x(k) + \mathrm{B}u(k), \\ y(k) = \mathrm{C}x(k-d). \end{cases} \tag{3.2}$$

The solution of (3.1) can easily be found by recursion and is given by

$$\begin{cases} x(k) = \mathrm{A}^k x(0) + \sum_{j=0}^{k-1} \mathrm{A}^{k-j-1}\mathrm{B}u(j-d), \\ y(k) = \mathrm{C}x(k) = \mathrm{C}\mathrm{A}^k x(0) + \mathrm{C}\left(\sum_{j=0}^{k-1} \mathrm{A}^{k-j-1}\mathrm{B}u(j-d)\right). \end{cases} \tag{3.3}$$

The solution to (3.2) can be found likewise. From (3.3) it becomes clear that the solution depends on the initial condition $x(0)$ and $\phi(k)$. One interesting fact about (3.1) and (3.2) is that they are input to output equivalent, meaning that they admit the same frequency domain model. Application of the z-transform to both of them lead to the representation

$$Y(z) = G(z)z^{-d}U(z), \tag{3.4}$$

where $G(z) = \mathrm{C}\,(z\mathrm{I} - \mathrm{A})^{-1}\,\mathrm{B}$ represents the delay-free part of the plant, and $U(z)$, $Y(z)$ are the z-transform of the input and output signals, respectively. This frequency-domain representation has been widely used by control engineers for the design of control systems. It is important to

remark that, as opposed to their continuous-time counterpart, (3.4) is of finite dimension, as there are a finite number of roots for their characteristic polynomial. We will not go into details over that since the contributions reported in the time delay part of this thesis deal with discrete-time systems.

3.2 Discrete-time state-delayed systems

Consider the linear discrete-time state-delayed system

$$\begin{cases} x(k+1) = \mathrm{A}x(k) + \mathrm{A_d}x(k-d_\mathrm{M}), \quad k \in \mathbb{Z}^+, \quad x(k) \in \mathbb{R}^n, \\ x(k) = \phi(k),\ k \in [-d_\mathrm{M}, 0]\,, \end{cases} \tag{3.5}$$

where A, $\mathrm{A_d}$ are matrices of appropriate dimension, $d_\mathrm{M} > 0$ is a constant delay and $\phi(k)$ is the initial condition at the interval $[-d_\mathrm{M}, 0]$. This type of system emerges when applying some closed-loop control strategy to systems (3.1) and (3.2). However, it can also naturally appear in open-loop processes. The fundamental distinction between (3.5) and non-delayed difference equations is that the state of 3.5 is given by the augmented vector $\bar{x}(k) = \begin{bmatrix} x(k)^\top & x(k-1)^\top & \cdots & x(k-d_\mathrm{M})^\top \end{bmatrix}^\top$ instead of simply $x(k)$. The solution of (3.5) can easily be found by recursion and is given by

$$x(k) = \mathrm{A}^k x(0) + \sum_{j=0}^{k-1} \mathrm{A}^{k-j-1}\mathrm{A_d}x(j-d_\mathrm{M}) \tag{3.6}$$

which clearly depends on the initial value sequence $\phi(k),\ k \in [-d_\mathrm{M}, 0]$. One option to analyse stability of (3.5) is to rewrite it as the following augmented delay-free system

$$\bar{x}(k+1) = \overline{\mathrm{A}}\bar{x}(k), \quad k \in \mathbb{Z}^+, \quad \bar{x}(k) \in \mathbb{R}^{(d_\mathrm{M}+1)n}, \tag{3.7}$$

$$\overline{\mathrm{A}} = \begin{bmatrix} \mathrm{A} & \overbrace{0 \quad \cdots \quad 0}^{(d_\mathrm{M}-1)\text{ times}} & \mathrm{A_d} \\ \mathrm{I} & 0 \quad \cdots \quad 0 & 0 \\ 0 & \mathrm{I} \quad \ddots \quad \vdots & \vdots \\ \vdots & \ddots \quad \ddots \quad 0 & 0 \\ 0 & \cdots \quad 0 \quad \mathrm{I} & 0 \end{bmatrix}, \tag{3.8}$$

and use the conventional quadratic Lyapunov function for delay-free systems $V(\bar{x}) = \bar{x}^\top \bar{\mathrm{P}}\bar{x}$, with $\bar{\mathrm{P}}$ in $\mathbb{S}^+_{(d_\mathrm{M}+1)n}$. This technique, however, may not be numerically robust to solve in case the order

of augmented system (3.7) is high. Other inconvenience appears when the delay is time-varying, that is, instead of the constant $d_{\mathrm{M}} > 0$ delay in (3.5), we have the time-varying delay d_k such that $0 \leq d_k \leq d_{\mathrm{M}}$. In this case, the augmented system becomes the switched one

$$\bar{x}(k+1) = \overline{\mathrm{A}}^{(j)}\,\bar{x}(k), \quad k \in \mathbb{Z}^+, \quad \bar{x}(k) \in \mathbb{R}^{(d_{\mathrm{M}}+1)n}, \tag{3.9}$$

where $j \in \mathcal{J} = \{0, 1, \ldots, d_{\mathrm{M}}\}$ and the value of the delay at each sampling time defines the matrix $\overline{\mathrm{A}}^{(j)}$ with

$$\overline{\mathrm{A}}^{(0)} = \begin{bmatrix} \mathrm{A}+\mathrm{A}_{\mathrm{d}} & 0 & \cdots & 0 & 0 \\ \mathrm{I} & 0 & \cdots & 0 & 0 \\ 0 & \mathrm{I} & \ddots & \vdots & \vdots \\ \vdots & \ddots & \ddots & 0 & 0 \\ 0 & \cdots & 0 & \mathrm{I} & 0 \end{bmatrix}, \overline{\mathrm{A}}^{(1)} = \begin{bmatrix} \mathrm{A} & \mathrm{A}_{\mathrm{d}} & \cdots & 0 & 0 \\ \mathrm{I} & 0 & \cdots & 0 & 0 \\ 0 & \mathrm{I} & \ddots & \vdots & \vdots \\ \vdots & \ddots & \ddots & 0 & 0 \\ 0 & \cdots & 0 & \mathrm{I} & 0 \end{bmatrix}, \cdots, \overline{\mathrm{A}}^{(d_{\mathrm{M}})} = \begin{bmatrix} \mathrm{A} & 0 & \cdots & 0 & \mathrm{A}_{\mathrm{d}} \\ \mathrm{I} & 0 & \cdots & 0 & 0 \\ 0 & \mathrm{I} & \ddots & \vdots & \vdots \\ \vdots & \ddots & \ddots & 0 & 0 \\ 0 & \cdots & 0 & \mathrm{I} & 0 \end{bmatrix}.$$

Although exploring the stability of systems with time-varying delays using the equivalent switched system is a nice idea which has attracted the attention in some important works (HETEL *et al.*, 2008; SUN *et al.*, 2008; ZHANG; YU, 2009), in this thesis we are more interested in applying so-called delay-dependent stability conditions through a special class of Lyapunov functionals, as contextualized in the next section.

3.3 Delay-Dependent Stability

In this section, bases for the stability analysis of discrete-time systems with time-varying delays are presented. As explained in the introduction, the motivation for the study of stability in the case of time-varying delays lies on the recent advance of networked controlled systems. In general, stability of time-delayed systems can be tackled by using either delay-independent or delay-dependent conditions. The later case (in which bounds on the delay are explicitly considered) is preferred in this work. For this, initially let us consider the following discrete-time linear system with time-varying delay d_k

$$\begin{cases} x(k+1) = \mathrm{A}x(k) + \mathrm{A}_{\mathrm{d}}x(k-d_k), \quad k \in \mathbb{Z}^+, \quad d_k \in \mathbb{N}, 0 \leq d_k \leq d_{\mathrm{M}}. \\ x(k) = \phi(k),\ k \in [-d_{\mathrm{M}}, 0] \end{cases} \tag{3.10}$$

where $\phi(k)$ is the initial condition at the interval $[-d_{\mathrm{M}}, 0]$. For simplicity, denote $\bar{x}(k) \triangleq x(k+j)$, $j = -d_M, -d_M+1, \ldots, 0$, and $d_k \triangleq d(k)$. In the Lyapunov-Krasoviskii framework, system (6.22)

is asymptotically stable if, for all $k \in \mathbb{Z}^+ = \{0,1,2,\dots\}$, there exists a functional

$$V_k \triangleq V(k,\bar{x}(k)) : \mathbb{Z}^+ \times \overbrace{\mathbb{R}^n \times \dots \times \mathbb{R}^n}^{d_M+1 \text{ times}} \to \mathbb{R}^+ \tag{3.11}$$

such that, for all $\bar{x}(k) \neq 0$, $V_k > 0$ and its forward difference is negative, i.e., $\Delta V_k = V_{k+1} - V_k < 0$. Basically, that implies that the problem of providing stability analysis for systems with delayed states can be solved by choosing an appropriate functional V_k. These are referred as Lyapunov-Krasovskii functionals and their choice and subsequent manipulation lead to sufficient conditions that can be more or less conservative in terms of bounds on the delay for which stability is assured. When dealing with stability of systems with time-varying delays, all Lyapunov-Krasovskii functionals (LKFs) employ summation terms that need to be upper bounded in order to derive tractable LMI conditions. Due to this, careful deliberation has been raised by the time delay research community in the last decades concerning the search and application of less conservative summation inequalities in LKFs. This is an active field of research, with many works published in the last ten years. For more details see, for example, the works of Zhu and Yang (2008), Zhang *et al.* (2008), Shao and Han (2011), Liu and Zhang (2012), Seuret *et al.* (2015). More discussion on this matter will be provided within Chapter 6, where we apply delay-dependent conditions for the stability analysis of a predictor controller structure in the presence of output time-varying delays and saturating input.

3.3.1 Sector conditions and stability of time-delayed systems

Consider now a modified version of the delayed system (3.10) interconnected with the deadzone nonlinearity $\varphi(v(k))$, $v = \mathrm{K}x$.

$$\begin{cases} x(k+1) = \mathrm{A}x(k) + \mathrm{A_d}x(k-d_k) + \mathrm{B}\varphi(v(k)), \quad k \in \mathbb{Z}^+, \quad d_k \in \mathbb{N}, 0 \leq d_k \leq d_{\mathrm{M}}. \\ x(k) = \phi(k),\ k \in [-d_{\mathrm{M}}, 0] \end{cases} \tag{3.12}$$

Let $\mathrm{V}_k : \underbrace{\mathbb{R}^n \times \dots \times \mathbb{R}^n}_{d_{\mathrm{M}}+1 \text{ times}} \to \mathbb{R}^+$ be a Lyapunov-Krasovskii functional, and $\Delta \mathrm{V}_k$ its forward difference along system trajectories. By using Lemma 2.3 with $v = \mathrm{K}x$ and $\theta = \mathrm{G}x$, where G is a free matrix, and applying the S-procedure (BOYD *et al.*, 1994), we find out that

$$\Delta \mathrm{V}_k - 2\varphi^\top(v(k))\mathrm{W}\Big[\varphi(v(k)) - \mathrm{G}x(k)\Big] < 0$$

implies that $\Delta \mathrm{V}_k < 0$, $\forall x(k) \in \mathscr{L}(\bar{u}) = \{x \in \mathbb{R}^n; |\mathrm{K}x - \mathrm{G}x| \leq \bar{u}\}$, where $\bar{u}$ is a symmetric saturation level. In this case, condition from Lemma 2.3 is locally satisfied. If we make $\mathrm{G} = \mathrm{K}$, then

condition (2.18) holds for $\forall x(k) \in \mathbb{R}^n$, thus Lemma 2.3 is globally satisfied. Since the state of (3.12) is given by the augmented vector $\tilde{x}(k) = \begin{bmatrix} x(k)^\top & x(k-1)^\top & \cdots & x(k-d_{\mathrm{M}})^\top \end{bmatrix}^\top$, and no longer by simply $x(k)^\top$ as in the delay-free case,it is necessary to estimate yet another set $\mathcal{D}(\tilde{x}(k))$ such that for all $\tilde{x}(k) \in \mathcal{D}(\tilde{x}(k))$, we guarantee that $x(k) \in \mathscr{L}(\bar{u})$, so that the sector condition can be effectively validated for the set of initial conditions of the delayed system. In order to guarantee regional asymptotic stability, the set of initial conditions must be contained within the region of attraction of the system. As the exact characterization of the region of attraction is almost impossible to accomplish, optimization procedures must take place in order to maximize the estimated sets. There exist different strategies in the literature of constrained time-delay systems to characterize such a set, which usually consists in using the LKF to find a set of norm bounded functions of the initial condition. It is important to remark that other approaches for the consideration of the saturation condition can be used instead of the sector conditions, such as the polytopic model approach (TARBOURIECH *et al.*, 2011), which we do not consider in this thesis. More details about the definition of the set initial conditions of a input-saturated state-delayed system with time-varying delays will be given within Chapter 6 of this thesis, where we will also characterize a set of functions of an input disturbance affecting the system for which stability is mathematically assured despite the presence of the saturating input and time-varying delays.

3.4 About the next chapters

For the sake of convenience, we will shortly refresh the reader's mind with a brief description of the upcoming chapters in the time delay part of this thesis:

- Chapter 4 provides an overview of some common control strategies for the control of input and output time-delay systems, with focus on predictive strategies.
- Chapter 5 presents a control plus anti-windup strategy that is suitable to deal in a unified way with both delay-free and delayed systems. Both the linear controller and the anti-windup are based on the model of the plant.
- Chapter 6 then addresses robust stability analysis of a simplified dead-time compensator, which is a variant of the Filtered Smith Predictor (FSP), for the case of systems with both output time-varying delays and saturating inputs. Some novelties regarding the definition of the region of attraction for this type of system are presented.

4 CONTROL STRATEGIES

In this chapter, we review some of the strategies that have historically been applied to the control of input delayed systems. Initially, we explain the paradigm of predictor strategies in the control of time delay systems. Then we briefly go through the celebrated Smith Predictor (SP). Later we contextualize what are the so-called Dead-time Compensators (DTCs) and review the Simplified Dead-time Compensator (SDTC) from Torrico *et al.* (2018). Much of the basic content regarding the predictor idea is inspired by other thesis dealing with the subject (SANZ, 2018; PRUDÊNCIO DE ALMEIDA FILHO, 2020). Even though Smith's idea was originally published in the Laplace domain for continuous-time systems, we will write the equivalent ideas for the case of discrete-time systems. In case the reader is already comfortable with the subject of prediction in time delay systems, there is no harm in going straight to section 4.4, where the base controller used in chapters 5 and 6 of this thesis is reviewed.

4.1 The predictor paradigm

Consider the control loop depicted in Figure 6, where $C(z)$ is the feedback controller and $P(z) = G(z)z^{-d}$ is the delayed plant. The input-output transfer functions from the reference r and the disturbance q are given by

$$H_{ry} = \frac{G(z)C(z)z^{-d}}{1 + G(z)C(z)z^{-d}}, \tag{4.1}$$

$$H_{qy} = \frac{G(z)z^{-d}}{1 + G(z)C(z)z^{-d}}. \tag{4.2}$$

As it can be observed, the delay appears in the characteristic equations of transfer functions (4.1)-(4.2). Bad behaviour of the closed loop such as oscillations in the output or even instability can occur, since the delay reduces the system phase margin in this situation. Consider now the ideal closed loop scheme in Figure 7. This implementation is unfeasible since we do not have access to measurements of the delay-free output $\bar{y}$. Such ideal feedback would yield the following input-output transfer functions

$$H_{ry} = \frac{G(z)C(z)z^{-d}}{1 + G(z)C(z)}, \tag{4.3}$$

$$H_{qy} = \frac{G(z)z^{-d}}{1 + G(z)C(z)}. \tag{4.4}$$

Figure 6 – Generic control structure for discrete time-delay system.

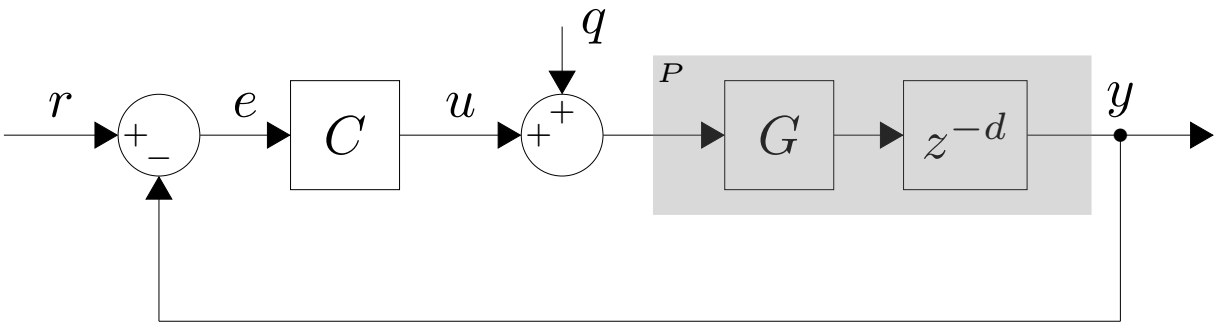

Source: The author.

Figure 7 – Ideal control loop for discrete time-delay system (unfeasible).

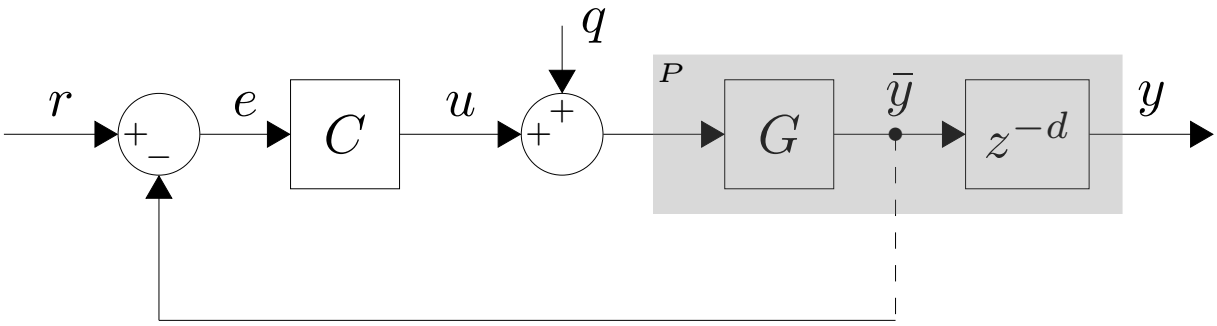

Source: The author.

One great advantage in this situation is that since the delay is eliminated from the feedback loop, it vanishes from the characteristic equations of (4.3)-(4.4). Thus, any appropriate control strategy for the delay-free plant $G(z)$ could be applied. The idea of predictive controllers for time-delay systems was born from the paradigm of estimating, somehow, the signal $\bar{y}(z) = y(z)z^d$, which corresponds to the output of the delay-free plant, in an attempt to obtain the same characteristics of the ideal feedback loop from Figure 7. In the case of state-space representation (3.1) this would be equivalent to estimating the value of $y(k+d)$. Suppose now that now that system (3.1) is affected by disturbances such the state equation is now written as:

$$x(k+1) = \mathrm{A}x(k) + \mathrm{B}u(k-d) + \mathrm{B}_q q(k), \tag{4.5}$$

where $q(k)$ is the disturbance signal. From the solution of (4.5), the exact prediction for

$y(k+d) = \mathrm{C}x(k+d)$ can be computed with

$$y(k+d) = \mathrm{C}\mathrm{A}^d x(k) + \mathrm{C}\left(\sum_{j=0}^{d-1} \mathrm{A}^{d-j-1}\mathrm{B}u(k-d+j) + \sum_{j=0}^{d-1} \mathrm{A}^{d-j-1}\mathrm{B}q(k+j)\right). \tag{4.6}$$

Nonetheless, implementation of this equation is also unfeasible since it implies knowledge of the values of q in the interval $[k, k+d-1]$, that is, it requires knowledge of future values of the disturbance. This is unthinkable in almost all real practical situations. A simplified version of (4.6), in which the terms due to the disturbance $q(k)$ are disregarded, takes place in the famous Artstein's predictor[1] strategy. Such simplification, however, leads to the inevitable existence of prediction errors. The development of strategies that envisage the minimization of such an error, and therefore an improvement of the prediction of $x(k+d)$, has been an active field of research. See, for example, the works of Castillo and García (2021), Sanz *et al.* (2016), Léchappé *et al.* (2015), dealing with the continuous-time counterpart of this problem.

4.2 The Smith Predictor

One of the most well-known strategies for the control of systems with inputs and output delays is the seminal Smith Predictor (SP). Smith's idea was introduced prior to Arstein's predictor, in Smith (1957), and was conceived in the frequency domain. The idea consists of eliminating the effect of the delay from the feedback loop by means of employing a model $P_n = G_n z^{-d_n}$ of the system to the feedback path. Henceforth, any strategy for delay-free systems could be efficiently applied. The structure of the Smith predictor is shown in Figure 8. Block diagram algebra leads to the following input-output transfer functions in the nominal case[2] ($P = P_n$):

$$H_{ry} = \frac{G_n(z)C^*(z)z^{-d}}{1 + G_n(z)C^*(z)}, \tag{4.7}$$

$$H_{qy} = \frac{G_n(z)z^{-d}}{1 + G_n(z)C^*(z)}. \tag{4.8}$$

As it can be seen from (4.7)-(4.8), the delay is successfully eliminated from the characteristic equation in case the model perfectly matches the plant. Therefore, under this circumstance,

[1] Although Artstein's original work considered the continuous counterpart of (4.5), we herein present the discrete version to keep consistency with the discrete time formulation in the thesis.

[2] The expression nominal case refers to a perfect modelling of the plant, i.e., $P = P_n$.

the primary controller $C^*(z)$ can be conceived using any design technique that applies to the delay-free plant $G(z)$, as was the case for the ideal control loop of Figure 7. Interestingly, Smith's visionary idea made use of the Laplace transform for continuous-time systems and could not be implemented with the tools available at the epoch. Only much later, with the advent of digital computers, it became possible to implement the strategy. Herein we have presented the discrete-time (z-transform) equivalent of his ideas.

Figure 8 – Smith Predictor conceptual structure. $P_n = G_n z^{-d_n}$ stands for the plant nominal model.

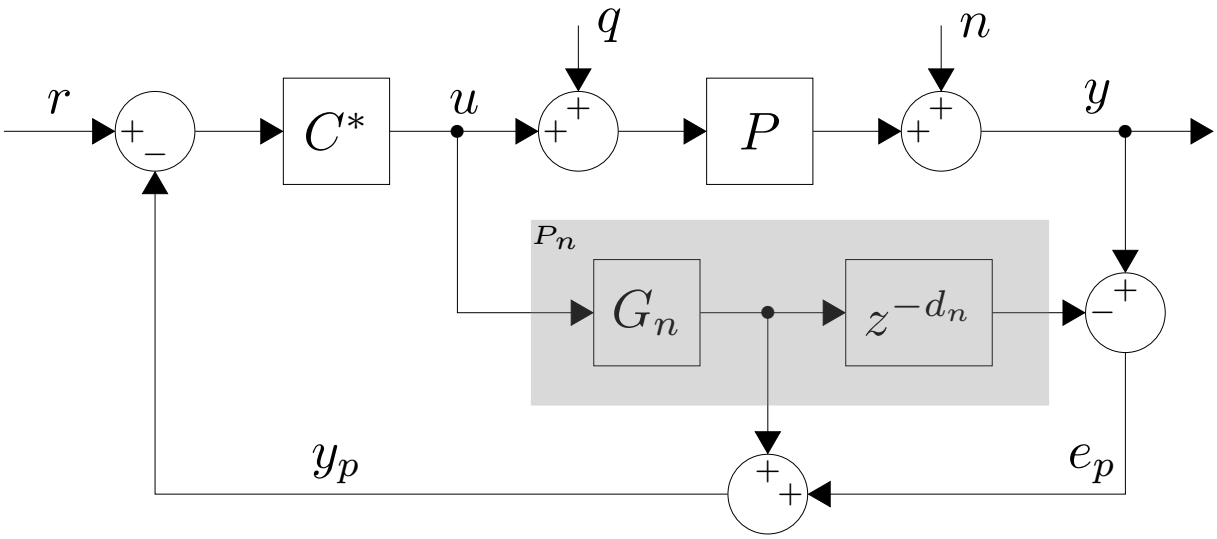

Source: The author.

4.3 Dead-time Compensators

One main drawback of the Smith Predictor is its inability to deal with open-loop unstable plants. This is due to the poles of the process model appearing in the disturbance rejection transfer function. Different solutions to overcome this limitation have been proposed over time, with special attention given to the Filtered Smith Predictor (FSP) presented in Normey-Rico *et al.* (1997), which solved this problem by means of the introduction of a so-called robustness filter to the path of the signal e_p in Figure 8 that is used to eliminate the unstable and/or integrative poles of the process model from the disturbance rejection response. Many other variations of the SP and the FSP have been proposed over time, which now form a family of predictive control strategies commonly known as Dead-time Compensators (DTCs) due to

their ability to *compensate*[3] the dead time[4] when the process model $P_n(z)$ perfectly matches that of the real process $P(z)$.

4.3.1 Frequency domain robust stability condition

Since all process models possess uncertainties, it important to use some condition to establish the robust stability of predictive structures. In the case of the traditional DTCs applied to linear systems, a widely used analysis tool is the frequency domain robust stability condition from Morari and Zafiriou (1989) briefly reviewed in this subsection. Consider again the closed loop in Figure 6. The SISO plant $P(z)$ can be written either as

$$P(z) = P_n(z) + \Delta P(z),$$

or

$$P(z) = P_n(z)\left(1 + \delta P(z)\right),$$

where $P_n(z)$ is the nominal process model, $\Delta P(z)$ and $\delta P(z)$ are the addictive and multiplicative modelling errors, respectively. Morari and Zafiriou (1989) uses the Nyquist criterion to establish the following robust condition in case of addictive uncertainties (here translated to the discrete-time case)

$$|I_r(\omega)|_{z=e^{j\omega T_s}} > |\Delta P(z)|_{z=e^{j\omega T_s}}, \forall \omega \text{ such that } 0 < \omega < \pi/T_s, \tag{4.9}$$

where $I_r(\omega) = \frac{|1+C(z)P_n(z)|}{|C(z)|}$ and T_s is the sampling time. In case of multiplicative uncertainty, the condition can be equivalently redefined as

$$|I_r(\omega)|_{z=e^{j\omega T_s}} > |\delta P(z)|_{z=e^{j\omega T_s}}, \forall \omega \text{ such that } 0 < \omega < \pi/T_s, \tag{4.10}$$

where $I_r(\omega) = \frac{|1+C(z)P_n(z)|}{|C(z)P_n(z)|}$. The stability of the closed loop in the presence of modelling uncertainties is then guaranteed if either the robust condition (4.9) or (4.10) is satisfied. These conditions can be graphically verified in a nice manner in order to compare the robustness of different control strategies.

---

[3] Compensate in this context means to eliminate the delay influence from the feedback loop.

[4] Dead time is another common expression to designate time delays. From now on we will use both interchangeably.

Remark 4.1: On the robustness of linear DTCs

By means of block diagram algebra, all DTC strategies can be rewritten as Figure 6 where C is actually a combination of the primary controller C^* and the predictor components. For example, in the case of the Smith predictor (section 4.2), one would use the relation $C(z) = \frac{C^*(z)}{1+C^*(G_n(z)-P_n(z))}$ to obtain valid robust stability conditions through substitution of $I_r(\omega)$ in (4.9) and (4.10) by $I_r(\omega) = \frac{|1+C^*(z)G_n(z)|}{|C^*(z)|}$ and $I_r(\omega) = \frac{|1+C^*(z)G_n(z)|}{|C^*(z)G_n(z)|}$, respectively.

4.4 The Simplified Dead-time Compensator

This section presents a review of the Simplified DTC (SDTC) strategy from Torrico *et al.* (2018), which is the base controller used for chapters 5 and 6 of this thesis. The controller scheme is presented first, followed by the tuning procedure for set-point tracking, robustness and disturbance rejection. Finally, the section is closed with discussion about the controller implementation structure and its usefulness dealing with delayed systems.

4.4.1 Conceptual scheme

The SDTC conceptual scheme is depicted in Fig. 9, where $P_n(z) = G_n(z)z^{-d_n}$ is the nominal process, with $G_n(z)$ and d_n being the fast model and the nominal dead time, respectively. The block $P(z) = G(z)z^{-d}$ represents the real process.

The input-output transfer functions for the nominal case ($P_n(z) = P(z)$) and the robust stability condition are given by

$$H_{ry}(z) = P_n(z)H(z)F_0, \tag{4.11}$$

$$H_{qy}(z) = P_n(z)T_d(z), \tag{4.12}$$

$$H_{nu}(z) = -P_n(z)H(z)F_r(z), \tag{4.13}$$

$$I_{\mathrm{r}}(\omega) = \left| \big(P_n(z)H(z)F_r(z)\big)^{-1} \right|_{z=e^{j\omega T_s}} > |\delta P(z)|_{z=e^{j\omega T_s}}, \tag{4.14}$$

where $H(z) = \big[1 + F_1(z) + G_n(z)F_2(z)\big]^{-1}$, $T_d(z) = \big(1 - F_r(z)P_n(z)H(z)\big)$; $H_{ry}(z)$, $H_{qy}(z)$, and $H_{nu}(z)$ are the input-output transfer functions of the closed loop in Fig. 9, which can be obtained by block diagram algebra; $I_r(\omega)$ is defined as the robustness index, T_s is the sampling time (with $0 < \omega < \pi/T_s$), and $|\delta P(z)|_{z=e^{j\omega T_s}}$ is the norm of the multiplicative uncertainty, as explained in the previous section. By inspection of transfer functions (4.11)-(4.13), note that the time delay has been properly eliminated from their characteristic equations, as required by DTC strategies.

Figure 9 – SDTC conceptual structure. $P_n = G_n z^{-d_n}$ stands for the plant nominal model.

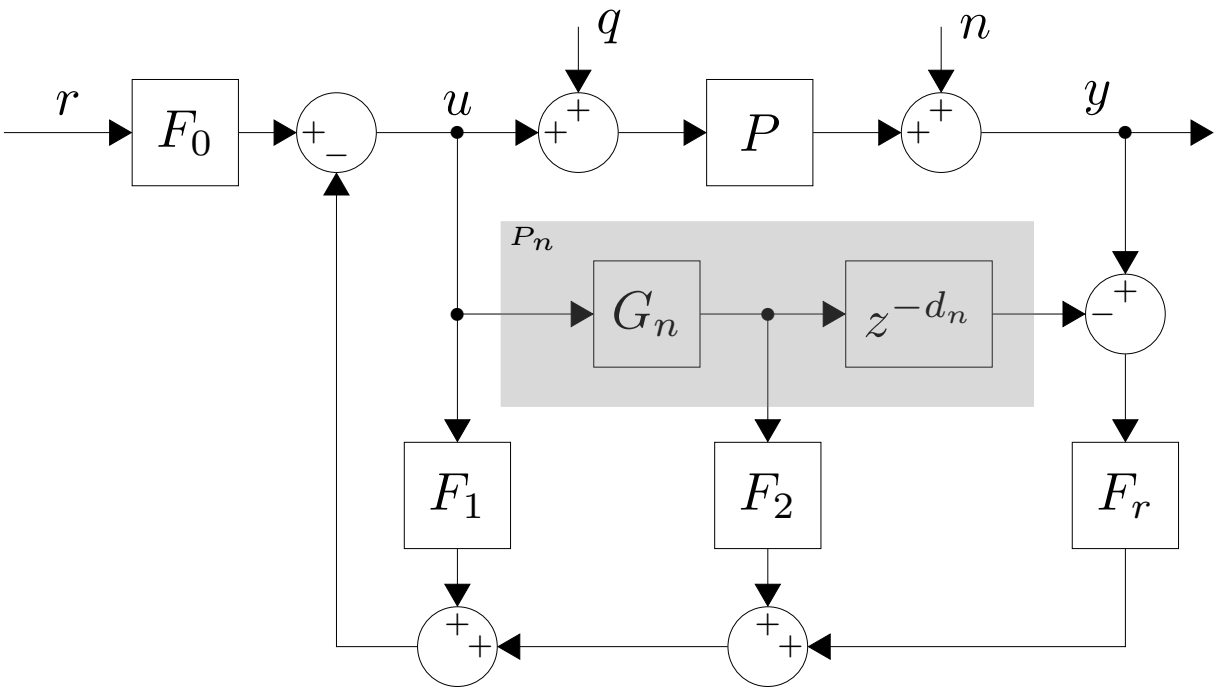

Source: The author.

It is important to highlight from (4.11) to (4.14) that the static gain F_0, and the filters $F_1(z)$ and $F_2(z)$ can be tuned in order to obtain a desired set-point tracking response, while the filter $F_r(z)$ can be set for disturbance rejection and robustness.

4.4.2 Set-point tracking response tuning

Tuning rules for the primary controller of the SDTC, defined by F_0, $F_1(z)$, and $F_2(z)$ are reviewed in this subsection. Consider feedback Finite Impulse Response (FIR) filters $F_1(z)$ and $F_2(z)$ as

$$F_1(z) = \sum_{i=1}^{n-1} f_{1_i} z^{-i}, \quad F_2(z) = \sum_{i=0}^{n-1} f_{2_i} z^{-i}, \tag{4.15}$$

where n is the order of the fast model $G_n(z)$. Coefficients of $F_1(z)$ and $F_2(z)$ are obtained by means of classical design techniques in order to reach a desired set-point tracking response, e.g. through pole placement in (4.11). The static gain F_0 is then computed to yield zero steady-state error between the reference and the output, i.e. $H_{ry}(z)\big|_{z=1} = 1$, yielding

$$F_0 = P_n^{-1}(z) H^{-1}(z)\Big|_{z=1}. \tag{4.16}$$

4.4.3 Robustness and disturbance rejection tuning

Robustness filter $F_r(z)$ is tuned aiming: (i) to reject undesired disturbances applied in the control signal; (ii) to eliminate the poles of the plant model $P_n(z)$ from $H_{qy}(z)$; (iii) to establish the desired compromise between robustness and disturbance rejection. Such goals can be met by applying the following filter

$$F_r(z) = \frac{1}{(1-\rho z^{-1})^{n+1}} \sum_{i=0}^{n} f_{r_i} z^{-i}, \tag{4.17}$$

where $0 < |\rho| < 1$ is the filter tuning parameter. In order to achieve objectives (i) and (ii), following conditions must be attended

$$\begin{cases} T_d(z)\big|_{z=p_i \neq 1} = 0, \quad i = 1...n_p \\ \\ \frac{d^j}{dz^j} T_d(z)\Big|_{z=1} = 0, \quad j = 0...m \end{cases} \tag{4.18}$$

where n_p are the number of stable and unstable delay-free process model poles, $m = m_1 + m_2 - 1$, m_1 is the order of the disturbance signal (1 for steps, 2 for ramps, etc) and m_2 is the number of integral poles of the plant. Equation (4.18) set a linear system so that coefficients f_{r_i} from (4.17) can be readily found, achieving design of the robustness filter $F_r(z)$ for a chosen value of the filter tuning parameter ρ. To reject other kinds of disturbance, (4.18) can be expanded to include the condition $T_d(z)\big|_{z=q_i} = 0$, where q_i, $i = 1...n_d$, are the n_d poles of the Laplace transform of the disturbance signal.

From (4.12) and (4.14) note that $F_r(z)$ appears in the numerator of $H_{qy}(z)$ and in the denominator of $I_r(w)$. That way, the objective (iii) can be met by user adjustment of $0 < |\rho| < 1$ parameter. By setting higher values of ρ, one can increase the robustness of the system, while smaller values of ρ speedup the disturbance rejection response. The noise attenuation characteristics can also be improved by using higher-order robustness filters (TORRICO *et al.*, 2018).

4.4.4 Implementation structure and discussion

A problem of many DTCs for unstable processes is that they cannot be implemented in its conceptual structure (NORMEY-RICO; CAMACHO, 2007). That way the structure shown in Fig. 10 must be used for implementation purposes, where $S(z) = F_1(z) + G_n(z)(F_2(z) - F_r(z)z^{-d_n})$. One can verify that proper design of $F_r(z)$ by following the rules established in the

Subsection 4.4.3 guarantees that $F_2(z) - F_r(z)z^{-d_n}$ cancels the poles of $G_n(z)$ in $S(z)$. That way, the implementation structure is always internally stable. Therefore, differently from the Smith Predictor, the SDTC is able to deal with stable, integrative, and unstable open-loop process.

Furthermore, some other characteristics of the SDTC strategy deserve to be discussed in further detail.

- The strategy does not add zeros in the closed-loop transfer function which may be dominant and cause undesired overshoot. This allows the reference filter to be defined as a simple gain (see (4.16)).
- The controller tuning is simplified due to the fact that the designer only needs to specify two tuning parameters, that is, the desired closed-loop set-point tracking poles (see Subsection 4.4.2) and the robustness filter $F_r(z)$ poles given by the ρ parameter (see Subsection 4.4.3). This makes the controller adjustment quite intuitive, and therefore quite useful for control engineers. Also, the discrete-time nature of the controller should provide a secure computer-based implementation.

Figure 10 – SDTC implementation scheme.

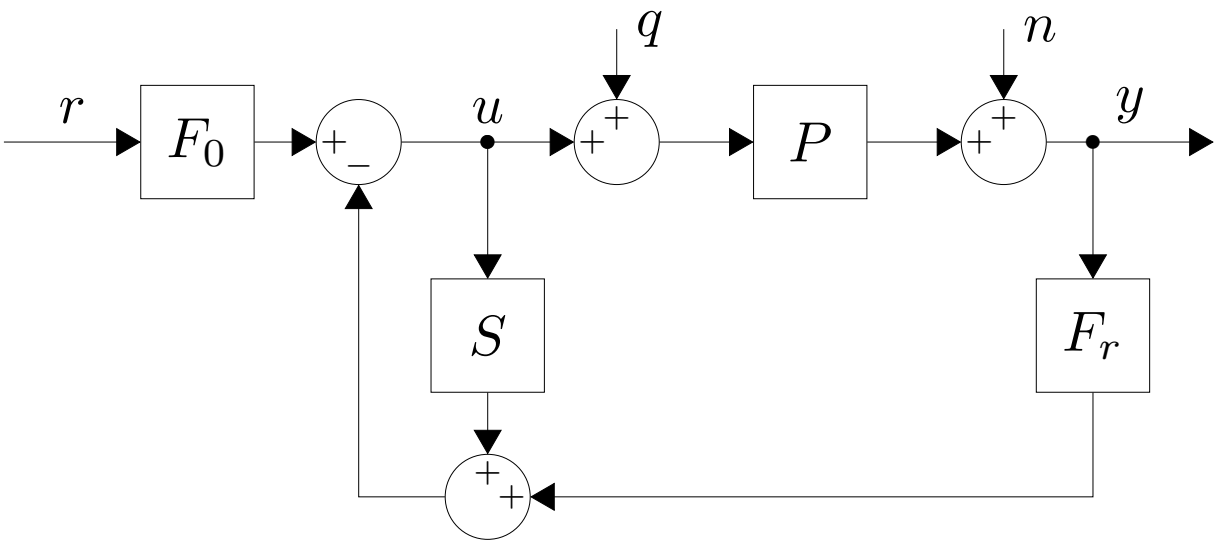

Source: The author.

4.5 Other Strategies

Many other strategies for the control of input and output time-delay systems have been explored in the literature. For example, regarding predictive strategies, many variations of model predictive controllers (MPCs) (CAMACHO; BORDONS, 2007; BOUOUDEN *et al.*,

2016) have been applied, specially when dealing with control constraints. Another variation of predictors consists of the so-called predictor observer structures. These are structures that do not suffer from the internal instability problems of the DTCs derived from the Smith predictor, which might represent an advantage since there is no need to define some strategy for the cancellation of the unstable and integrative poles of the plant model. In this context see, for example, chapter 3 in Krstic (2009) and the extended observer ideas in Sanz *et al.* (2020), Sanz *et al.* (2018b). We will go through more details on the relevant literature of controllers for time-delay systems within the next two chapters, as the main objective of the current chapter was to present the basis related to predictors with particular focus to dead-time compensators (DTCs), which is the class of controllers explored in this thesis.

5 A PRACTICAL ANTI-WINDUP STRATEGY

This chapter presents a predictor-based structure that is suitable to deal with both time-delayed and delay-free systems with saturating actuators. Such condition, well known in the literature to cause the windup phenomenon, is usually coped within the control area by techniques that commonly lead to the controller augmentation. However, it seems to exist a lack of simple approaches to deal with the design of linear controllers for both systems with and without delay. Thus, this chapter addresses the saturation problem by both proposing a linear controller design and an associated anti-windup compensator design. The controller tuning is realized in three distinct phases, initially considering set-point tracking adjustment, then robustness and disturbance rejection tuning, and finally the associated anti-windup compensator synthesis. Linear matrix inequalities (LMIs) which include both performance and stability requirements are employed for the anti-windup synthesis. The proposed controller presents better results when compared with recently published anti-windup controllers as well as a constrained MPC algorithm. Experimental results on a neonatal intensive care unit are also presented in order to validate the usefulness of the proposed strategy.

5.1 Introduction

Dead-time compensators (DTCs) is a class of predictor-based controllers that have been widely studied for about the past 25 years mainly due to their ability to improve the performance of classical proportional-integral (PI) and/or proportional-integral-derivative (PID) controllers when the process presents time delay between the input and output. The first DTC was proposed by Smith (1957), also known in the literature as the Smith Predictor (SP). Some drawbacks of the proposal have limited its applications as it is restricted to open-loop stable plants, while the slow poles of the plant dominate the disturbance rejection response (NORMEY-RICO; CAMACHO, 2007). Since then several extensions have been proposed to improve robustness, disturbance rejection, and measurement noise attenuation characteristics of the SP (ASTROM *et al.*, 1994; MATAUSEK; MICIC, 1996; MATAUSEK; MICIC, 1999; RAO *et al.*, 2007; KAYA, 2003; RAO; CHIDAMBARAM, 2008; NORMEY-RICO; CAMACHO, 2008b; KIRTANIA; CHOUDHURY, 2012; DE OLIVEIRA *et al.*, 2017; SANZ *et al.*, 2018a; GARCÍA *et al.*, 2006; ALBERTOS; GARCÍA, 2009; GARCÍA; ALBERTOS, 2008; RAO; CHIDAMBARAM, 2005). However, a problem with the aforementioned works is that they are not concerned with actuator

saturation, which places a nonlinearity into the otherwise linear DTC structures, thus causing their effectiveness to drop. Such a condition is common in practical applications and can cause problems due to two reasons:

Problem 5.1

Slow and/or integral poles in the primary controller have been historically related to windup issues.

Problem 5.2

Differences between the controller output and the actual plant input can cause prediction errors; thus it is essential to include the saturation model to the control structure.

Some previous works have proposed different approaches to deal with saturating actuators in the control of time-delay systems with model-based controllers. An appropriate solution of the modified Smith predictor (MATAUSEK; MICIC, 1996; MATAUSEK; MICIC, 1999) with anti-windup was proposed in Matausek and Ribic (2012), although an optimization procedure is necessary to define some desired robustness and noise sensitivity constraints. In Huba (2013), a predictive disturbance observer-based filtered PI control for first-order plus dead-time (FOPDT) processes is presented. Recently, in Flesch *et al.* (2017) an anti-windup structure for the filtered SP (FSP) was proposed. Another alternative to deal with input constraints considers the use of model-based predictive controllers (MPCs) (CAMACHO; BORDONS, 2007; NORMEY-RICO; CAMACHO, 2007). However, in the MPC case, a constrained quadratic problem needs to be solved at each sampling time. Non-model-based approaches have also successfully been applied in the control of time-delay systems with actuator saturation. As an example, Fridman *et al.* (2003) deals with the regional stabilization problem by designing a constant state-feedback controller, while Tarbouriech *et al.* (2003) solves the problem of computing an anti-windup compensator in order to maximize the region of stability of the closed-loop system when a dynamic output feedback controller is supposed to have been previously designed.

Much of the modern approach for dealing with actuator saturation considers the design of anti-windup structures that are only activated during saturation of the control signal. In this manner, very often the goal of the design is to improve performance by forcing the closed-loop out of the nonlinear region so that the system response is preserved as close as possible to

the linear case. Some classical works containing well established anti-windup design techniques with this goal can be found in Turner and Postlethwaite (2004), Weston and Postlethwaite (2000), Turner *et al.* (2004), Gomes da Silva Jr. and Tarbouriech (2005).

The inclusion of the saturation model leads to a nonlinear approach to the control synthesis, so that, many works related to nonlinear control have dealt with windup issues (GALEANI *et al.*, 2007; TEEL; KAPOOR, 1997; MEGRETSKI, 1996; TEEL, 1996). More recently, the design of nonlinear anti-windup techniques that improve the performance of previously designed low-order and full-order anti-windup controllers have been searched, as in Turner and Kerr (2018). Despite many works dealing with anti-windup compensator design, and even the design of anti-windup compensators for systems with time delays (GOMES DA SILVA JR. *et al.*, 2006; TARBOURIECH *et al.*, 2004; TARBOURIECH; GOMES DA SILVA JR., 2000), relatively few papers treat the delay and the delay-free case in a simple and unified framework. Furthermore, many approaches do not consider, explicitly, practical issues such as tracking, robustness and disturbance rejection.

5.1.1 The simplified approach for the control of time-delay systems

In Torrico *et al.* (2013), simple tuning rules were proposed for the Filtered Smith Predictor (FSP) applied to the control of stable, integrative, and unstable first-order plus dead-time processes. The primary controller is free from integral action, differently from the traditional FSP, and ensures a good trade-off among disturbance rejection, robustness, and noise attenuation. In Torrico *et al.* (2016), the results obtained in Torrico *et al.* (2013) were extended to the case of multiple-delay SISO systems of any model order; this is referred to as the Simplified Dead-Time Compensator (SDTC), which was recently further explored in Torrico *et al.* (2018). Works above, however, do not consider the design for delay-free or input saturated systems.

5.1.2 Contribution

A gap has been noticed in the control field, whereby there does not appear to be a simple approach to design a linear controller for both the time-delay and delay-free case. This work addresses this by developing the SDTC for time-delay and delay-free SISO systems and, also, providing LMIs for the design of anti-windup compensation if saturating actuators are present; this was not explored in Torrico *et al.* (2016) or Torrico *et al.* (2018). To summarize, this chapter presents:

- A new methodology for linear controller design which deals directly with actuator saturation. The key feature of this scheme is that it employs a predictor-based structure that implements integral action implicitly, thereby avoiding integrator wind-up traditionally associated with actuator saturation.
- A unified framework which can be used to deal with the design of controllers for systems with actuator saturation, both with and without time-delays.
- By means of an analysis structure which decouples the system into linear and nonlinear loops, it is shown that stability of the nominal nonlinear loop neither depends on the delay (which is compensated by the conditioning scheme) nor the robustness filter.
- Such nice aspects allow for the design of the controller in a three-degree of freedom fashion, such that set-point tracking, disturbance rejection, and anti-windup compensation are independently tuned. Therefore, although the whole proposed controller structure (including the anti-windup filter) can be seen as one entity, the tuning is realized in three distinct phases. Furthermore, performance constraints related to the anti-windup compensator dynamics are included in the LMIs by using $\mathbb{D}$-stability regions. This is a new approach for including pre-specified dynamic requirements within the anti-windup design.

It is emphasized that the approach not only deals with the joint problems of time-delays and saturation but also considers disturbances, tracking, and robustness. This makes the approach proposed here quite practical and useful for the engineer.

Simulation results are used to analyze the tuning and establish a fair comparison with the anti-windup strategies presented in Flesch *et al.* (2017), Turner and Kerr (2018), Li *et al.* (2016), Zhang and Jiang (2008). Also, a constrained model predictive controller (MPC) is considered where constraints are set to deal with the saturating issue. Furthermore, an experiment was performed for temperature control in a neonatal intensive care unit.

5.2 Preliminaries

Consider a discrete-time LTI system $P(z)$ described by the following equations

$$P(z) \sim \begin{cases} x_p(k+1) = \mathrm{A}x_p(k) + \mathrm{B}[u(k-d) + w(k-d)], \\ y(k) = \mathrm{C}x_p(k) + \mathrm{D}[u(k-d) + w(k-d)] + n(k), \end{cases} \tag{5.1}$$

where $x_p(k) \in \mathbb{R}^n$ is the state vector, $u(k) \in \mathbb{R}$ is the actual plant input, $y(k) \in \mathbb{R}$ is the measured output, $w(k)$ is a matched input disturbance, and $n(k)$ is due to measurement noise, respectively. Matrices $\mathrm{A} \in \mathbb{R}^{n\times n}$, $\mathrm{B} \in \mathbb{R}^n$, $\mathrm{C}^\top \in \mathbb{R}^n$, $\mathrm{D} \in \mathbb{R}$, and delay $d \geq 0$ are all constant and known. Following assumptions are taken:

Assumption 5.1

The pair (A, B) is controllable.

Assumption 5.2

The unknown disturbance signal is bounded by $|w(k)| < D_w$, and is locally integrable.

Assumption 5.3

The process input, $u(k)$, is given by $u(k) = sat(v(k))$, where $v(k)$ is the computed control action and the saturation function is defined as

$$sat(v(k)) = sign(v(k)) \times min\{|v(k)|, \bar{u}\}, \bar{u} > 0, \tag{5.2}$$

where $\bar{u}$ denotes the control amplitude bound.

This work makes use of some critical conditions which are necessary for anti-windup synthesis with guaranteed regions of stability. Therefore, they are briefly reviewed as follows.

5.2.1 Sector Condition

For this chapter, consider the deadzone operator $\varphi(\cdot)$ defined in (2.11) and the classical sector condition from Equation (2.15). Also consider the associated set given by

$$\mathscr{L}(v, \bar{u}) = \{v \in \mathbb{R}; -\eta\bar{u} \leq v \leq \eta\bar{u}\}, \tag{5.3}$$

where $\eta = \dfrac{1}{1-\Lambda}$, $0 \leq \Lambda < 1 \ \in \mathbb{R}$.

5.2.2 Quadratic Lyapunov Function

Consider the discrete-time system

$$x(k+1) = f(x(k)) \tag{5.4}$$

where $f(x(k)) = \mathrm{A}x(k) + \mathrm{B}\varphi(v(k))$, $v(k) = \mathrm{K}x(k)$. Then, making use of the sector condition, the origin of the above system is locally asymptotically stable if there exists a positive definite function $\mathrm{V}(x(k))$ such that

$$\Delta\bar{\mathrm{V}}(x(k)) := \mathrm{V}(x(k+1)) - \mathrm{V}(x(k)) - 2\varphi(v)^\top \mathrm{W}[\varphi(v) - \Lambda v] < 0, \forall x(k) \in \mathscr{L}(\mathrm{K}x(k), \bar{u}),$$

where $\mathscr{L}(\mathrm{K}x(k), \bar{u})$ is a region of the state space obtained from application of the sector condition. Furthermore, if $\mathscr{L}(\mathrm{K}x(k), \bar{u})$ is the whole state-space, the system is globally asymptotically stable.

In this chapter, we chose to use the quadratic Lyapunov function

$$\mathrm{V}(x(k)) = x^\top(k)\mathrm{Q}x(k),$$

where $\mathrm{Q} = \mathrm{Q}^\top$ is a positive definite matrix. Furthermore, the ellipsoid $\varepsilon(\mathrm{Q}, 1) = \{x \in \mathbb{R}^n; x^\top \mathrm{Q}x \leq 1\}$ is a region of asymptotic stability (RAS) of (5.4) if the following restriction is satisfied

$$x^\top \mathrm{K}^\top \mathrm{K}x \leq x^\top \mathrm{Q}x\eta^2\bar{u}^2,$$

which ensures inclusion of $\varepsilon(\mathrm{Q}, 1)$ in the set $\mathscr{L}(\mathrm{K}x(k), \bar{u})$.

5.2.3 $\mathcal{L}_2$ gain

One import measure of performance of anti-windup strategies in saturated systems is the so-called $\mathcal{L}_2$ gain. A nonlinear system with input $\psi(k)$ and output $\Omega(k)$ has an induced $\mathcal{L}_2$ gain of γ when

$$\forall \psi \in l_2, \ \|\Omega\| < \gamma\|\psi\| + \theta \tag{5.5}$$

where $\|\psi(k)\|$ denotes $\sqrt{\sum_{k=0}^{\infty} \left(\psi(k)^\top \psi(k)\right)}$, and θ is a positive constant. Moreover, whenever the vector valued function $\psi(k)$ obeys $\|\psi(k)\| < \infty$, we say that $\psi \in l_2$. The $\mathcal{L}_2$ gain, defined in equation (5.5), represents a bound on the root mean square energy gain of a nonlinear system. The following condition is sufficient to ensure $\mathcal{L}_2$ gain less than γ from an input ψ to an output Ω (while also holding stability guarantees)

$$\Delta\mathrm{V}(x(k)) + \Omega^\top\Omega - \gamma^2\psi^\top\psi - 2\varphi(v)^\top \mathrm{W}[\varphi(v) - \Lambda v] < 0, \tag{5.6}$$

which is a combination of the quadratic Lyapunov functional from Subsection 5.2.2, the classical sector condition (2.15), and the term $\Omega^\top\Omega - \gamma^2\psi^\top\psi$ which is used to ensure a level of $\mathcal{L}_2$

performance. Note that since the sector condition guarantees $-2\varphi(v)^\top \mathrm{W}[\varphi(v) - \Lambda v] > 0$, equation (5.6) implies that

$$\Delta \mathrm{V}(x(k)) + \Omega^\top \Omega - \gamma^2 \psi^\top \psi < 0 \tag{5.7}$$

also holds for a Lyapunov function $\mathrm{V}(x(k))$ and for all $x(k)$ in the set resulting from the application of a sector condition. Then, by computing

$$\sum_{j=0}^{\infty} \Big(\Delta \mathrm{V}(x(j)) + \Omega(j)^\top \Omega(j) - \gamma^2 \psi(j)^\top \psi(j) \Big) < 0, \tag{5.8}$$

it follows that

$$\mathrm{V}(x(\infty)) - \mathrm{V}(x(0)) + \sum_{j=0}^{\infty} \Big(\Omega(j)^\top \Omega(j) \Big) - \gamma^2 \sum_{j=0}^{\infty} \Big(\psi(j)^\top \psi(j) \Big) < 0, \tag{5.9}$$

which, by taking square roots and using the facts that $\sqrt{a^2+b^2} \leq a+b$ for $a,b \in \mathbb{R}^+$, and $\mathrm{V}(x) > 0$, leads to

$$\|\Omega\| < \gamma \|\psi\| + \sqrt{\mathrm{V}(x(0))} \tag{5.10}$$

for all initial conditions $x(0)$ inside the stability set. The reader is referred to the work in Herrmann *et al.* (2006) to see other details regarding the explanation of condition (5.6).

5.2.4 $\mathbb{D}$*-Stability*

Although the previously presented conditions are sufficient to provide performance and stability analysis conditions, it might be desired to include some dynamical information to the anti-windup design. This is done in this work by using the concept of $\mathbb{D}$-stability regions. So let us borrow the following definition from Duan and Yu (2013).

Definition 5.1

Let $\mathbb{D}$ be a domain on the complex plane, which is symmetric about the real axis. Then, a matrix $\mathrm{A} \in \mathbb{R}^{n \times n}$ is said to be $\mathbb{D}$-stable if

$$\lambda_i \in \mathbb{D}, \;\; i = 1, 2 \ldots n, \text{ where } \lambda_i \text{ are the } n \text{ eigenvalues of A.}$$

In this work, the following particular case of $\mathbb{D}$-stability is employed

$$\mathbb{D} = \mathbb{H}_{\zeta_a, \zeta_b} = \{ \lambda = \sigma + j\omega \mid \zeta_b < \sigma < \zeta_a \}, \tag{5.11}$$

such that the following proposition holds (see Duan and Yu (2013) for the proof).

Proposition 5.1

The matrix $\mathrm{A} \in \mathbb{R}^{n\times n}$ is $\mathbb{H}_{\zeta_a,\zeta_b}$-stable if and only if there exists a positive definite matrix $\mathrm{Q} = \mathrm{Q}^\top$ such that

$$\begin{cases} \mathrm{A}^\top\mathrm{Q} + \mathrm{Q}\mathrm{A} - 2\zeta_a\mathrm{Q} < 0, \\ \mathrm{A}^\top\mathrm{Q} + \mathrm{Q}\mathrm{A} - 2\zeta_b\mathrm{Q} > 0. \end{cases} \tag{5.12}$$

5.3 Unified anti-windup controller

The proposed unified anti-windup SDTC (AW-SDTC) control structure to deal with both time-delayed and delay-free SISO systems with saturating actuators is depicted in Fig. 11, where $P_n(z) = G_n(z)z^{-d_n}$ is the nominal process, with $G_n(z)$ and d_n being the fast model and nominal dead time, respectively. Plant $P(z) = G(z)z^{-d}$ is the model of the real process. Additive uncertainty enters the system such that $P(z) = P_n(z) + \Delta P(z)$. $M(z)$ is the anti-windup conditioning filter, while $F_r(z)$ and $S(z)$ are calculated to improve set-point tracking, disturbance rejection and robustness properties of the controller.

Figure 11 – Proposed unified anti-windup scheme.

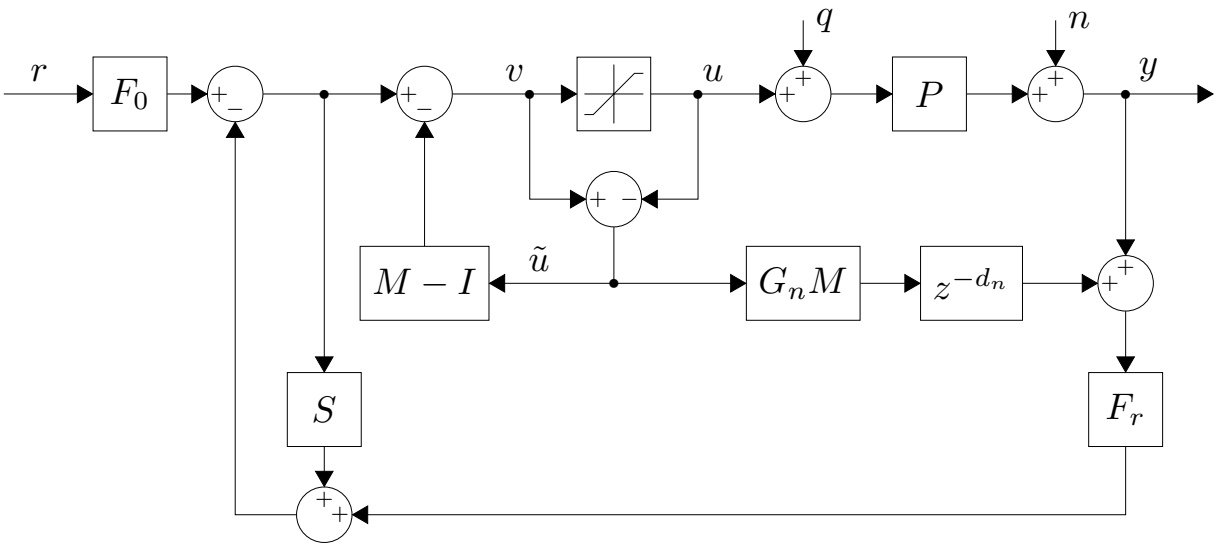

Source: The author.

By using the deadzone nonlinearity identity (2.11), the AW-SDTC scheme in Fig. 11 is redrawn in a equivalent form depicted by Fig. 12. The equivalency between the two structures is valid if and only if

$$S(z) = F_1(z) + G_n(z)(F_2(z) - F_r(z)z^{-d_n}) \text{ and } H(z) = \left[1 + F_1(z) + G_n(z)F_2(z)\right]^{-1}. \tag{5.13}$$

Figure 12 – Mismatch equivalent structure for analysis.

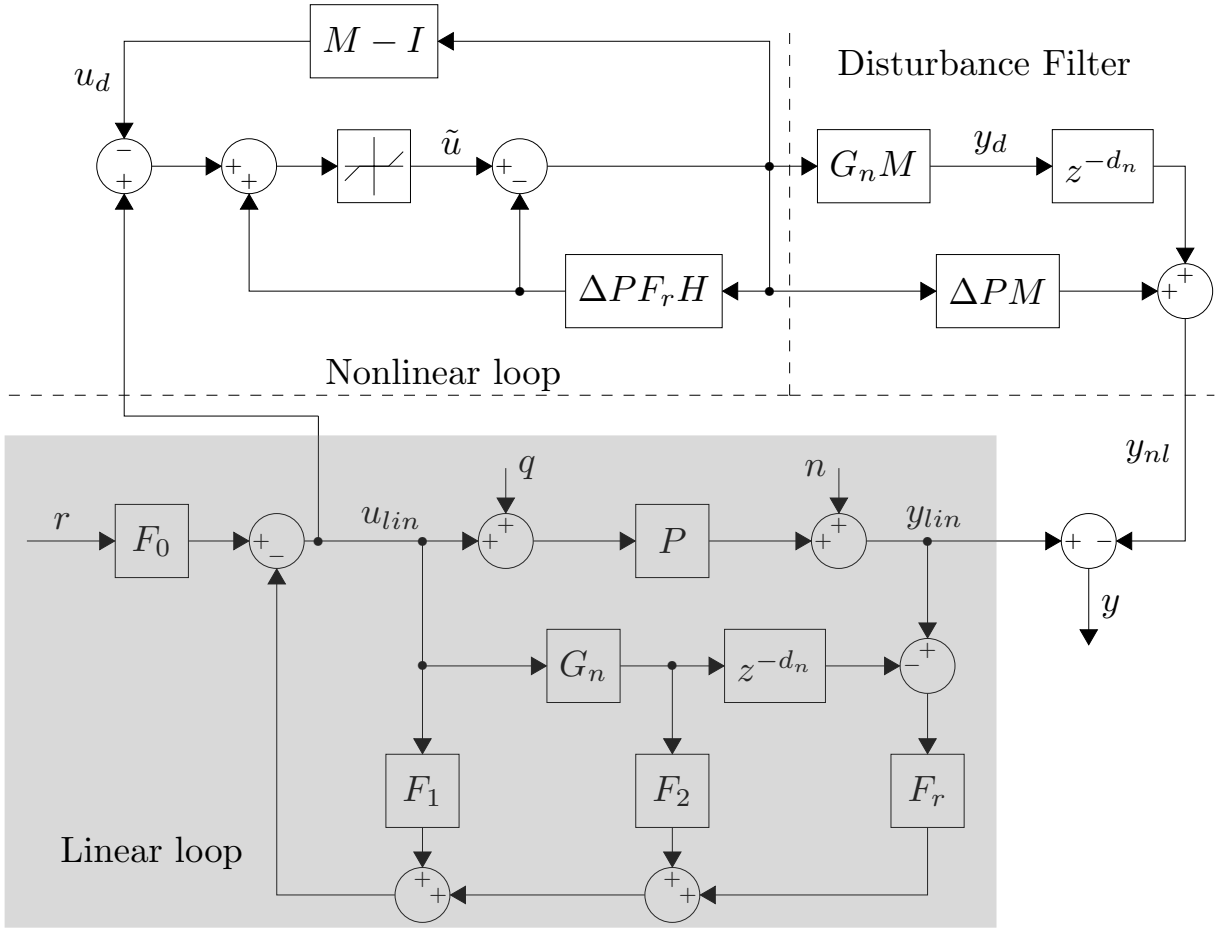

Source: The author.

From Fig. 12 note that the system is conveniently divided into three parts, namely the linear loop, the nonlinear loop and the disturbance filter, with output given by $y(k) = y_{lin}(k) - y_{nl}(k)$. This kind of decoupled structure is widely used for design and analysis of closed-loop systems under input saturation (see Turner and Postlethwaite (2007) and Turner *et al.* (2007) for instance). Some of the aspects which make this structure attractive for the work herein are described as follows.

First, note that the linear loop determines the system behavior in the absence of control saturation. This allow us to design the system to obtain a desired response in the nominal case, i.e. $P_n(z) = P(z)$ and $u(k) = v(k)$. For this, the linear loop is tuned in a two-degree of freedom fashion, where $F_1(z)$ and $F_2(z)$ can be used to achieve a desired set-point tracking response, whilst $F_r(z)$ can be adjusted to deal with disturbance rejection, robustness and noise attenuation characteristics of the proposed controller. Note that the structure of the linear loop exactly matches that of the linear SDTC presented in Chapter 4.

On the other hand, note that both the disturbance filter and the nonlinear loop depend on the anti-windup conditioning filter $M(z)$. Also recall that when saturation events end, the output of the dead-zone nonlinearity $\tilde{u}(k)$ becomes null. Nevertheless, possible windup effects caused by the saturation are not instantaneously over, as the states of the disturbance filter are not instantaneously null. Therefore, the disturbance filter is responsible for determining both speed and manner of recovery of the closed-loop system after saturation ceases. On what concerns stability, by considering that the linear loop is stable (which obviously should be by proper design of $F_1(z)$, $F_2(z)$ and $F_r(z)$), the stability of the proposed structure depends solely on the stability of the nonlinear loop. Thereby, it is evident that the design of the conditioning filter $M(z)$ should tackle both performance and stability issues of the system under saturation.

5.3.1 Tuning of the linear loop

The input-output transfer functions for the unsaturated nominal case ($P_n(z) = P(z)$ and $u(k) = v(k)$) are given by

$$H_{ry}(z) = \frac{Y(z)}{R(z)} = P_n(z)H(z)F_0, \tag{5.14}$$

$$H_{qy}(z) = \frac{Y(z)}{Q(z)} = P_n(z)T_d(z), \tag{5.15}$$

$$H_{nu}(z) = \frac{U(z)}{N(z)} = -P_n(z)H(z)F_r(z), \tag{5.16}$$

where $T_d(z) = \big(1 - F_r(z)P_n(z)H(z)\big)$; $U(z)$, $Y(z)$, $R(z)$, $N(z)$ and $Q(z)$ refer to the Z-transform of the linear control action $u_{lin}(k)$, process linear output $y_{lin}(k)$, reference $r(k)$, measurement noise $n(k)$, and input load disturbance $q(k)$, respectively, and $H(z)$ has been defined in (5.13).

For this situation, robust stability of the linear loop is achieved if the condition

$$I_{\mathrm{r}}(\omega) = \left| \big(P_n(z)H(z)F_r(z)\big)^{-1} \right|_{z=e^{j\omega T_s}} > |\delta P(z)|_{z=e^{j\omega T_s}}, \tag{5.17}$$

is satisfied, where T_s is the sampling time, $0 < \omega < \pi/T_s$, $\delta P(z)$ is the multiplicative uncertainty, and $I_r(w)$ is defined as the robustness index, as explained in the previous chapter. The multiplicative uncertainty enters the system such that $P(z) = P_n(z) + \Delta P(z) = P_n(z)[1 + \delta P(z)]$.

It is important to highlight from equations (5.14) to (5.17) that F_0, $F_1(z)$ and $F_2(z)$ can be tuned in order to obtain a desired set-point tracking, while the filter $F_r(z)$ is set to obtain a desired trade-off between disturbance rejection and robustness.

5.3.1.1 Set-point tracking

Tuning rules for the primary controller, defined by F_0, $F_1(z)$, and $F_2(z)$ are established in this subsection. For this, consider feedback FIR filters $F_1(z)$ and $F_2(z)$ as

$$F_1(z) = \sum_{i=0}^{n-1} f_{1_i} z^{-i}, \quad F_2(z) = \sum_{i=0}^{n-1} f_{2_i} z^{-i} \tag{5.18}$$

where n is the order of the fast model $G_n(z)$. Coefficients of $F_1(z)$ and $F_2(z)$ are obtained through standard pole placement design procedure in order to reach a desired set-point tracking response (5.14). Notice that in this strategy, FIR filter $F_1(z)$ has the additional term f_{1_0} when compared with the SDTC strategy from the previous chapter. This allows to compute pole placement for delay-free systems with instantaneous response. For this, one must solve an equation of the type $\Gamma c = o$, with

$$\Gamma = \begin{bmatrix} 1 & 0 & \dots & 0 & b_0 & 0 & \dots & 0 \\ a_1 & 1 & & \vdots & b_1 & b_0 & & \vdots \\ \vdots & a_1 & & 0 & \vdots & b_1 & & 0 \\ a_n & \vdots & & 1 & b_n & \vdots & & b_0 \\ 0 & a_n & & a_1 & 0 & b_n & & b_1 \\ \vdots & 0 & & a_2 & \vdots & 0 & & b_2 \\ 0 & \vdots & & \vdots & 0 & \vdots & & \vdots \\ \underbrace{0 \quad 0 \quad a_n}_{n} & & & & \underbrace{0 \quad 0 \quad b_n}_{n} & & & \end{bmatrix}, c = \begin{bmatrix} f_{1_0} \\ \vdots \\ f_{1_{n-1}} \\ f_{2_0} \\ \vdots \\ f_{2_{n-1}} \end{bmatrix}, o = \begin{bmatrix} 0 \\ s_1 - a_1 \\ \vdots \\ s_n - a_n \\ s_{n+1} \\ \vdots \\ s_{2n-1} \end{bmatrix}, \tag{5.19}$$

where Γ is a non-singular $2n$ square matrix, $a_1 \dots a_n$ and $b_0 \dots b_n$ are the coefficients of the delay-free model

$$G_n(z) = \frac{b_0 + b_1 z^{-1} + b_2 z^{-2} \dots b_n z^{-n}}{1 + a_1 z^{-1} + a_2 z^{-2} \dots a_n z^{-n}}, \tag{5.20}$$

and $s_1 \dots s_{2n-1}$ are the coefficients of the desired characteristic polynomial

$$1 + s_1 z^{-1} + s_2 z^{-2} + \dots + s_{2n-1} z^{-2n+1} = (1 - \alpha_1 z^{-1})(1 - \alpha_2 z^{-1}) \dots (1 - \alpha_{2n-1} z^{-1}). \tag{5.21}$$

Therefore, closed-loop poles $\alpha = [\alpha_1 \dots \alpha_{2n-1}]$, with $0 \leq |\alpha_i| < 1$, are the set-point tracking tuning parameter. For example, if faster set-point is desired, then smaller values of α_i can be chosen, and *vice-versa*. The static gain F_0 is then computed to yield zero steady-state error, that is $F_0 = P_n^{-1}(z) H^{-1}(z)\Big|_{z=1}$.

5.3.1.2 *Disturbance rejection and robustness*

Robustness filter $F_r(z)$ is tuned aiming: (i) to reject step-like disturbances applied in the control signal; (ii) to eliminate the modes of the plant model $P_n(z)$ from the disturbance rejection $H_{qy}(z)$ response; (iii) to obtain a desired trade-off between robustness and disturbance rejection. Such goals can be met by applying the filter (4.17), where $0 < |\rho| < 1$ is the filter tuning parameter.

5.3.2 *Tuning of the nonlinear loop and the disturbance filter*

Previous works have shown that most conditioning schemes for systems with actuator saturation can be interpreted as different choices of conditioning filter $M(z)$ (WESTON; POSTLETHWAITE, 2000). For the proposed structure, such filter is defined as

$$M(z) = \frac{D_g(z)}{(1-\nu_1 z^{-1})(1-\nu_2 z^{-1})\dots(1-\nu_n z^{-1})}, \tag{5.22}$$

with $G_n(z) = N_g(z)/D_g(z)$. Note that the zeros of $M(z)$ are equal to the poles of the process model while the ν_i poles of $M(z)$ can be defined in order to meet certain criteria. Such choice yield some interesting characteristics for the strategy in this work. The equivalent disturbance filter is given by

$$G_n(z)M(z) = \frac{N_g(z)}{(1-\nu_1 z^{-1})(1-\nu_2 z^{-1})\dots(1-\nu_n z^{-1})},$$

so that the poles of $G_n(z)$ are canceled by the numerator of $M(z)$; therefore the disturbance filter is always stable with user-defined poles ν_i. On the other hand, poles ν_i define system recover manner after saturation while also playing a role on the stability of the nonlinear loop. Then, it is clear that there exists a trade-off between performance and stability of the saturated system. For $|\nu_i| \to 0$, the system should present faster recover from saturation events. On the other hand, for poles $|\nu_i| \to 1$ the nonlinear loop region of stability should increase.

From Fig. 12, note that due to uncertainties in the system, the filter $F_r(z)$ plays some influence in both the linear and the nonlinear loops. Even though this is true, notice that the linear and nonlinear loops are decoupled, i.e., their responses are not feedbacked to each other. Furthermore, since robustness filter $F_r(z)$ is previously designed to deal with uncertainty and yield robustness characteristics of the linear loop, the design of the anti-windup conditioning filter $M(z)$ is done considering the nominal system behavior, i.e., $\Delta P(z) = 0$.

5.3.2.1 Anti-windup synthesis

Works using the mismatch equivalent representation (Fig. 12) often consider that the goal of the anti-windup design is to maintain the response of the system as close as possible to the response of the linear system, that is, the response of the system had saturation not been present. Moreover, previous studies have proven that global stability of the closed-loop in the presence of actuator saturation cannot be achieved by a bounded input in the case of unstable processes (SONTAG, 1984; LASSERRE, 1993). Therefore, another common goal in anti-windup design is to seek a compensator which enlarges the region of attraction of the closed-loop system.

Consider the analysis structure in Fig. 12. As previously explained, all the poles of the disturbance filter should be within the unit circle, therefore considering that the linear loop is stable through robust condition (5.17), stability under actuator saturation depends only upon the stability of the nonlinear loop. Therefore, the goal of the proposed strategy is to design $M(z)$ such that there are guaranteed regions of stability while also keeping desired output performance. In this work, the first goal is met by using classical Lyapunov theorem along with the classical sector condition, while performance characteristics are introduced employing $\mathbb{D}$-stability conditions (5.12), which allow the designer to allocate the poles of $M(z)$ within a desired region.

Herein, anti-windup design for both the regional and global stability cases is established using LMIs, which are suitable to assure stability conditions for stable, integrative and unstable open loop plants. Consider the state-space realization of the process fast model $G_n(z)$, given by matrices $\mathrm{A}, \mathrm{B}, \mathrm{C}$, D. The state-space equivalent representation of $M(z)$ in (5.22) is given as

$$M(z) \sim \left[\begin{array}{c|c} \mathrm{A}+\mathrm{BK} & \mathrm{B} \\ \hline \mathrm{K} & \mathrm{I} \end{array}\right] \tag{5.23}$$

where the v_i poles of the conditioning filter $M(z)$ are equal to the eigenvalues of $\mathrm{A}+\mathrm{BK}$. Therefore, computation of $M(z)$ is accomplished by finding a suitable matrix $\mathrm{K} \in \mathbb{R}^{1\times n}$ which attends to pre-specified stability and performance design requirements. Since $M(z)-I$ is always strictly proper, no direct feedthrough exists from $\tilde{u}(k)$ to $u_d(k)$, thus the system is well conditioned.

In order to find the gain K, consider the mapping $\tau_{pn} : u_{lin} \to y_d$ defined as

$$\tau_{pn} \triangleq \begin{cases} x(k+1) = (\mathrm{A}+\mathrm{BK})x(k) + \mathrm{B}\tilde{u}(k), \\ y_d(k) = (\mathrm{C}+\mathrm{DK})x(k) + \mathrm{D}\tilde{u}(k), \\ u_d(k) = \mathrm{K}x(k), \\ \tilde{u}(k) = \varphi(u_{lin}(k) - u_d(k)) \end{cases}, \tag{5.24}$$

It is important to highlight that this mapping is defined for the nominal case, i.e. $\Delta P(z) = 0$ in Fig. 12. Therefore, although the presence of delays indeed influence the closed-loop behavior in the uncertain case, they do not affect the anti-windup design. The following theorem establish conditions to find the anti-windup conditioning filter $M(z)$ with guaranteed regions of stability.

Theorem 5.1

There exists an anti-windup conditioning filter $M(z)$ if there exist matrices X in $\mathbb{S}_n^+$, J in $\mathbb{S}_1^+$, L in $\mathbb{R}^{1\times n}$, and scalar $\gamma > 0$ such that LMIs

$$\begin{bmatrix} -\mathrm{X} & -\mathrm{L}^\top\Lambda & 0 & \mathrm{XC}^\top + \mathrm{L}^\top\mathrm{D} & \mathrm{XA}^\top + \mathrm{L}^\top\mathrm{B}^\top \\ \star & -2\mathrm{J} & \Lambda & \mathrm{JD}^\top & \mathrm{JB}^\top \\ \star & \star & -\gamma\mathrm{I} & 0 & 0 \\ \star & \star & \star & -\gamma\mathrm{I} & 0 \\ \star & \star & \star & \star & -\mathrm{X} \end{bmatrix} \prec 0, \tag{5.25}$$

and

$$\begin{bmatrix} \mathrm{X} & \mathrm{L}^\top \\ \star & \eta^2\bar{u}^2 \end{bmatrix} \succeq 0, \tag{5.26}$$

are feasible for given $\eta = 1/(1-\Lambda)$. Additionally, the poles of the conditioning filter $M(z)$ will be within a $\mathbb{H}_{\zeta_a,\zeta_b}$-region in the unit circle (see Fig. 13) if following LMIs hold along with (5.25) and (5.26)

$$\begin{cases} \mathrm{XA}^\top + \mathrm{L}^\top\mathrm{B}^\top + \mathrm{AX} + \mathrm{BL} - 2\zeta_a\mathrm{X} \prec 0, \\ \mathrm{XA}^\top + \mathrm{L}^\top\mathrm{B}^\top + \mathrm{AX} + \mathrm{BL} - 2\zeta_b\mathrm{X} \succ 0, \end{cases} \tag{5.27}$$

where ζ_a, ζ_b are scalars to be chosen. Then, a suitable K achieving finite $\mathcal{L}_2$ gain γ of the τ_{pn} operator is given by $\mathrm{K} = \mathrm{LX}$. Moreover, the ellipsoid $\varepsilon(\mathrm{Q},1) = \{x \in \mathbb{R}^n; x^\top\mathrm{Q}x \leq 1\}$, with $\mathrm{Q} = \mathrm{X}^{-1}$, is a region of asymptotic stability (RAS) of the nonlinear loop in Fig. 12.

Figure 13 – $\mathbb{H}_{\zeta_a,\zeta_b}$-region inside unit circle on the complex plane.

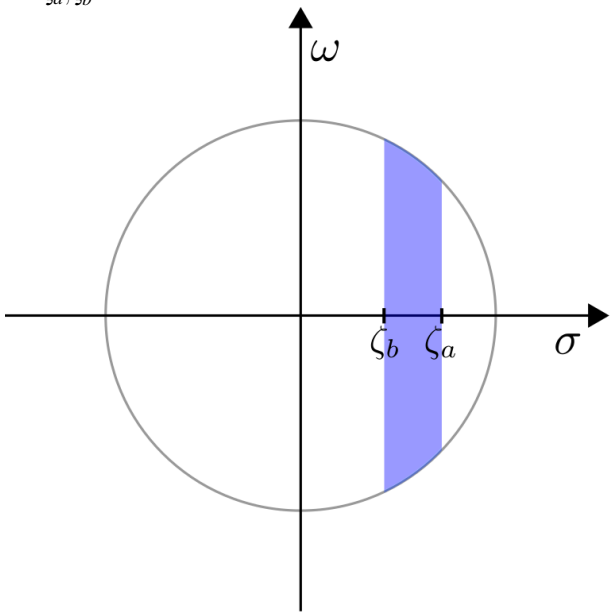

Source: The author.

Proof. Using the previously defined Lyapunov functional, sector condition, and $\mathcal{L}_2$ gain, a sufficient condition for stability of τ_{pn} is written as (TURNER; POSTLETHWAITE, 2007)

$$\Delta V(x(k)) + {y_d}^\top y_d - \gamma^2 {u_{lin}}^\top u_{lin} - 2\tilde{u}^\top W[\tilde{u} - \Lambda(u_{lin} - u_d)] < 0. \tag{5.28}$$

Then, by defining $\lambda = \begin{bmatrix} x^\top & \tilde{u}^\top & {u_{lin}}^\top \end{bmatrix}^\top$, we can write inequality (5.28) in an equivalent quadratic form given by (5.29), where $\Upsilon_{11} = (A+BK)^\top Q(A+BK) - Q + (C+DK)^\top (C+DK)$ and $\Upsilon_{12} = (A+BK)^\top QB + (C+DK)^\top D - K^\top \Lambda W$.

$$\lambda^\top \begin{bmatrix} \Upsilon_{11} & \Upsilon_{12} & 0 \\ \star & B^\top QB - 2W & W\Lambda \\ \star & \star & -\gamma^2 I \end{bmatrix} \lambda < 0. \tag{5.29}$$

By applying Schur complement twice to the matrix in (5.29), one obtains

$$\begin{bmatrix} -Q & -K^\top \Lambda W & 0 & C^\top + K^\top D^\top & A^\top + K^\top B^\top \\ \star & -2W & W\Lambda & D^\top & B^\top \\ \star & \star & -\gamma I & 0 & 0 \\ \star & \star & \star & -\gamma I & 0 \\ \star & \star & \star & \star & -Q^{-1} \end{bmatrix} \prec 0. \tag{5.30}$$

Next, by using $\mathrm{diag}(\mathrm{Q}^{-1},\mathrm{W}^{-1},\mathrm{I},\mathrm{I},\mathrm{I})$ to apply a congruence transformation with (5.30), the following matrix inequality is obtained

$$\begin{bmatrix} -\mathrm{Q}^{-1} & -\mathrm{Q}^{-1}\mathrm{K}^{\top}\Lambda & 0 & \mathrm{Q}^{-1}(\mathrm{C}^{\top}+\mathrm{K}^{\top}\mathrm{D}^{\top}) & \mathrm{Q}^{-1}(\mathrm{A}^{\top}+\mathrm{K}^{\top}\mathrm{B}^{\top}) \\ \star & -2\mathrm{W}^{-1} & \Lambda & \mathrm{W}^{-1}\mathrm{D}^{\top} & \mathrm{W}^{-1}\mathrm{B}^{\top} \\ \star & \star & -\gamma\mathrm{I} & 0 & 0 \\ \star & \star & \star & -\gamma\mathrm{I} & 0 \\ \star & \star & \star & \star & -\mathrm{Q}^{-1} \end{bmatrix} \prec 0. \tag{5.31}$$

Finally, by defining new variables $\mathrm{X}=\mathrm{Q}^{-1}$, $\mathrm{J}=\mathrm{W}^{-1}$, and by making the change of variables $\mathrm{L}=\mathrm{K}\mathrm{Q}^{-1}$, LMI (5.25) is obtained, with $\mathrm{X}\succ 0$, $\mathrm{J}\succ 0$ and $\gamma>0$. In order to ensure that $\varphi(\cdot)$ is within the sector $[0,\Lambda]$, when $u_{lin}=0$, it is necessary that

$$|u_d| = |\mathrm{K}x| \leq \eta^2\bar{u}^2. \tag{5.32}$$

Then, LMI (5.26) is used in order to guarantee that the ellipsoidal set $\varepsilon=\{x\in\mathbb{R}^n : x\mathrm{Q}x\leq 1\}$ is an estimation on the region of attraction of the nonlinear loop (5.24). This holds if

$$x^{\top}\mathrm{K}^{\top}\mathrm{K}x \leq x^{\top}\mathrm{Q}x\eta^2\bar{u}^2, \tag{5.33}$$

which is equivalent to

$$\begin{bmatrix} \mathrm{Q} & \mathrm{K}^{\top} \\ \star & \eta^2\bar{u}^2 \end{bmatrix} \succeq 0. \tag{5.34}$$

LMI (5.26) is then obtained by applying a congruence transformation to (5.34) using $\mathrm{diag}(\mathrm{Q}^{-1},\mathrm{I})$. Consider now equations (5.12). In order to obtain (5.27), replace A by $\mathrm{A}+\mathrm{BK}$, apply congruence transformation with Q^{-1} and make $\mathrm{X}=\mathrm{Q}^{-1}$, $\mathrm{L}=\mathrm{K}\mathrm{Q}^{-1}$. This completes the proof. □

Additionally, for the case of stable processes, it is useful to establish the following corollary.

Corollary 5.1

The origin is globally asymptotically stable for the nominal ($P_n(z) = P(z)$) closed-loop system in Fig. 11 if there exist matrices X in $\mathbb{S}_n^+$, J in $\mathbb{S}_1^+$ such that LMI

$$\begin{bmatrix} -\mathrm{X} & -\mathrm{L}^\top & 0 & \mathrm{XC}^\top + \mathrm{L}^\top \mathrm{D} & \mathrm{XA}^\top + \mathrm{L}^\top \mathrm{B}^\top \\ \star & -2\mathrm{J} & \mathrm{I} & \mathrm{JD}^\top & \mathrm{JB}^\top \\ \star & \star & -\gamma \mathrm{I} & 0 & 0 \\ \star & \star & \star & -\gamma \mathrm{I} & 0 \\ \star & \star & \star & \star & -\mathrm{X} \end{bmatrix} \prec 0 \tag{5.35}$$

is feasible. Furthermore, the poles of the conditioning filter $M(z)$ will be contained within a $\mathbb{H}_{\zeta_a,\zeta_b}$-region in the unit circle (see Fig. 13) if (5.35) holds along with (5.27). Then, a suitable K gain is given by $\mathrm{K} = \mathrm{LX}$.

Proof. Proof of corollary 5.1 is straightforward. In the global stability case it suffices to replace Λ by I in the classical sector condition, then (5.25) becomes (5.35). □

5.4 Simulation results

Some works dealing with the saturating issue point out that although it is possible to achieve global stability for open-loop stable systems, the local stability relaxation can often be preferred in order to obtain improved local performance (see Turner and Postlethwaite (2007), for instance). Furthermore, systems usually operate within a desired region of the space, so that the local assumption can often be enough. Therefore, the local approach was preferred for all the examples in this section, even the open-loop stable ones.

5.4.1 Delay-free examples

This subsection presents simulation results for systems without time-delay recently presented in Turner and Kerr (2018) and Li *et al.* (2016).

5.4.1.1 Example 1 - Comparison with nonlinear anti-windup

Consider the example recently used in Turner and Kerr (2018) to illustrate a nonlinear anti-windup technique where the plant is a third-order SISO system with input constraint given

Figure 14 – Simulation results for example 1.

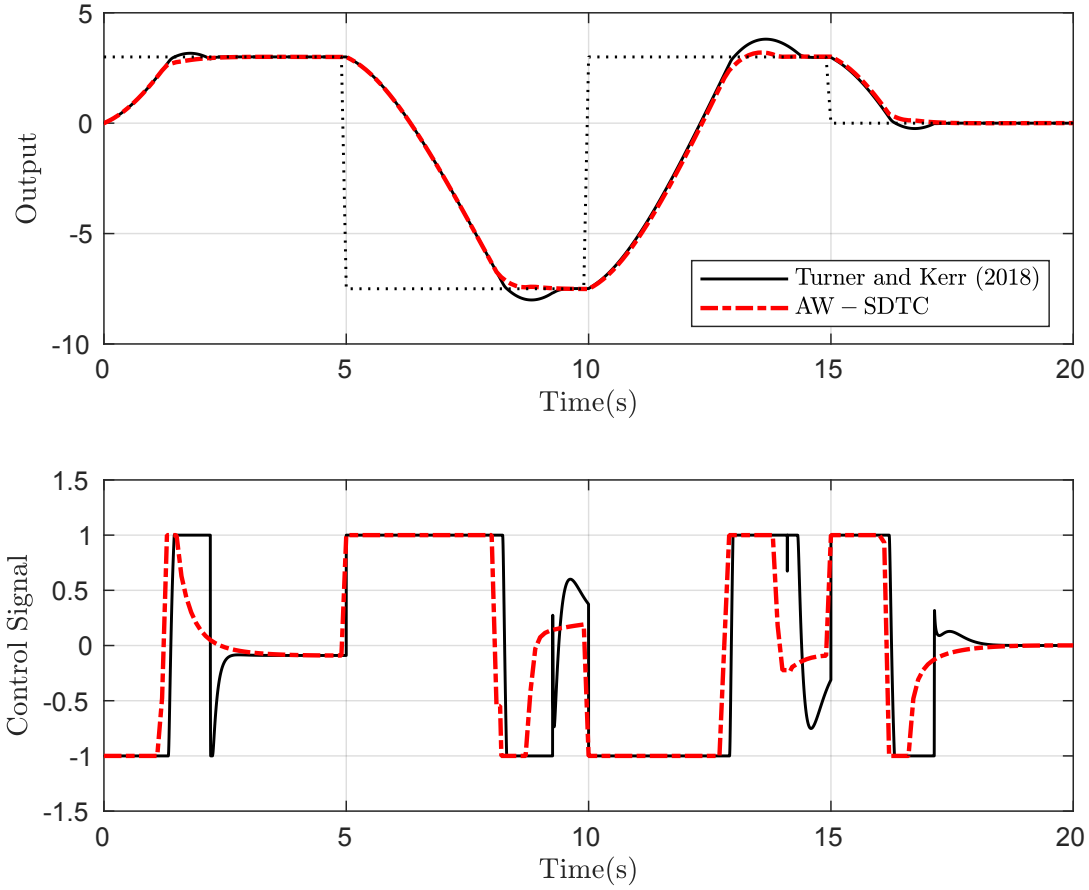

Source: The author.

by $\overline{u} = 1$. By using a zero-order hold and sampling time of $T = 0.1s$ the following discrete-time transfer-function model is obtained:

$$P(z) = \frac{-0.1045z^{-1} + 0.1216z^{-2} - 0.03547z^{-3}}{1 - 2.309z^{-1} + 1.656z^{-2} - 0.3465z^{-3}}.$$

The AW-SDTC was initially tuned to obtain set tracking response similar with the compared controller leading to $\alpha = \begin{bmatrix} 0.8 & 0.3 & 0 & 0 & 0 \end{bmatrix}$ and $\rho = 0.9$. Then, for the tuning of the anti-windup conditioning filter $M(z)$, Theorem 5.1 was used with $\Lambda = 0.855$, $\zeta_b = 0$ and $\zeta_a = 1$, yielding $\nu = \begin{bmatrix} 0.777 & 0.384 & 0.096 \end{bmatrix}$ and $\gamma = 87.3443$.

Fig. 14 shows output and control signals for a sequence of steps in the reference. From the output graph, one may notice that the AW-SDTC controller does not exhibit overshoots and undershoots while the nonlinear controller from Turner and Kerr (2018) does. Hence, settling time is much smaller for the proposed controller herein. It is important to highlight that the control signal of the AW-SDTC does not present high-frequency ripples as the controller from Turner and Kerr (2018), thus being better behaved. Furthermore, it is evident that the AW-SDTC controller recovers faster from saturation events while presenting better output results. This

behavior will be shown to exist in all further simulation examples. It should be highlighted that the better behavior of the approach herein comes with the cost of providing regional stability only, whereas the approach from Turner and Kerr (2018) guarantees global stability. This illustrates the trade-off between local stability relaxation and performance that was mentioned in the beginning of Section 5.4. The region of stability obtained by using Theorem 5.1 is shown in Fig. 15.

Figure 15 – Ellipsoidal region of stability for example 1.

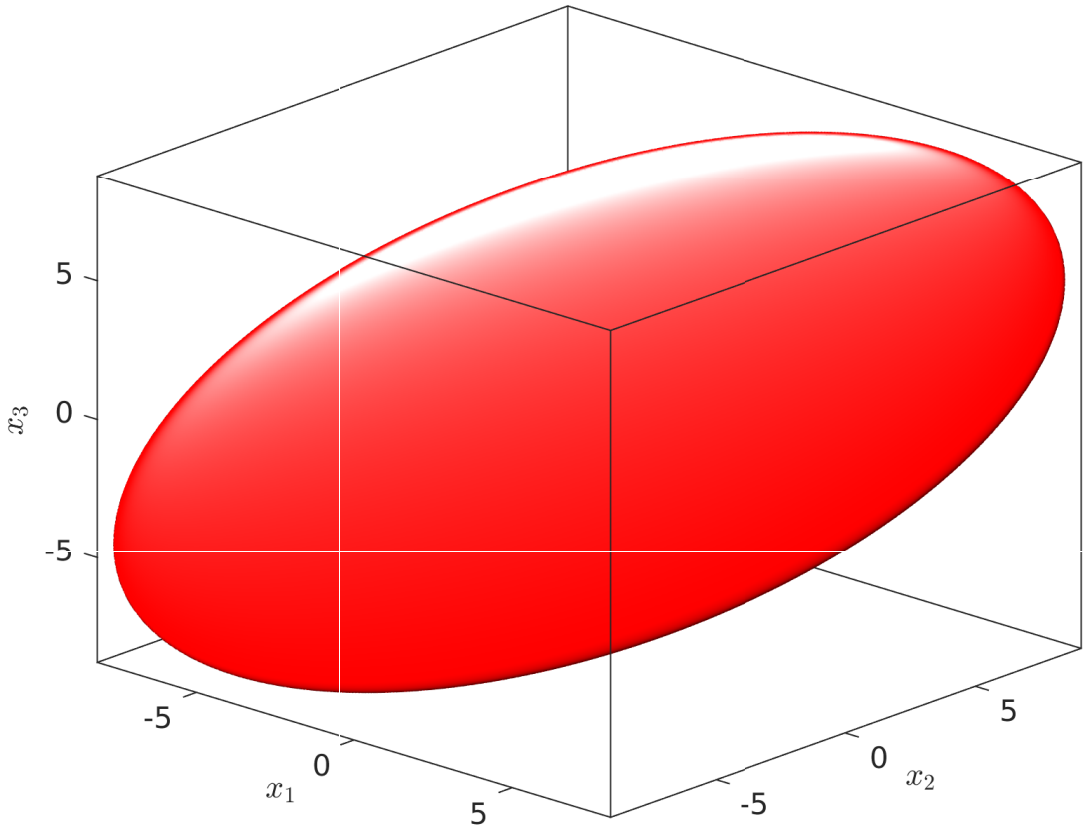

Source: The author.

5.4.1.2 *Example 2 - Comparison with 4-degree-of-freedom anti-windup*

Consider the second-order SISO plant

$$G(s) = \frac{0.5s^2 + 0.5s + 1}{s^2 + 0.2s + 0.2},$$

with input constraint such that $\overline{u} = 0.5$. By using a zero-order hold and sampling time of $T = 0.1s$ the following discrete-time transfer-function model is obtained:

$$P(z) = \frac{-0.5 + 0.941z^{-1} - 0.4549z^{-2}}{1 - 1.978z^{-1} + 0.9802z^{-2}}.$$

In this example, comparison with the recent 4-degree-of-freedom anti-windup from Li *et al.* (2016) and the classical low-order IMC anti-windup scheme from Turner and Postlethwaite (2004)

are presented. Controllers from Li *et al.* (2016) and Turner and Postlethwaite (2004) are defined as therein. The AW-SDTC controller is tuned with $\alpha = \begin{bmatrix} 0.947+0.128i & 0.947-0.128i & 0 \end{bmatrix}$ and $\rho = 0.7$. The poles $\nu = \begin{bmatrix} 0.945+0.129i & 0.945-0.129i \end{bmatrix}$ of the anti-windup conditioning filter were found by applying Theorem 5.1 with $\Lambda = 0.45$, $\zeta_b = 0.946$ and $\zeta_a = 0.948$, yielding $\gamma = 9.4416$.

Fig. 16 shows the results for a step change in the reference, followed by a negative input load disturbance of magnitude 0.5. For the set-point tracking the AW-SDTC and the controller from Li *et al.* (2016) exhibit very similar responses. However, it is possible to note that the AW-SDTC is the first controller to reject the input disturbance completely.

Figure 16 – Simulation results for example 2 - Set-point tracking and input disturbance.

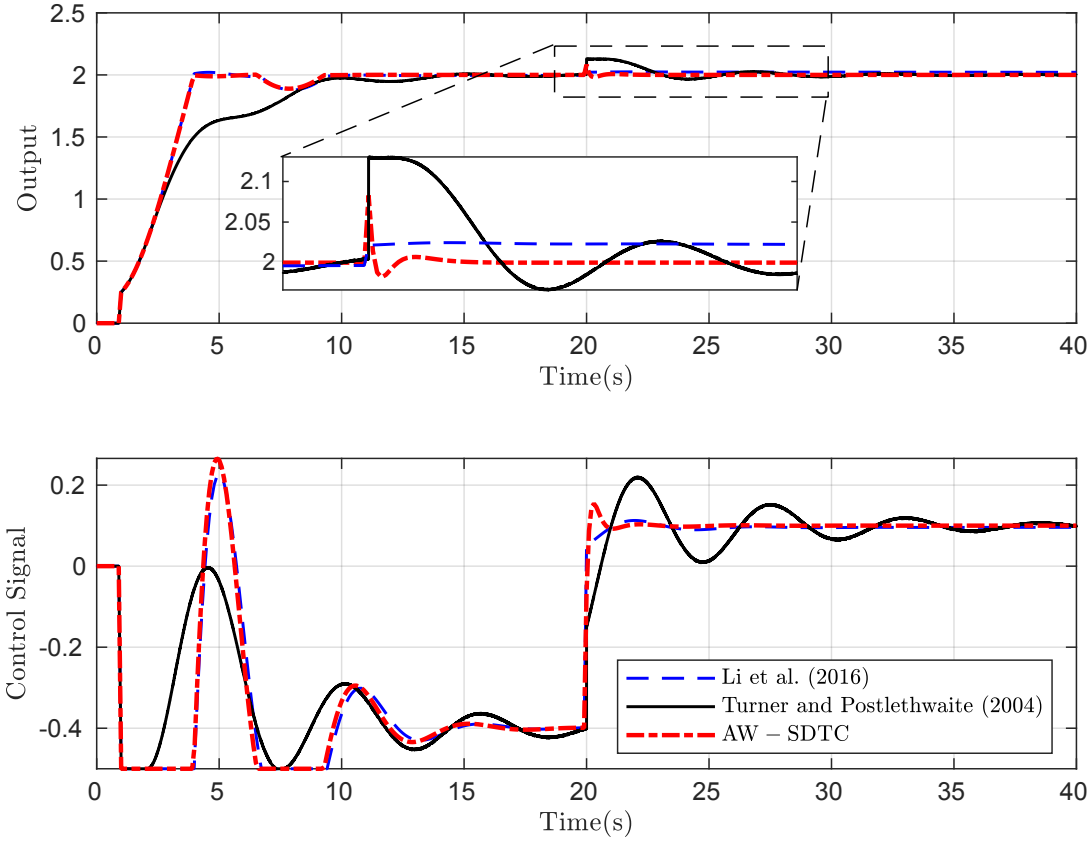

Source: The author.

As in Li *et al.* (2016), a second simulation (shown in Fig. 17) was realized in order to evaluate performance against output disturbance. Although both the AW-SDTC and the controller from Li *et al.* (2016) seem to present similar rejection of the disturbance, there is a slight advantage to the AW-SDTC, which completely rejects the disturbance faster and in a less oscillatory manner.

Figure 17 – Simulation results for example 2 - Output disturbance rejection.

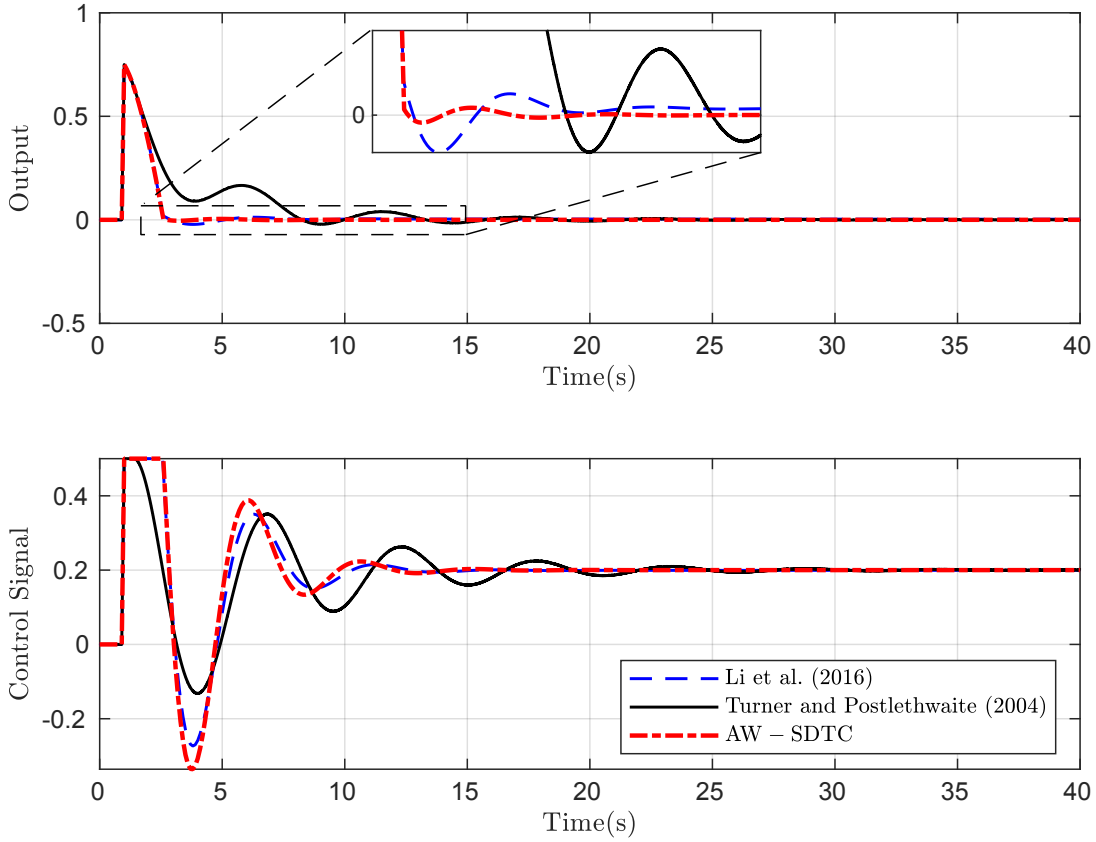

Source: The author.

It is worth to mention, once more, that the proposal herein preferred to use the local assumption for stability in order to prioritize performance. On the other hand, other approaches as the one from Turner and Postlethwaite (2004) are suitable to guarantee global stability for this plant. The ellipsoidal region of stability for this example obtained employing Theorem 5.1 is shown in Fig. 18.

5.4.2 Time-delay examples

This subsection presents two simulation case studies using the integrative plant presented in Zhang and Jiang (2008) and the unstable process recently presented in Flesch *et al.* (2017). Comparison with a constrained MPC is also performed. Evaluated controllers are compared under input saturation, dead-time uncertainties, input and output disturbances, and step reference variations.

Figure 18 – Guaranteed ellipsoidal region of stability for example 2.

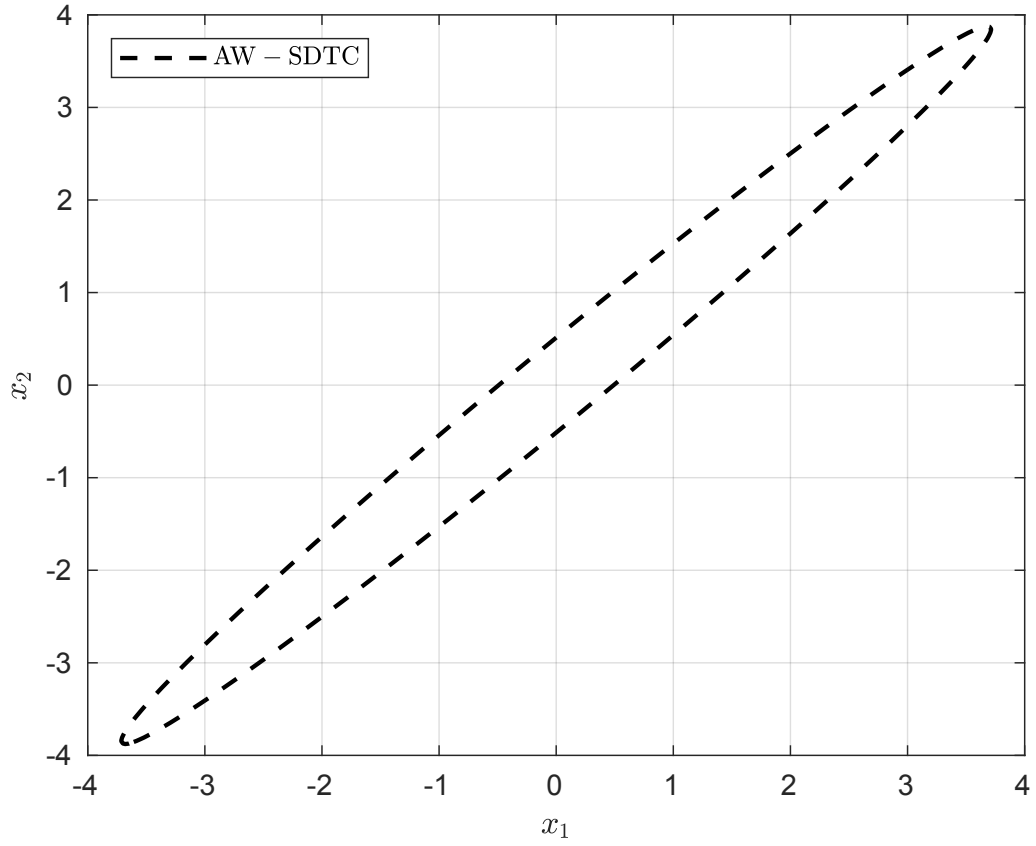

Source: The author.

5.4.2.1 Example 3 - Integrating case

This example presents comparative simulation results obtained with the following controllers: an input constrained MPC from Camacho and Bordons (2007), controller reported in Zhang and Jiang (2008), the recently published strategy in Flesch *et al.* (2017) and the proposed AW-SDTC. For this purpose, the following process model presented in Zhang and Jiang (2008) is considered:

$$P(s) = \frac{e^{-5s}}{s}.$$

The input limit is given by $\bar{u} = 1$. By using a zero-order hold and sampling time of $T = 0.2s$ the following discrete-time transfer-function model is obtained:

$$P(z) = \frac{-0.5 + 0.941z^{-1} - 0.4549z^{-2}}{1 - 1.978z^{-1} + 0.9802z^{-2}}.$$

Parameters of the controller from Zhang and Jiang (2008) are defined as therein. The MPC from Camacho and Bordons (2007) was tuned in order to present a step response quite similar to the controller from Zhang and Jiang (2008) in the nominal case without input saturation.

The MPC from Camacho and Bordons (2007) uses the Controlled Auto-Regressive Integrated Moving-Average (CARIMA) model to compute predictions and is adjusted with the limits of the prediction window as $N_1 = d_n + 1$, $N_2 = d_n + 100$, the control horizon $N_u = 70$, and the control weights given by $\phi_1 = 0$ and $\phi_i = 250$, $i = 2, \ldots, N_u$.

For the AW-SDTC controller two different tunings are considered. The first one, named AW-SDTC$_1$, was tuned aiming to improve disturbance rejection, leading to the following parameters $\alpha = 0.955$ and $\rho = 0.865$. The pole $\nu = 0.9548$ of the anti-windup conditioning filter was found by applying Theorem 5.1 with $\Lambda = 0.7$, $\zeta_b = 0.95$, yielding $\gamma = 113.1629$. Figs. 19 and 20 show simulation results for a step reference. An input disturbance pulse with amplitude of -1.5 was applied from $t = 40$ s to $t = 50$ s. A step input disturbance with amplitude of -0.5 was applied at $t = 100$ s.

Fig. 19 shows simulation results without uncertainties. One can observe that all the controllers follow the reference in a similar way. However, in the case of both input pulse disturbance and input saturation, the proposed AW-SDTC$_1$ controller is the only not presenting overshoot at recovery. Regarding the step input disturbance performance, all controllers perform in very similar manner, as the control signals do not saturate.

Figure 19 – Simulation results for example 3 (no uncertainties).

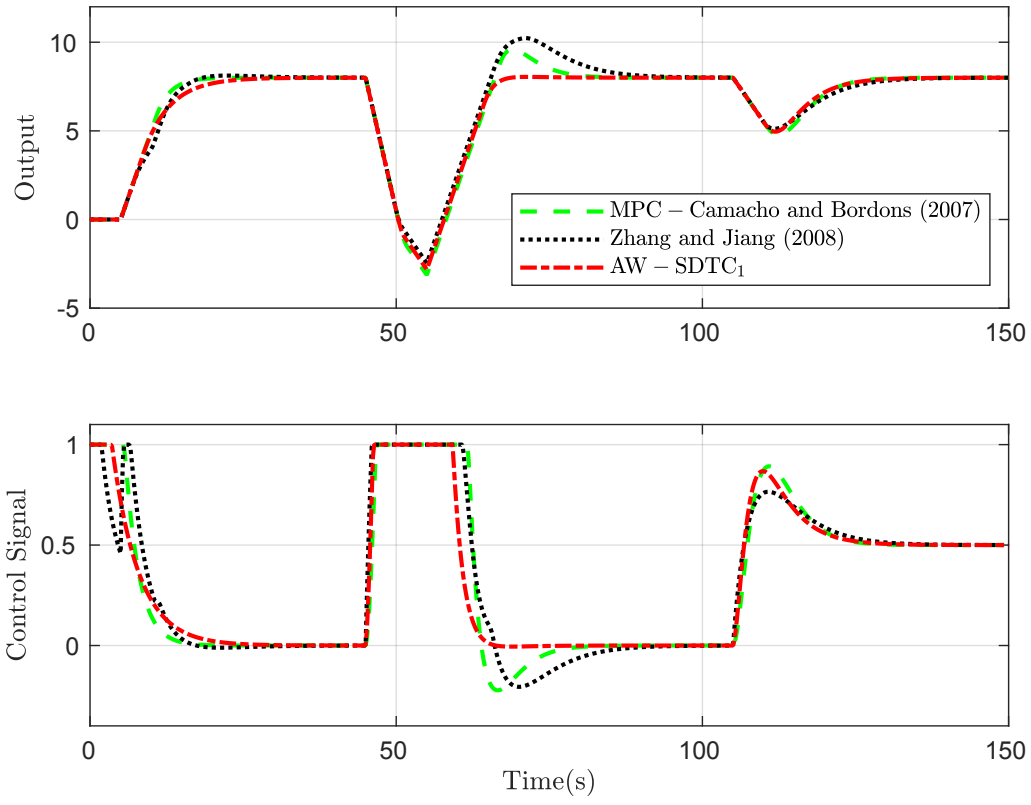

Source: The author.

Fig. 20 shows simulation results using +20% dead-time uncertainty. It can be seen that the proposed AW-SDTC$_1$ retains better output performance for pulse disturbance while may be taken as equivalent to the compared controllers for step disturbance. It is important to highlight that the proposed AW-SDTC achieves better performance than the MPC, which is a much more complex controller.

Figure 20 – Simulation results for example 3 (20% dead-time uncertainty).

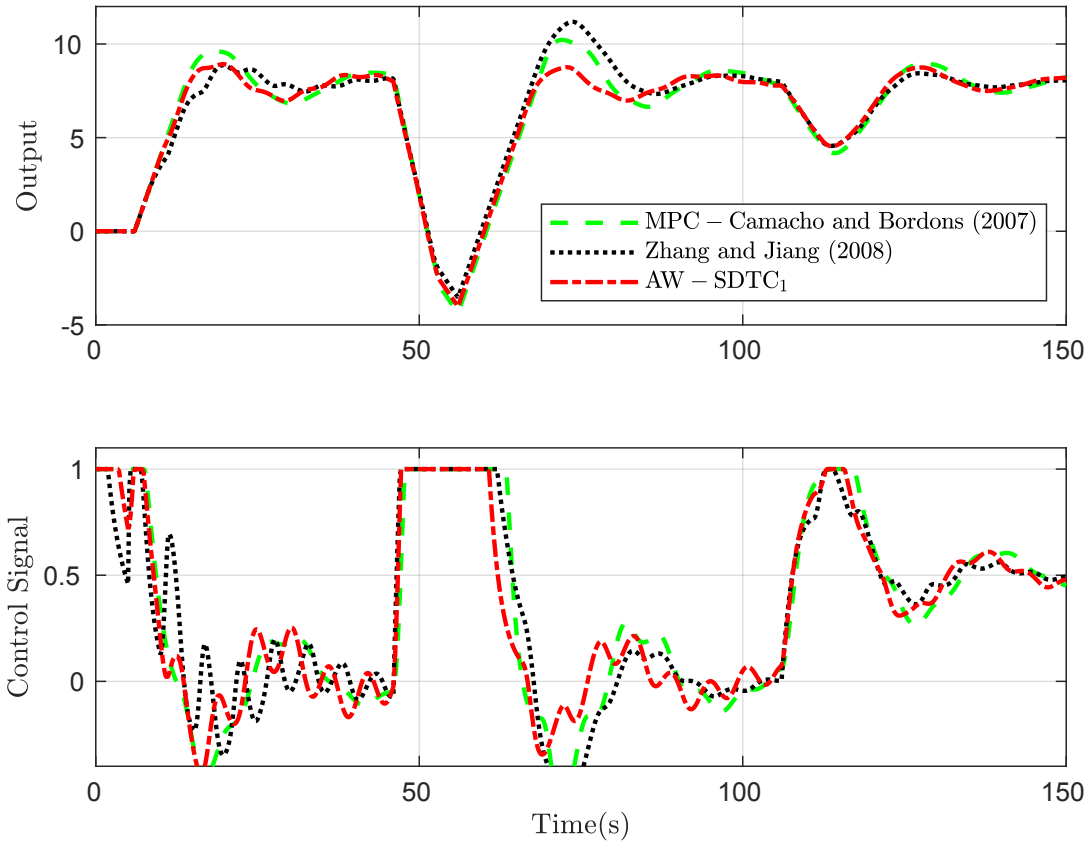

Source: The author.

In order to establish comparison with the anti-windup strategy in Flesch *et al.* (2017), the AW-SDTC$_2$ was tuned to yield a similar set-point tracking response by using the following parameters $\alpha = 0.5$ and $\rho = 0.3$. The pole $\nu = 0.493$ of the anti-windup conditioning filter was found by applying Theorem 5.1 with $\Lambda = 0.96$, and $\zeta_b = 0.45$, yielding $\gamma = 560.4146$. The increase in the $\mathcal{L}_2$ gain can be justified by the more aggressive tuning of the anti-windup filter.

Fig. 21 shows the results for the nominal case, while Fig. 22 presents the results using +5% dead-time uncertainty. Notice that, contrary to the controller from Flesch *et al.* (2017), the AW-SDTC$_2$ does not present overshoot for either pulse or step disturbances in the nominal case. Also, note from Fig. 22 that even in the uncertain case, the proposed controller had improved performance against the compared controller.

Figure 21 – Simulation results for example 3 (no uncertainties).

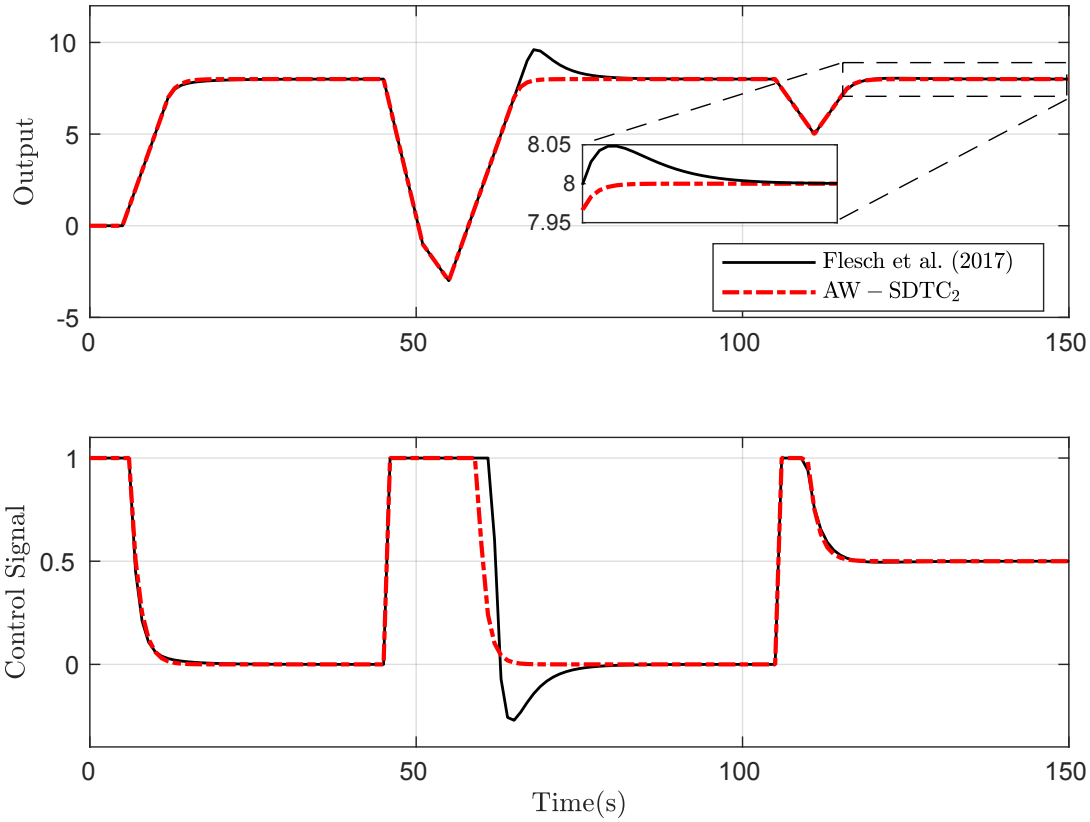

Source: The author.

Figure 22 – Simulation results for example 3 (5% dead-time uncertainty).

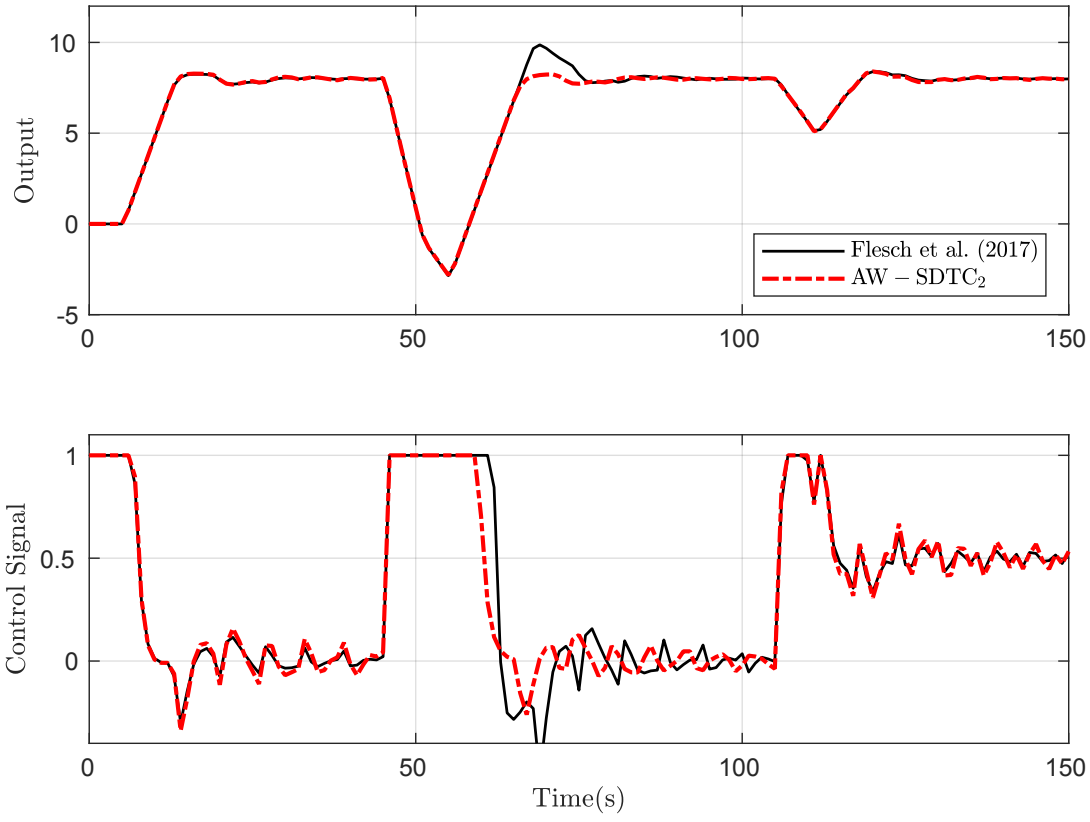

Source: The author.

5.4.2.2 *Example 4 - Unstable case*

This example also compares the proposed AW-SDTC with the strategy proposed in Flesch *et al.* (2017). The controlled process, which represents an isothermal chemical reactor, has been studied in many works and is originally found in Liou and Yu-Shu (1991). The following differential equation gives the nonlinear model

$$\frac{dC}{dt} = \frac{Q}{V}(C_f - C) - \frac{k_1 C}{(k_2 C + 1)^2},$$

where C_f and C are the process control and output variables, respectively, given in mol/L. The operating parameters are given as k_1 = 10 L/s, k_2 = 10 L/mol, V = 1 L and Q=0.03333 L/s. The bound on the process input is given by $\bar{u} = 0.05$.

An unstable linearized model obtained around the steady-state condition with C_f = 3.288 mol/L and C = 1.316 mol/L is given by

$$P(s) = \frac{3.433}{103.1s - 1} e^{-20s},$$

where a measurement delay of $L = 20s$ is considered. By using a zero-order hold and sampling time of $T = 5s$ the discrete-time model is obtained as

$$P(z) = \frac{0.1706 z^{-1}}{1 - 1.0497 z^{-1}} z^{-4}.$$

The controller from Flesch *et al.* (2017) is defined as therein. Once more, the AW-SDTC was tuned to obtain set tracking response similar to the compared controller. However, faster disturbance rejection was aimed with AW-SDTC controller tuned with $\alpha = 0.68$ and $\rho = 0.65$. The pole $\nu = 0.6804$ of the anti-windup conditioning filter was found by using Theorem 5.1 with $\Lambda = 0.5$, and $\zeta_b = 0.65$, yielding $\gamma = 38.2798$.

The process nonlinear model is used in all simulations for a step reference of 0.1 mol/L at time $t = 0$ s, in addition to application of input and output disturbances of amplitude 0.015 mol/L and 0.02 mol/L in t = 200 s and t = 500 s, respectively.

From Fig. 23, one may note the controller from Flesch *et al.* (2017) exhibits slower rejection for both input and output disturbances and undershoot in the rejection of the output disturbance due to the dominant zero imposed by its primary controller. On the other hand, the proposed AW-SDTC does not present any of these issues which may become inconvenient. It may be interesting to comment that the proposed AW-SDTC overall better performance might be related to the addition of the tuning parameters ζ_a and ζ_b, which allow fine adjustment of the

poles of the anti-windup conditioning filter. On the other hand, the anti-windup technique from Flesch *et al.* (2017) does not employ any tuning parameters.

Figure 23 – Example 4 - Simulation results for unstable case.

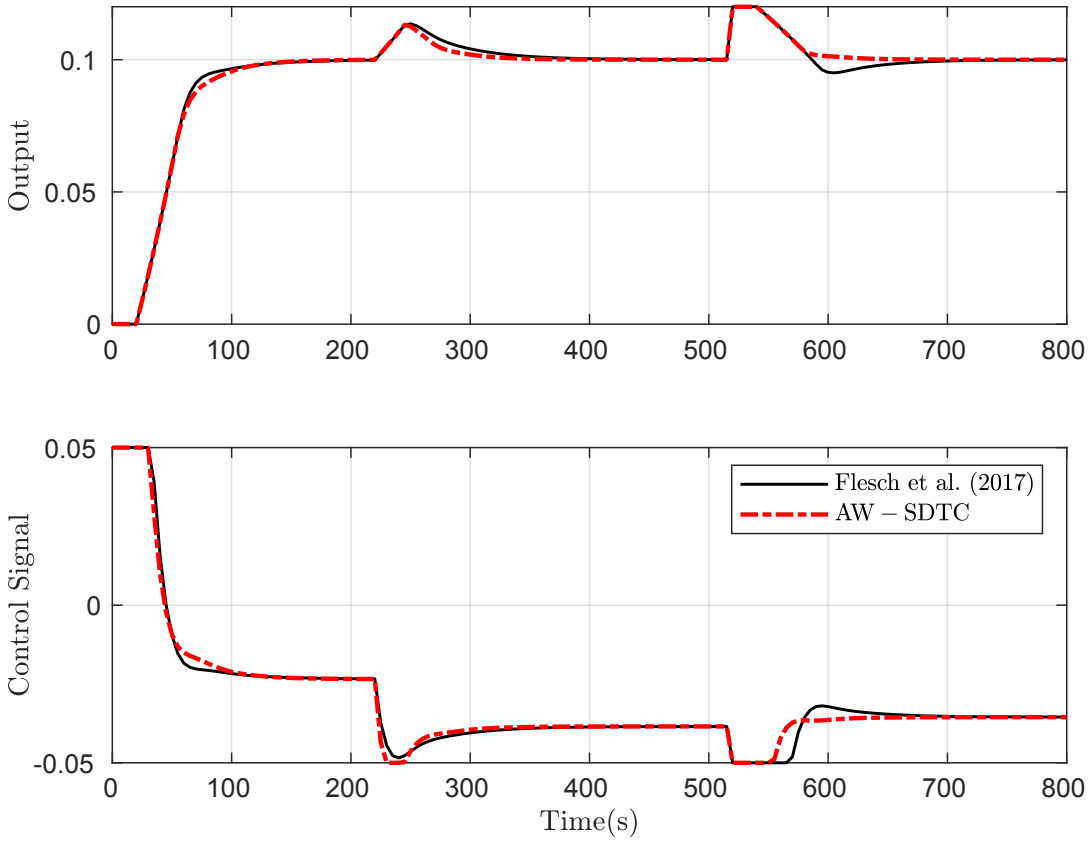

Source: The author.

Consider now that the process measurement delay is actually 10% larger, $L = 22s$. As shown by Fig. 24, the AW-SDTC maintains its performance characteristics related to disturbances rejection even under such circumstances, while issues mentioned earlier for the nominal case remains unchanged to the comparing controller. It is important to highlight that for the proposed strategy such results are obtained by using simple gains in the primary controller, and a first-order robustness filter. On the other hand, the strategy from Flesch *et al.* (2017) applies a PI as the primary controller, a first-order reference filter and a second-order robustness filter, which clearly shows a design advantage in favor of the AW-SDTC algorithm as it becomes much simpler than the compared one. Table 1 summarizes the results for other modeling uncertainty cases in Examples 3 and 4. The Integral Square Error (ISE) of the output signal and the control signal variance were calculated. Overall, the proposed strategy presents betters results, in addition to being simpler, as previously explained.

Figure 24 – Example 4 - Simulation results for unstable case with 10% dead-time uncertainty.

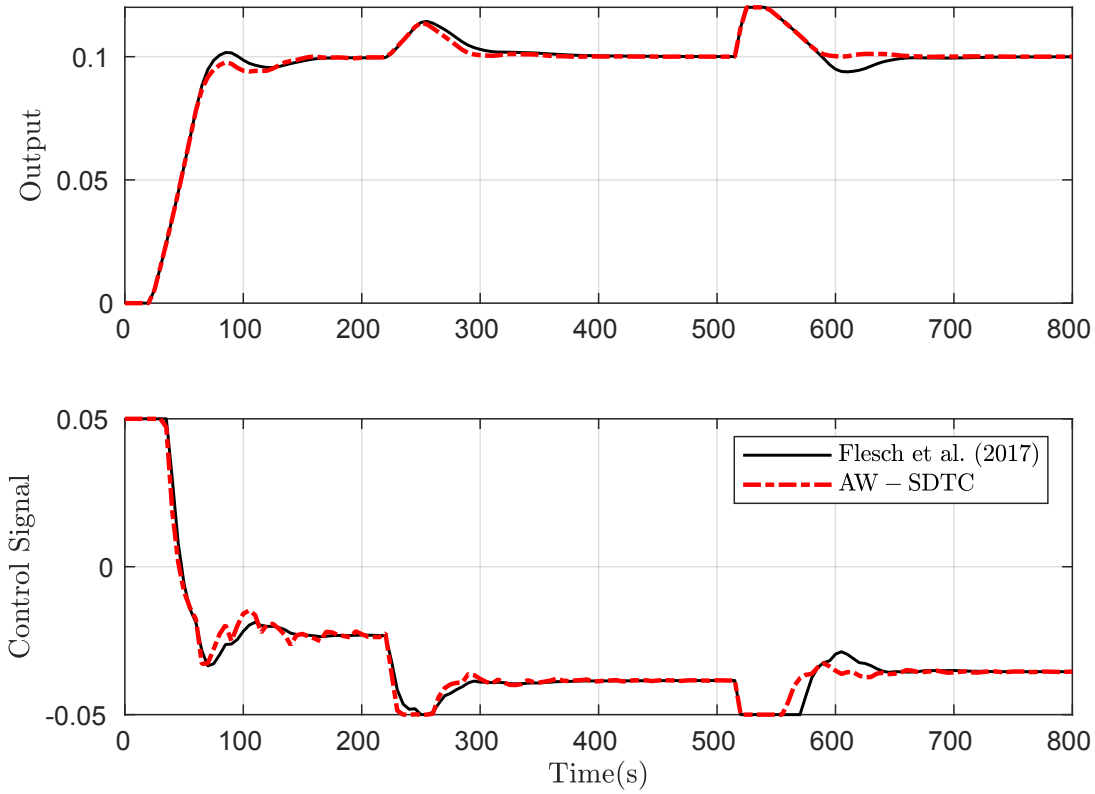

Source: The author.

Table 1 – Output ISE and control variance for dead-time simulation examples.

	Example 3			
Dead-time	Output Signal ISE		Control Signal Variance	
uncertainty (%)	AW – $SDTC_2$	Ref. (FLESCH *et al.*, 2017)	AW – $SDTC_2$	Ref. (FLESCH *et al.*, 2017)
0	1540.40	1550.51	0.1449	0.1592
2	1543.88	2311.56	0.1475	0.2805
5	1543.11	1163.23	0.1561	0.5459
10	1502.72	1059.56	0.4308	0.3035
20	2551.09	2619.82	0.7154	0.6037
	Example 4			
Dead-time	Output Signal ISE		Control Signal Variance	
uncertainty (%)	AW – SDTC	Ref. (FLESCH *et al.*, 2017)	AW – SDTC	Ref. (FLESCH *et al.*, 2017)
0	0.3953	0.3961	0.00040	0.00042
10	0.4122	0.4140	0.00043	0.00044
20	0.4609	0.4394	0.00059	0.00049
40	0.5907	0.5117	0.00085	0.00065
70	0.8141	0.8454	0.00083	0.00080

Source: The author.

5.5 Experimental results

This section intends to show the usefulness of the proposed AW-SDTC, applied for temperature control of a commercial neonatal intensive care unit (NICU) depicted in Fig. 25. The plant has been identified using a step-test identification procedure (NORMEY-RICO;

CAMACHO, 2007), whose model is given by

$$P_n(s) = \frac{0.483e^{-10.2s}}{254.7s+1},$$

where the time is measured in minutes and the control is constrained within the range from 0 to 100 % as it is the current flowing through a heating resistor, which is limited by its maximum power. The following discrete-time model is obtained using a sampling time of $T = 0.2$ min

$$P_n(z) = \frac{0.0003791}{z-0.9992}z^{-51}.$$

Figure 25 – Picture of the neonatal intensive care unit.

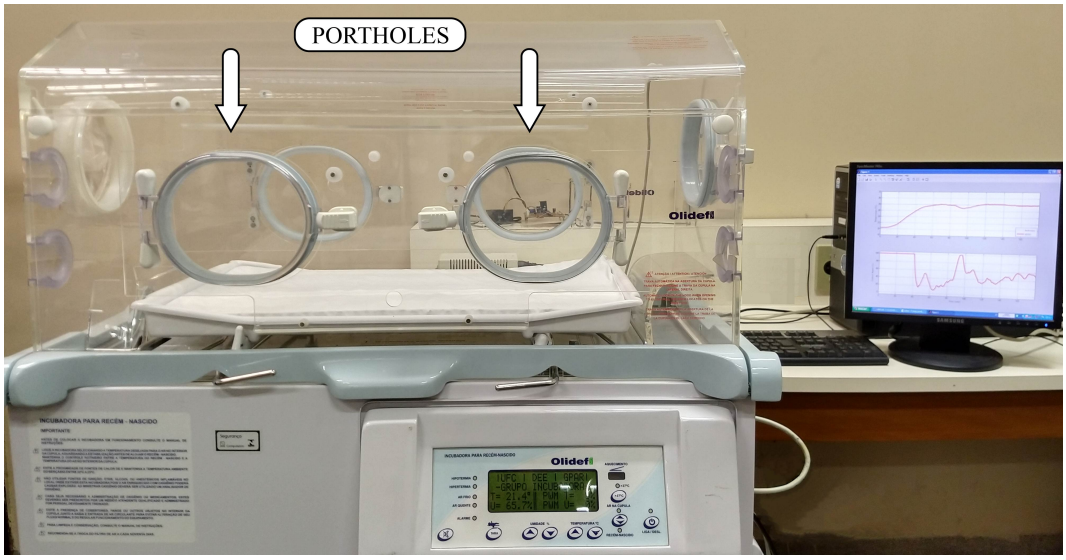

Source: The author.

The AW-SDTC control structure was tuned with $\alpha = 0.92$, $\rho = 0.98$ and $\nu = 0.9203$. The pole of the anti-windup conditioning filter was found by running Corollary 5.1 with $\zeta_a = 0.925$ and $\zeta_n = 0.915$, thus global stability of the system has been guaranteed. It is important to notice that with this controller the nominal desired closed-loop transfer function $H_{ry}(z)$ is chosen to obtain much faster set-point tracking response than the open-loop plant, thus justifying the choice of small sampling time. Furthermore, the robustness filter $F_r(z)$ increases system robustness with a proper measurement noise attenuation.

Experimental results using the proposed structure for a temperature set-point of 28^oC are shown in Fig. 26. The initial temperature inside the NICU is 21.3^oC, whilst the temperature of the room was kept around 18^oC during the whole experiment. It is important to remark that the acrylic dome which involves the NICU does not provide a good level of thermal

isolation between the internal and external environments. Therefore, the external temperature is an unmodeled disturbance which is present during the experiment. Due to saturation, the reference tracking response is not as fast as designed to be. However, observe that, as expected, the output can track the reference without oscillations. Furthermore, it is important to note that even though the plant input became saturated during the first 41 minutes, the controller did not present windup issues.

In order to assess controller robustness, portholes of the NICU were kept opened between $t = 85$ min and $t = 95$ min leading to an undershoot of 1.2^oC. However, such disturbance was adequately rejected as set-point was achieved again within 30 minutes. Note that even though the control signal saturated again during the disturbance rejection phase, no windup issues emerged, which further demonstrates the strategy ability to deal with the saturation condition.

Figure 26 – Experimental results: temperature control of a NICU.

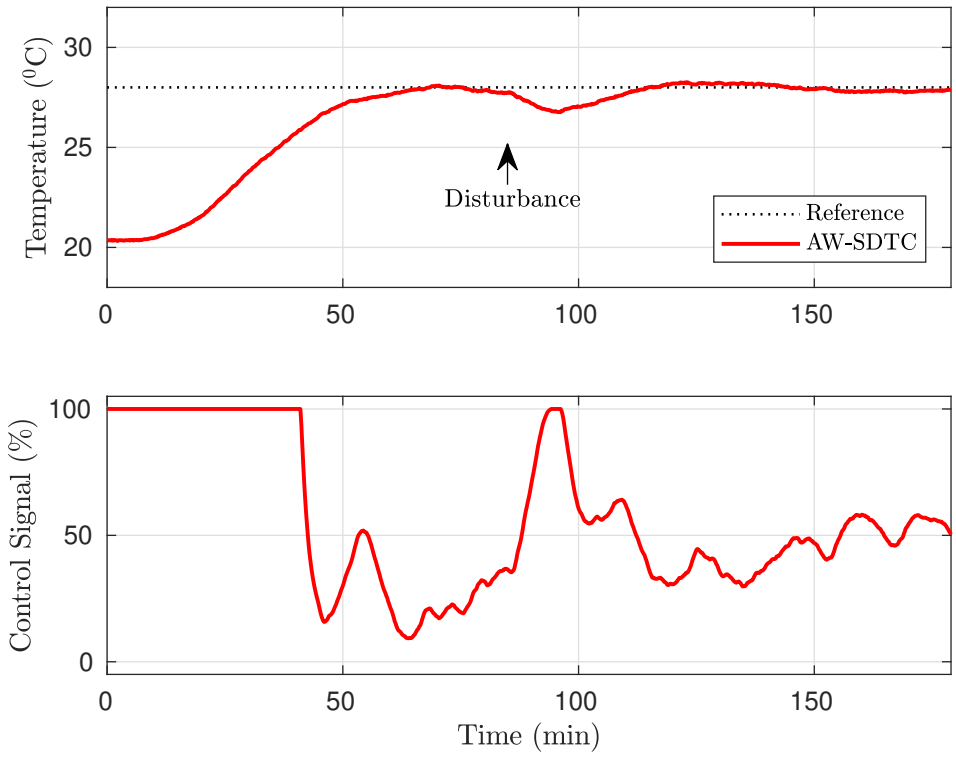

Source: The author.

5.6 Discussion

An anti-windup strategy along with a linear DTC structure applied to the control of both time-delayed and delay-free SISO systems of any order with saturating actuators has

been presented. LMIs which incorporate $\mathbb{D}$-stability regions have been used to synthesize the anti-windup compensator in order to guarantee good performance of the design. Different from most previous saturation related works, this work addresses the problem of saturation in a practical manner such that problems as tracking, robustness, and disturbance rejection are explicitly considered. Furthermore, it has been shown that disturbance rejection response of the proposed AW-SDTC during saturation events presents better results when compared to strategies previously proposed in the literature.

The developed experiment effectively assures that the proposed strategy does not present windup issues, while keeps the excellent performance of a conventional linear SDTC. Due to its inherent simplicity, the proposed scheme is supposed to present great potential to be implemented in practical applications, therefore being quite useful for control engineers. The discrete-time nature of the controller should provide a secure computer-based implementation.

6 A SATURATED DTC STRATEGY WITH TIME-VARYING DELAYS

Dead-time compensators (DTCs) are a family of classical controllers derived from the Smith Predictor (SP). Their main characteristic is that they explicitly employ the model of the open-loop process to feedback a predicted value of the non-delayed system, thus obtaining *compensation* of the delay. Such a perfect compensation is not achievable in the case of time-varying delays. In this chapter, we address stability analysis of a DTC structure in this situation, in addition to considering saturating actuators and disturbances of limited energy. Specific challenges related to the DTC closed loop are taken into account in the developed theoretical conditions, which are expressed in terms of linear matrix inequalities (LMIs) by using an adequate Lyapunov-Krasovskii functional (LKF) and generalized sector conditions. Furthermore, a new approach for the definition of the set of initial conditions in an augmented space in conjunction with the LKF is presented. Besides theoretical innovations, practical discussion about the relation between the tuning of DTC controllers and robustness for this class of systems is presented through numerical examples. An experimental application on a neonatal incubator prototype is carried out to emphasize the effectiveness of the results.

6.1 Introduction

Time delay, which appears in many industrial processes, is a challenging issue in the process control area since the transport delay can lead the system to undesired oscillatory closed-loop response or even instability (NORMEY-RICO; CAMACHO, 2007). According to Fridman (2014), Seuret and Gouaisbaut (2013), the stability analysis and the robust control of time-delay systems are also of theoretical importance since it belongs to the wide class of infinite-dimensional systems (in the continuous-time case), which are not so easy to handle theoretically.

Besides time delay, another major topic in control systems is actuator saturation (TARBOURIECH *et al.*, 2011; ZACCARIAN; TEEL, 2011). Most variables in industrial processes work near or at their maximum and minimum limits in order to optimize production. The nonlinear nature of the closed loop can also lead to instability. Therefore, such constraints must be taken into account during closed-loop stability analysis prior to the controller practical implementation. The presence of isolated nonlinearities, as the actuator saturation, is yet an active topic of research, see e.g. Wang *et al.* (2018), Wang and Ji (2020), Hu *et al.* (2020). The

problem of sensor saturation has also recently been studied in Zhang and Zhou (2019), Shen *et al.* (2020).

Regarding time delays, the so-called dead-time compensators (DTCs) have been widely studied over the years due to their ability to improve the performance and robustness of the closed-loop system for processes with constant input or output time delay (NORMEY-RICO; CAMACHO, 2007). The first DTC was proposed in Smith (1957), also known in the literature as the Smith predictor (SP). Since then, several extensions have been proposed to deal with stable, unstable, and integrative processes, and to improve robustness, disturbance rejection, and measurement noise attenuation (NORMEY-RICO; CAMACHO, 2008a). Some recent works intended to improve these characteristics can be found in García and Albertos (2013), Liu *et al.* (2018), Sanz *et al.* (2018a), Torrico *et al.* (2018), Torrico *et al.* (2019), among others. Other solutions not involving the classical DTCs have also been proposed in recent years, for example in Sun and Fu (2016) the adaptive control of a class of time-varying nonlinear systems with constant delay is investigated. The robust control of nonlinear systems with constant delays was also explored in Yang and Sun (2019). In Rodríguez *et al.* (2020), tuning rules for low-order controllers (including proportional-integral-derivative (PID) controllers) are revisited and the robust control of time-delayed single-input single-output (SISO) is addressed.

Nonetheless, due to the growing importance of Networked Control Systems (NCSs) (YANG, 2006; GUPTA; CHOW, 2010; ZHANG *et al.*, 2017) the problem of time-varying delays started to gain more importance in the recent years when compared to the case of constant delays (even if the constant delay is uncertain). To cite a few works, the stability of structures for the control of time-varying delay systems has recently been studied along the problems of linear time-varying (LTV) processes (SANZ *et al.*, 2019), nonlinear systems (SANZ *et al.*, 2020), non-minimum phase systems (GENG *et al.*, 2019), and mismatched disturbances (GONZALEZ *et al.*, 2019). In this case, the traditional DTC will no longer be able to provide perfect compensation of the delay, that is, will not be able to eliminate the delay from the feedback loop, which is its main characteristic. Due to this problem, the work in Normey-Rico *et al.* (2012) develops stability analysis of the Filtered Smith Predictor (FSP) for the case of time-varying delay processes in order to evaluate the FSP ability to deal with this case. However, saturating actuators, which is common in practical applications and places an undesired nonlinearity in the closed-loop system, has not been considered in the aforementioned work.

Concerning the classical DTCs, in Normey-Rico and Camacho (2007), it is argued

that one strategy to take the saturation into account in DTC structures is to include the model of the saturation at the input of the model of the plant. As highlighted by the authors, the fundamental property of the Smith Predictor still holds in this situation: the dead time is eliminated from the main feedback loop in the case of no modelling errors and no disturbances. However, time-varying delays are not considered and formal stability analysis with the characterization of a set of initial conditions of the plant and/or disturbances for which the internal stability of the closed loop is preserved is not presented by the authors. In Alves Lima *et al.* (2020), which inspired Chapter 5, a practical solution for the control of systems with constant delay and input saturation is presented based on the design of a DTC for the linear system plus the addition of anti-windup to deal with saturation aspects. Nevertheless, a procedure for estimating the region of attraction of the plant and the DTC controller in the case of uncertain (or time-varying) delays is not presented either.

In the current chapter, we revisit the DTC structure to provide theoretical conditions, expressed through linear matrix inequalities (LMIs), for the stability analysis of the closed loop considering systems with both input saturation and output time-varying delays. One of the objectives is to characterize the region of admissible initial conditions for which the closed-loop stability is ensured despite the presence of saturating input. To do this, we consider an adequate Lyapunov-Krasovskii functional and generalized sector conditions. Additionally, we aim at using the analysis to relate the tuning of DTCs with both robustness and performance of the closed loop. Although seminal works addressing the joint problems of time delays and input saturation can be found in the literature (TARBOURIECH; GOMES DA SILVA JR., 2000; FRIDMAN *et al.*, 2003; GOMES DA SILVA JR. *et al.*, 2006; GOMES DA SILVA JR. *et al.*, 2008), fundamental differences can be cited: i) All of them consider state delays, while we consider output delays, a different kind of delay present in numerous applications, as in chemical reaction processes. ii) All of them are in continuous-time since they do not deal with model-based controls. On the other hand, we propose the use of DTCs, which are high-order predictive controllers employing the model of the process and that have been frequently used in practical applications in the last decades. Since all strategies employing the plant model for the control of time-delay systems need to be, in practice, digitally implemented, we work in the discrete-time domain which is more realistic in this case. iii) Neither of them deals with time-varying delays, which appear in many real applications and are more difficult to treat in a theoretical point of view. Additionally, in this chapter, we propose a new methodology for the estimate on the region of stability along

with Lyapunov-Krasovskii functionals which might lead to less conservative results than those commonly used (see Sections 2.3 and 4.1 of the chapter). Such a novel methodology can be applied in any work using LKFs for the stability of discrete-time time-delayed systems and is, therefore, a technical contribution not necessarily linked with the DTC controller.

The chapter is organized as follows. Section 6.2 describes the complete system under consideration, the involved contributions, and states the mathematical problem we intend to solve. Section 6.3 is dedicated to some preliminary results. In Section 6.4, the main results are presented. Section 6.5 brings simulation results of the DTC, followed by the experimental application in Section 6.6. Finally, concluding remarks are brought in the last section of the chapter.

6.2 Problem formulation

6.2.1 General view

In the chapter, we consider a discrete-time system controlled by a DTC and subject to input saturation. The structure is depicted in Fig. 27 constituted by a plant $\mathcal{P}$, a reference filter $\mathcal{F}_0$, subsystem $\mathcal{S}$ and a filter $\mathcal{F}_r$. In this chapter, we consider the regulatory case, with reference $r = 0$, and the simplified DTC controller from Torrico *et al.* (2018), presented in Chapter 4. However, the developed LMIs can easily be applied to other variations of the Filtered Smith Predictor. The complete system under consideration issued from the connection of the plant, the system $\mathcal{S}$, and the filter $\mathcal{F}_r$ is described as follows:

$$\mathcal{P} \triangleq \begin{cases} x_{p_{k+1}} = \mathrm{A}_p x_{p_k} + \mathrm{B}_p \left(u_k + q_k\right) \\ y_k = \mathrm{C}_p x_{p_{k-d_k}} \end{cases} \tag{6.1}$$

$$\mathcal{S} \triangleq \begin{cases} x_{s_{k+1}} = \mathrm{A}_s x_{s_k} + \mathrm{B}_s u_k \\ y_{s_k} = \mathrm{C}_s x_{s_k} \end{cases} \tag{6.2}$$

$$\mathcal{F}_r \triangleq \begin{cases} x_{f_{k+1}} = \mathrm{A}_f x_{f_k} + \mathrm{B}_f y_k \\ y_{f_k} = \mathrm{C}_f x_{f_k} + \mathrm{D}_f y_k \end{cases} \tag{6.3}$$

where $x_{p_k} \in \mathbb{R}^{n_p}$ is the plant state vector, $x_{s_k} \in \mathbb{R}^{n_s}$ is the state of $\mathcal{S}$, and $x_{f_k} \in \mathbb{R}^{n_f}$ is the state of $\mathcal{F}_r$. $y_k \in \mathbb{R}$ is the measured output and $u_k \in \mathbb{R}$ is the control input, while $y_{s_k} \in \mathbb{R}$ and $y_{f_k} \in \mathbb{R}$

Figure 27 – Saturated DTC controller implementation scheme.

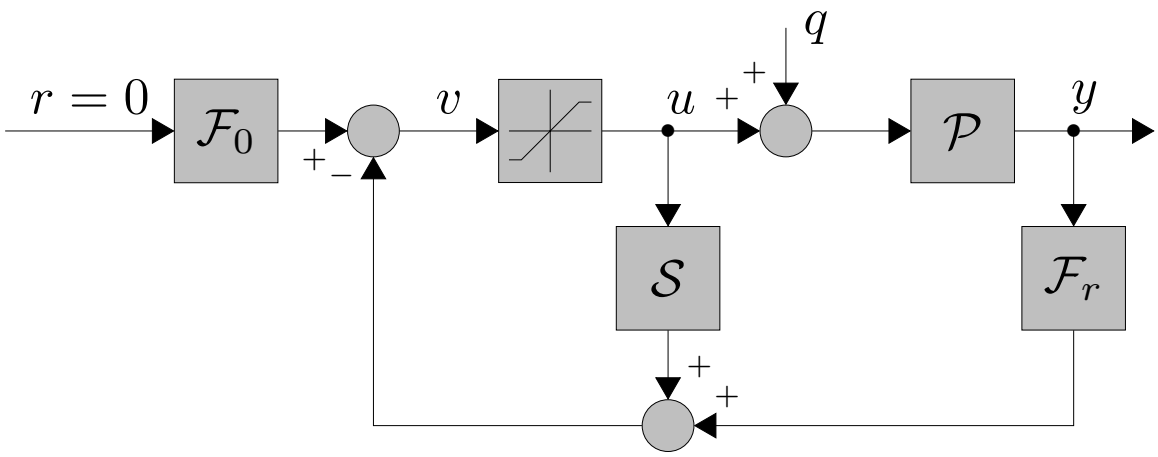

Source: The author.

are the outputs of $\mathcal{S}$ and $\mathcal{F}_r$, respectively. Matrices A_p, B_p, and C_p are all constant, known, and of appropriate dimensions. The plant output delay is bounded and time-varying such as $1 \leq d_m \leq d_k \leq d_\mathrm{M}$, and can arbitrarily vary within such limits. Integers d_m and d_M are known, whereas the value of d_k at each sampling time is unknown. Additionally, the plant is subject to an input disturbance q_k which supposedly belongs to the following set of functions

$$\mathcal{Q} = \{q_k : \mathbb{R}^+ \mapsto \mathbb{R}; \sum_{k=0}^{\infty} q_k^\top q_k \leq \delta\}, \tag{6.4}$$

where $\delta > 0$ represents a bound on the signal energy of q_k. The connection between $\mathcal{P}$, $\mathcal{S}$ and $\mathcal{F}_r$ is realized by

$$\begin{aligned} u_k &= sat(v_k) \\ v_k &= -y_{s_k} - y_{f_k} \end{aligned} \tag{6.5}$$

where the saturation is classically defined as

$$sat(v_k) = sign(v_k) \times min\{|v_k|, \bar{u}\}, \bar{u} > 0, \tag{6.6}$$

$\bar{u}$ being the level of saturation.

Then, the closed-loop system (6.1), (6.2), (6.3) and (6.5) reads:

$$\begin{cases} x_{k+1} = \mathrm{A}x_k + \mathrm{A_d}x_{k-d_k} + \mathrm{B}sat(v_k) + \mathrm{B}_q q_k \\ v_k = \mathrm{K}x_k + \mathrm{K_d}x_{k-d_k} \\ x_k = \phi_k,\ k \in [-d_\mathrm{M}, 0] \\ y_k = \mathrm{C}x_{k-d_k} \end{cases} \tag{6.7}$$

with

$$\mathrm{A} = \begin{bmatrix} \mathrm{A}_p & 0 & 0 \\ 0 & \mathrm{A}_s & 0 \\ 0 & 0 & \mathrm{A}_f \end{bmatrix}, \mathrm{A_d} = \begin{bmatrix} 0 & 0 & 0 \\ 0 & 0 & 0 \\ \mathrm{B}_f\mathrm{C}_p & 0 & 0 \end{bmatrix},$$

$$\begin{bmatrix} \mathrm{K} \\ \mathrm{K_d} \\ \mathrm{C} \end{bmatrix} = \begin{bmatrix} 0 & -\mathrm{C}_s & -\mathrm{C}_f \\ -\mathrm{D}_f\mathrm{C}_p & 0 & 0 \\ \mathrm{C}_p & 0 & 0 \end{bmatrix}, \begin{bmatrix} \mathrm{B} & \mathrm{B}_q \end{bmatrix} = \begin{bmatrix} \mathrm{B}_p & \mathrm{B}_p \\ \mathrm{B}_s & 0 \\ 0 & 0 \end{bmatrix},$$

where $x_k = \begin{bmatrix} x_{p_k}^\top & x_{s_k}^\top & x_{f_k}^\top \end{bmatrix}^\top \in \mathbb{R}^n$, $n = n_p + n_s + n_f$, and ϕ_k is the initial condition at the interval $[-d_\mathrm{M}, 0]$.

Remark 6.1

There is no loss of generality in considering the regulatory case, since industrial processes can be modelled around an operation point, and a simple change of variables can transform the desired output in zero.

6.2.2 Notes on the controller design

The controller matrices A_s, B_s, C_s, A_f, B_f, C_f and D_f have been designed following the steps in Torrico *et al.* (2018), presented in Section 4.4, that is, to establish a desired response of the nominal linear system. In other words, the controller design considered that the time delay d_k was constant $d_k = d_n$, and the non-occurrence of the saturation. Since the objective of this chapter is not the controller design, but rather closed-loop stability analysis, we just briefly review some properties of the controller. The computation of $\mathcal{S}$ depends on the process model with nominal delay d_n[1], the desired $2n_p - 1$ closed-loop tracking poles, and the robustness filter $\mathcal{F}_r$. Furthermore, $\mathcal{S}$ provides perfect delay compensation for the nominal case, that is, nominal delay and no input saturation. The robustness filter $\mathcal{F}_r$ should be designed to guarantee an internally stable implementation structure (A_f and A_s must be Schur stable matrices), to make the equivalent controller have integral action, and to establish a desired compromise between robustness and disturbance rejection.

The state matrix A_f can be defined as $\mathrm{A}_f = \rho \mathrm{I}_{n_p+1}$, where $0 < \rho < 1$ is the robustness filter tuning parameter. In the linear time-invariant (LTI) case, by setting higher values of ρ, one

[1] The nominal delay d_n is defined as the rounding to the nearest integer of $(d_m + d_\mathrm{M})/2$.

can increase the robustness of the system to modelling uncertainties, while smaller values of ρ speedup the disturbance rejection response. More details on the design and tuning of DTC structures for LTI systems can be found in its vast literature (NORMEY-RICO *et al.*, 2012; SANZ *et al.*, 2018a).

Remark 6.2

In DTC structures, the choice of the robustness filter parameter ρ is essential, being its most important tuning variable since it deals with the trade-off between disturbance rejection performance and overall system robustness. Also, although ρ designates the robustness filter $\mathcal{F}_r$ poles, its value directly influences almost all of the other controller matrices (A_s, C_s, B_f, C_f, D_f), which hampers the development of LMI based stabilization of the whole system due to the difficulty to deal with nonlinearities. This will be subject of a succeeding work.

6.2.3 More details on the formulation and contributions

Although the open-loop process (6.1) has output delay, the closed-loop system representation (6.7) is in the form of a state-delayed discrete-time system with control saturation. Many works can be cited regarding the continuous counterpart of this kind of system (CHEN *et al.*, 2015; CHEN *et al.*, 2017; SEURET *et al.*, 2019). Fewer are dedicated to the discrete-time case, however, one can cite Chen and Fei (2014), Naamane *et al.* (2017), and most recently de Souza *et al.* (2019), which deals with the linear parameter varying (LPV) case. Besides dealing with the LPV case, it is important to highlight other differences from the formulation in this work. First of all, the control law in de Souza *et al.* (2019) does not deal with the NCS case where the delay appears in the plant output rather than in the plant state. Furthermore, the formulation proposed in de Souza *et al.* (2019) implements a control law that assumes knowledge of the full history of the plant state, that is the extended state $\overline{x_{p_k}} = \begin{bmatrix} x_{p_k}^\top & x_{p_{k-1}}^\top & \cdots & x_{p_{k-d_\mathrm{M}}}^\top \end{bmatrix}^\top$, and its closed-loop representation does not contain the term $K_d x_{k-d_k}$ since it would require knowledge of the value d_k at each sampling time. This is not the case in this work since the actual implemented control law only requires knowledge/measurement of the output y_k, and thus the control v_k in (6.7) is just the equivalent system for analysis.

It is also interesting to comment that, although works in this area usually employ Lyapunov-Krasovskii functionals, de Souza *et al.* (2019) uses the approach of augmented Lyapunov. As highlighted by the authors therein, the main drawback of the works based in the

Lyapunov-Krasovskii approach is that all of them characterize the region of attraction based on the norm of the sequence of initial conditions, which often leads to conservative estimates. In order to deal with this problem, in de Souza *et al.* (2019) the estimate on the region of attraction is characterized in an augmented space, which is convenient by means of the use of the augmented functional approach.

One of the theoretical innovations in this work comes from a mix of the ideas above. When dealing with DTC structures, it is necessary to keep in mind the problem of high order dimensions of the closed loop, which increases proportionally to the nominal delay d_n and the plant order n_p. The total order of the closed loop (6.7) is given by $n = n_p + n_s + n_f$, with $n_f = n_p + 1$, $n_s = n_f + d_n$, resulting in $n = 3n_p + d_n + 2$. As DTCs are usually applied to control systems with big delays (where conventional controllers such as PID and feedback gains alone are not as effective), the LMI conditions should, ideally, have a low number of decision variables to avoid tractability problems due to the high dimensionality of (6.7). Due to that, the augmented functional approach of de Souza *et al.* (2019) is not practical and can lead to high numerical complexity. On the other hand, differently from the works based on Lyapunov-Krasoviskii functionals, we define the initial conditions in an augmented space, avoiding the conservatism linked with the norm of the sequence approach therein.

On the practical side, we apply the developed conditions to link the DTC tuning variable ρ with the system robustness in the case of time-varying delays and input saturation. The specific challenges related to the DTC closed loop are taken into account in the developed theoretical conditions, and the relation between the tuning of DTCs and the robustness of the closed loop is established. To the best of our knowledge, no work in the literature of DTC has done that for the case of both time-varying delays and saturation. The experimental application considering both these conditions is also unprecedented.

6.2.4 Problem statement

The central objective with respect to system (6.7) can then be summarized as follows:

Problem 6.1

Given a process model defined by A_p, B_p, C_p and the nominal delay d_n, the controller matrices A_s, B_s, C_s, A_f, B_f, C_f, and D_f, provide LMI-based stability analysis in the case of simultaneous output time-varying delays and control saturation. More specifically, one

aims at providing adequate conditions to estimate:

i. The size of sets of guaranteed asymptotic stability for the closed loop.
ii. The energy bound on the external disturbance belonging to the set $\mathcal{Q}$.
iii. Lower and upper bounds on the time-varying delay.

Then, by means of numerical examples, one aims at using the solution to Problem 6.1 to relate the DTC tuning parameter ρ to items (i), (ii) and (iii).

6.3 Preliminary Results

In general, the stability of time-delayed systems can be tackled by using either delay-independent or delay-dependent conditions (FRIDMAN, 2014). The latter case (in which bounds on the delay are explicitly considered) is adopted in this work. The problem of providing stability guarantees for systems with delayed states can be solved by choosing an appropriate Lyapunov functional V_k and its consequent manipulation, which can lead to more or less conservative results. In recent years, many works have been dedicated to the construction of such Lyapunov functionals. All these methods are relying on an appropriate choice of a Lyapunov Krasovskii functional (LKF), and the way to upper bound some sums. Recently, many researchers have been dedicated to the goal of decreasing the conservatism inherent of these upper-bounds by discovering new inequalities. For more details, see the works of Zhang *et al.* (2008), Shao and Han (2011), Liu and Zhang (2012), Seuret *et al.* (2015), Hien and Trinh (2016), Zhang *et al.* (2017), Seuret and Gouaisbaut (2018). However, in this work, we choose to use the classical Jensen's inequality (ZHU; YANG, 2008), which in combination with the use of Finsler's Lemma and the reciprocally convex approach (PARK *et al.*, 2011) can potentially yield a good compromise between numerical complexity and the level of conservatism of the developed condition, as it will be shown later. Although the use of more complex inequalities could be interesting, it will be done in the future.

6.3.1 Auxiliary lemmas

In the development of our conditions, we apply Finsler's Lemma (DE OLIVEIRA; SKELTON, 2001), the discrete-time version of the Jensen's inequality, taken from Zhu and Yang (2008), Hien and Trinh (2016), and the reciprocally convex approach (PARK *et al.*, 2011; SEURET; GOUAISBAUT, 2013), stated in the following three Lemmas.

Lemma 6.1

(DE OLIVEIRA; SKELTON, 2001) Consider $\gamma \in \mathbb{R}^n$, $\Upsilon = \Upsilon^\top \in \mathbb{R}^{n\times n}$, and $\Gamma \in \mathbb{R}^{m\times n}$. The following facts are equivalent:

i. $\gamma^\top \Upsilon \gamma < 0$, $\forall \gamma$ such that $\Gamma\gamma = 0$, $\gamma \neq 0$.

ii. ${\Gamma^\perp}^\top \Upsilon \Gamma^\perp \prec 0$, where $\Gamma\Gamma^\perp = 0$.

iii. $\exists \mathrm{J} \in \mathbb{R}^{n\times m}$ such that $\Upsilon + \mathrm{J}\Gamma + \Gamma^\top \mathrm{J}^\top \prec 0$.

Lemma 6.2

(ZHU; YANG, 2008; HIEN; TRINH, 2016) For integers $a < b$, a function $f : \mathbb{Z}[a,b] \to \mathbb{R}^n$ and a matrix $\mathrm{R} \succ 0$, the following inequality holds

$$\sum_{k=a}^{b} f_k^\top \mathrm{R} f_k \geq \frac{1}{l}\left(\sum_{k=a}^{b} f_k^\top\right) \mathrm{R} \left(\sum_{k=a}^{b} f_k\right), \tag{6.8}$$

where $l = b - a + 1$ denotes the length of interval $[a,b]$ in $\mathbb{Z}$.

Lemma 6.3

(PARK *et al.*, 2011; SEURET; GOUAISBAUT, 2013) For given positive integers n, m, a scalar $\alpha \in (0,1)$, a matrix R_1 in $\mathbb{S}_n^+$ and two matrices W_1, W_2 in $\mathbb{R}^{n\times m}$. Define, for all vector $\zeta \in \mathbb{R}^m$, the function $\Theta(\alpha, \mathrm{R}_1)$ given by:

$$\Theta(\alpha, \mathrm{R}_1) = \frac{1}{\alpha}\zeta^\top \mathrm{W}_1^\top \mathrm{R}_1 \mathrm{W}_1 \zeta + \frac{1}{1-\alpha}\zeta^\top \mathrm{W}_2^\top \mathrm{R}_1 \mathrm{W}_2 \zeta.$$

If there exists $\mathrm{U}_{12} \in \mathbb{R}^{n\times n}$ such that $\begin{bmatrix} \mathrm{R}_1 & \mathrm{U}_{12} \\ \star & \mathrm{R}_1 \end{bmatrix} \succeq 0$, then the following inequality holds

$$\min_{\alpha\in(0,1)} \Theta(\alpha, \mathrm{R}_1) \geq \begin{bmatrix} \mathrm{W}_1\zeta \\ \mathrm{W}_2\zeta \end{bmatrix}^\top \begin{bmatrix} \mathrm{R}_1 & \mathrm{U}_{12} \\ \star & \mathrm{R}_1 \end{bmatrix} \begin{bmatrix} \mathrm{W}_1\zeta \\ \mathrm{W}_2\zeta \end{bmatrix}.$$

6.3.2 Stability in the unsaturated case

We initially develop results for the unsaturated case (i.e. $u_k = v_k$) with no disturbance ($q_k = 0$). This is an important step in order to check if the trade-off between the numerical complexity of the condition and the obtained results is well balanced. Especially, the ideal scenario for analysis of DTCs is to obtain conditions that have fewer decision variables and work

well with bigger delays. Also, some of the content of the proof in this section will be used in the main results in section 4. The developed conditions will be tested in a benchmark example from the literature.

The simplified version of (6.7) by taking into account the connection $u_k = v_k$, and $q_k = 0$, is given by:

$$\begin{cases} x_{k+1} = \mathbb{A}x_k + \mathbb{A}_{\mathrm{d}}x_{k-d_k} \\ x_k = \phi_k,\ k \in [-d_{\mathrm{M}}, 0] \end{cases} \tag{6.9}$$

where $1 \leq d_m \leq d_k \leq d_{\mathrm{M}}$, $x_k \in \mathbb{R}^n$, ϕ_k is the initial condition at the interval $[-d_{\mathrm{M}}, 0]$, $\mathbb{A} = \mathrm{A} + \mathrm{BK}$, and $\mathbb{A}_{\mathrm{d}} = \mathrm{A}_{\mathrm{d}} + \mathrm{BK}_{\mathrm{d}}$. The system (6.9) has the same format of those studied in Seuret *et al.* (2015), Nam *et al.* (2015), for example. The following theorem establishes a sufficient condition to prove stability of system (6.9).

Theorem 6.1

Consider $d_\Delta = d_{\mathrm{M}} - d_m$, and assume the existence of matrices Q, R, U, R_1, U_1 in $\mathbb{S}_n^+$, and matrix U_{12} in $\mathbb{R}^{n\times n}$ such that:

$$\mathrm{T} = \begin{bmatrix} \mathrm{R}_1 & \mathrm{U}_{12} \\ \star & \mathrm{R}_1 \end{bmatrix} \succeq 0,\ \ {\Gamma^{\perp}}^{\top} \Upsilon \Gamma^{\perp} \prec 0 \tag{6.10}$$

where $\Gamma^{\perp} = \begin{bmatrix} \mathbb{A} & 0 & 0 & \mathbb{A}_{\mathrm{d}} \\ & & \mathrm{I}_{4n} & \end{bmatrix}$ and

$$\Upsilon = \begin{bmatrix} \Upsilon_{11} & \Upsilon_{12} & 0 & 0 & 0 \\ \star & \Upsilon_{22} & \mathrm{R} & 0 & 0 \\ \star & \star & \Upsilon_{33} & \mathrm{U}_{12} & \mathrm{R}_1 - \mathrm{U}_{12} \\ \star & \star & \star & -\mathrm{U}_1 - \mathrm{R}_1 & \mathrm{R}_1 - \mathrm{U}_{12}^{\top} \\ \star & \star & \star & \star & \Upsilon_{55} \end{bmatrix},$$

with

$$\begin{aligned}
\Upsilon_{11} &= \mathrm{Q} + \mathrm{R}d_m^2 + \mathrm{R}_1 d_\Delta^2, \\
\Upsilon_{12} &= -\mathrm{R}d_m^2 - \mathrm{R}_1 d_\Delta^2, \\
\Upsilon_{22} &= \mathrm{R}d_m^2 - \mathrm{R} + \mathrm{R}_1 d_\Delta^2 - \mathrm{Q} + \mathrm{U}, \\
\Upsilon_{33} &= \mathrm{U}_1 - \mathrm{R}_1 - \mathrm{R} - \mathrm{U}, \\
\Upsilon_{55} &= \mathrm{U}_{12} + \mathrm{U}_{12}^\top - 2\mathrm{R}_1.
\end{aligned}$$

Then system (6.9) is asymptotically stable for any time-varying delay $d_m \leq d_k \leq d_\mathrm{M}$.

Proof. Consider the following Lyapunov-Krasovskii functional from Fridman (2014), which is the discrete-time counterpart of the functional used for continuous-time systems in Fridman (2006):

$$\mathrm{V}_k = \mathrm{V}_{\mathrm{Q}_k} + \mathrm{V}_{\mathrm{R}_k} + \mathrm{V}_{\mathrm{U}_k} + \mathrm{V}_{\mathrm{U}_{1_k}} + \mathrm{V}_{\mathrm{R}_{1_k}} \tag{6.11}$$

with

$$\begin{aligned}
\mathrm{V}_{\mathrm{Q}_k} &= x_k^\top \mathrm{Q} x_k, \\
\mathrm{V}_{\mathrm{R}_k} &= d_m \sum_{m=-d_m}^{-1} \sum_{j=k+m}^{k-1} \eta_j^\top \mathrm{R} \eta_j, \\
\mathrm{V}_{\mathrm{U}_k} &= \sum_{j=k-d_m}^{k-1} x_j^\top \mathrm{U} x_j, \\
\mathrm{V}_{\mathrm{U}_{1k}} &= \sum_{j=k-d_\mathrm{M}}^{k-d_m-1} x_j^\top \mathrm{U}_1 x_j, \\
\mathrm{V}_{\mathrm{R}_{1k}} &= d_\Delta \sum_{m=-d_\mathrm{M}}^{-d_m-1} \sum_{j=k+m}^{k-1} \eta_j^\top \mathrm{R}_1 \eta_j,
\end{aligned}$$

where $\eta_j = x_{j+1} - x_j$ and $\mathrm{Q}, \mathrm{U}, \mathrm{R}, \mathrm{U}_1$, and R_1 are matrices in $\mathbb{S}_n^+$. Evaluating $\Delta \mathrm{V}_k = \mathrm{V}_{k+1} - \mathrm{V}_k$ along the trajectories of (6.9), one gets

$$\Delta \mathrm{V}_{\mathrm{Q}_k} = x_{k+1}^\top \mathrm{Q} x_{k+1} - x_k^\top \mathrm{Q} x_k \tag{6.12}$$

$$\Delta \mathrm{V}_{\mathrm{R}_k} = d_m^2 \eta_k^\top \mathrm{R} \eta_k - d_m \sum_{j=k-d_m}^{k-1} \eta_j^\top \mathrm{R} \eta_j \tag{6.13}$$

$$\Delta \mathrm{V}_{\mathrm{U}_k} = x_k^\top \mathrm{U} x_k - x_{k-d_m}^\top \mathrm{U} x_{k-d_m} \tag{6.14}$$

$$\Delta \mathrm{V}_{\mathrm{U}_{1k}} = x_{k-d_m}^\top \mathrm{U}_1 x_{k-d_m} - x_{k-d_\mathrm{M}}^\top \mathrm{U}_1 x_{k-d_\mathrm{M}} \tag{6.15}$$

$$\Delta \mathrm{V}_{\mathrm{R}_{1k}} = d_\Delta^2 \left(\eta_k^\top \mathrm{R}_1 \eta_k - \sum_{j=k-d_\mathrm{M}}^{k-d_m-1} \frac{\eta_j^\top \mathrm{R}_1 \eta_j}{d_\Delta} \right) \tag{6.16}$$

By applying Lemma 6.2 to the summation term in the right-hand side of equation (6.13) we obtain the bound

$$d_m \sum_{j=k-d_m}^{k-1} \eta_j^\top \mathrm{R} \eta_j \geq \frac{d_m}{d_m} \left(\sum_{j=k-d_m}^{k-1} \eta_j^\top \right) \mathrm{R} \left(\sum_{j=k-d_m}^{k-1} \eta_j \right).$$

Since $\left(\sum_{j=k-d_m}^{k-1} \eta_j^\top\right) \mathrm{R} \left(\sum_{j=k-d_m}^{k-1} \eta_j\right) = \left(x_k^\top - x_{k-d_m}^\top\right) \mathrm{R} \left(x_k - x_{k-d_m}\right)$, we obtain

$$\Delta \mathrm{V}_{\mathrm{R}_k} \leq \eta_k^\top \mathrm{R} d_m^2 \eta_k - \left(x_k^\top - x_{k-d_m}^\top\right) \mathrm{R} \left(x_k - x_{k-d_m}\right),$$

which is equivalent to

$$\Delta \mathrm{V}_{\mathrm{R}_k} \leq \begin{bmatrix} x_{k+1} \\ x_k \\ x_{k-d_m} \end{bmatrix}^\top \begin{bmatrix} \mathrm{R} d_m^2 & -\mathrm{R} d_m^2 & 0 \\ \star & \mathrm{R} d_m^2 - \mathrm{R} & \mathrm{R} \\ \star & \star & -\mathrm{R} \end{bmatrix} \begin{bmatrix} x_{k+1} \\ x_k \\ x_{k-d_m} \end{bmatrix}. \tag{6.17}$$

To deal with the summation term in (6.16), first note that it can be split in two parts, one gathering terms in the interval $k-d_k$ to $k-d_m-1$ and the second between $k-d_\mathrm{M}$ and $k-d_k-1$. Then, apply Lemma 6.2 to get $d_\Delta \sum_{j=k-d_m}^{k-d_m-1} \eta_j^\top \mathrm{R}_1 \eta_j \geq \mathbb{H}_1$ and $d_\Delta \sum_{j=k-d_\mathrm{M}}^{k-d_k-1} \eta_j^\top \mathrm{R}_1 \eta_j \geq \mathbb{H}_2$, where

$$\mathbb{H}_1 = \frac{d_\Delta}{d_k - d_m} \left(x_{k-d_m}^\top - x_{k-d_k}^\top\right) \mathrm{R}_1 \left(x_{k-d_m} - x_{k-d_k}\right),$$
$$\mathbb{H}_2 = \frac{d_\Delta}{d_\mathrm{M} - d_k} \left(x_{k-d_k}^\top - x_{k-d_\mathrm{M}}^\top\right) \mathrm{R}_1 \left(x_{k-d_k} - x_{k-d_\mathrm{M}}\right).$$

Consider then Lemma 6.3 with $\Theta(\alpha, \mathrm{R}_1) = \mathbb{H}_1 + \mathbb{H}_2$, $\alpha = \frac{d_k - d_m}{d_\Delta}$, $\zeta_k = \begin{bmatrix} x_{k-d_m}^\top & x_{k-d_\mathrm{M}}^\top & x_{k-d_k}^\top \end{bmatrix}^\top$, $\mathrm{W}_1 = \begin{bmatrix} \mathrm{I} & 0 & -\mathrm{I} \end{bmatrix}$, $\mathrm{W}_2 = \begin{bmatrix} 0 & -\mathrm{I} & \mathrm{I} \end{bmatrix}$ to obtain $\mathbb{H}_1 + \mathbb{H}_2 \geq \chi_k^\top \mathrm{T} \chi_k$, where

$$\chi_k = \begin{bmatrix} x_{k-d_m} - x_{k-d_k} \\ x_{k-d_k} - x_{k-d_\mathrm{M}} \end{bmatrix}, \text{ and } \mathrm{T} = \begin{bmatrix} \mathrm{R}_1 & \mathrm{U}_{12} \\ \star & \mathrm{R}_1 \end{bmatrix} \succeq 0,$$

for some full matrix U_{12}, leading to:

$$\Delta \mathrm{V}_{\mathrm{R}_{1k}} \leq d_\Delta^2 \left(x_{k+1}^\top - x_k^\top\right) \mathrm{R}_1 \left(x_{k+1} - x_k\right) - \chi_k^\top \mathrm{T} \chi_k. \tag{6.18}$$

Adding (6.12), (6.14), (6.15), (6.17), and (6.18), and considering extended vector

$$\gamma_k = \begin{bmatrix} x_{k+1}^\top & x_k^\top & x_{k-d_m}^\top & x_{k-d_\mathrm{M}}^\top & x_{k-d_k}^\top \end{bmatrix}^\top,$$

we obtain the bound $\Delta V_k \leq \gamma_k^\top \Upsilon \gamma_k$, $\forall \gamma$ such that $\Gamma\gamma = 0$, $\gamma \neq 0$, with $\Gamma = \begin{bmatrix} -I & \mathbb{A} & 0 & 0 & \mathbb{A}_d \end{bmatrix}$. Thus, by guaranteeing that $\gamma_k^\top \Upsilon \gamma_k < 0$, we ensure that $\Delta V_k < 0$ and the asymptotically stability of system (6.9). By application of Lemma 6.1, this holds if ${\Gamma^\perp}^\top \Upsilon \Gamma^\perp \prec 0$, where $\Gamma^\perp$ is a basis for the null space of Γ, thus completing the proof of Theorem 6.1. □

Remark 6.3

The condition in Theorem 6.1 could also be obtained by means of the equivalent form (iii) of Lemma 6.1. However, this would lead to an increase of $5n^2$ in the total number of decision variables. In fact, the use of (iii) is more advantageous in case of controller synthesis, due to the flexibility to choose special forms for the Lagrange multiplier J.

6.3.3 Benchmark test of Theorem 6.1

In order to understand the level of conservatism of the conditions in Theorem 6.1, an example usually employed in the literature is recovered. Consider system (6.9) with:

$$\mathbb{A} = \begin{bmatrix} 0.8 & 0.0 \\ 0.05 & 0.9 \end{bmatrix}, \quad \mathbb{A}_d = \begin{bmatrix} -0.1 & 0.0 \\ -0.2 & -0.1 \end{bmatrix}$$

Table 2 shows the obtained results in comparison with others from the literature (see Table 1 in Pandey *et al.* (2018)). Although there is a clear disadvantage in the results for lower bounds on the minimum delay $d_m \leq 10$, we can see an interesting improvement as it becomes higher. As a matter of fact, the obtained results are very close to the best obtained for delays with lower bound $d_m \geq 25$. Also, note that the numerical complexity of the condition is much lower than that of most of the other approaches. This is very important since DTCs are frequently applied to systems with big delay, and the order of the closed loop depends on it, with $n = 3n_p + d_n + 2$, as highlighted earlier in the chapter. For comparison, for a process model with plant order $n_p = 2$ and nominal delay $d_n = 4$, the number of variables of the second condition with least variables (SHAO; HAN, 2011) is 122% higher than the approach here, and the number of variables in Kwon *et al.* (2013) is 648% higher. This is a huge difference that could impact the numerical performance of the conditions. Therefore, we conclude that the choice of LKF and its manipulation has been adequate for the DTC problem in this work, although it can be improved in future research. In the next section, we use this LKF in conjunction with a generalized sector condition to provide stability analysis to system (6.7).

Table 2 – Admissible upper bound d_{M} for various d_m applying Theorem 6.1. Other results from the literature come from Table 1 in Pandey *et al.* (2018).

Methods	d_m= 2	4	6	7	10	15	20	25	30	No. of variables
Theorem 6.1	17	17	17	18	20	23	27	31	35	$3.5n^2+2.5n$
Proposition 1 (SHAO; HAN, 2011)	17	17	18	18	20	23	27	31	35	$8n^2+3n$
Theorem 2 (KWON *et al.*, 2013)	22	22	22	22	23	25	28	32	36	$27n^2+9n$
Theorem 5 (SEURET *et al.*, 2015)	20	21	21	22	23	25	29	32	36	$10.5n^2+3.5n$
Theorem 7 (HIEN; TRINH, 2016)	20	21	21	22	23	25	29	32	36	$20n^2+5n$

6.4 Main results

In this section, we present stability analysis conditions for the saturated closed-loop system (6.7). Theoretical preliminaries are initially reviewed, including the generalized sector condition and the definition of a set of initial conditions for which stability guarantees will be inspected.

6.4.1 Theoretical preliminaries

Consider the deadzone nonlinearity φ, defined as follows

$$\varphi(v_k) = v_k - sat(v_k), \tag{6.19}$$

and the following set

$$\mathscr{L}(v-\theta,\bar{u}) = \{v \in \mathbb{R}; \theta \in \mathbb{R}; -\bar{u} \leq v-\theta \leq \bar{u}\}. \tag{6.20}$$

We then recall the following result which was introduced in Gomes da Silva Jr. and Tarbouriech (2005), here adapted for the simpler case of systems with a one-dimensional control input.

Lemma 6.4: Generalized sector condition

If v and θ belong to set $\mathscr{L}$, then the deadzone nonlinearity $\varphi(v)$ satisfies the following inequality, which is true for any matrix W in $\mathbb{S}_1^+$

$$\varphi^\top(v)\mathrm{W}[\varphi(v)-\theta] \leq 0. \tag{6.21}$$

By taking into account the original system (6.7) and the identity (6.19), the following

equivalent closed-loop representation is obtained

$$\begin{cases} x_{k+1} = \mathbb{A}x_k + \mathbb{A}_{\mathrm{d}}x_{k-d_k} - \mathrm{B}\varphi(v_k) + \mathrm{B}_{\mathrm{q}}q_k \\ v_k = \mathrm{K}x_k + \mathrm{K}_{\mathrm{d}}x_{k-d_k} \\ x_k = \phi_k,\ k \in [-d_{\mathrm{M}}, 0] \end{cases} \tag{6.22}$$

where $\mathbb{A} = \mathrm{A} + \mathrm{BK}$ and $\mathbb{A}_{\mathrm{d}} = \mathrm{A}_{\mathrm{d}} + \mathrm{BK}_{\mathrm{d}}$. This representation allows us to analyze the system stability using a combination of the Lyapunov functional (6.11) and the generalized sector condition provided in Lemma 6.4. Due to the saturating actuator, we need to analyse regional stability of (6.22), i.e. we need to find a set of initial conditions ϕ_k for which the asymptotic stability of the closed loop is ensured. First of all, note that we can rewrite the Lyapunov-Krasovskii functional (6.11) in the following augmented form $\mathrm{V}_k = \bar{x}_k^\top \mathbb{P} \bar{x}_k$, with $\bar{x}_k = \begin{bmatrix} x_k^\top & x_{k-1}^\top & \cdots & x_{k-d_{\mathrm{M}}}^\top \end{bmatrix}^\top$ and:

$$\mathbb{P} = \begin{bmatrix} \mathbb{P}_0 & \mathbb{P}_{b_1} & 0 & \cdots & 0 & \cdots & 0 \\ \star & \mathbb{P}_{a_1} & \ddots & \ddots & \vdots & \ddots & \vdots \\ \star & \ddots & \ddots & \mathbb{P}_{b_{d_m}} & 0 & \cdots & 0 \\ \vdots & \ddots & \star & \mathbb{P}_{a_{d_m}} & \mathbb{P}_{d_1} & \ddots & \vdots \\ \star & \cdots & \star & \star & \mathbb{P}_{c_1} & \ddots & 0 \\ \vdots & \ddots & \vdots & \ddots & \ddots & \ddots & \mathbb{P}_{d_{d_\Delta}} \\ \star & \cdots & \star & \cdots & \star & \star & \mathbb{P}_{c_{d_\Delta}} \end{bmatrix},$$

where

$$\begin{aligned} \mathbb{P}_0 &= \mathrm{Q} + \mathrm{R}d_m^2 + \mathrm{R}_1 d_\Delta^2, \\ \mathbb{P}_{a_i} &= \mathrm{U} + 2\mathrm{R}_1 d_\Delta^2 + \mathrm{R}d_m(2d_m - 2i + 1), \\ \mathbb{P}_{b_i} &= -\mathrm{R}_1 d_\Delta^2 - \mathrm{R}d_m(d_m - i + 1), \\ \mathbb{P}_{c_j} &= \mathrm{U}_1 + \mathrm{R}_1 d_\Delta(2d_\Delta - 2j + 1), \\ \mathbb{P}_{d_j} &= -\mathrm{R}_1 d_\Delta(d_\Delta - j + 1), \end{aligned}$$

for $i \in [1, d_m]$ and $j \in [1, d_\Delta]$. Then, we define the set of initial conditions as $\mathbb{D}_\phi = \{\phi_k \in \mathbb{R}^{(d_{\mathrm{M}}+1)\times n}; \phi_k^\top \mathbb{P}\phi_k \leq \beta\}$, with $\beta > 0$.

6.4.2 Stability in the saturated case

The following theorem provides a solution to Problem 6.1.

Theorem 6.2

For given positive scalar σ, assume the existence of matrices Q, R, U, R_1, U_1 in $\mathbb{S}_n^+$, matrices U_{12} in $\mathbb{R}^{n\times n}$, Z in $\mathbb{R}^{1\times n}$, W in $\mathbb{S}_1^+$, and positive scalars δ, μ such that

$$T = \begin{bmatrix} R_1 & U_{12} \\ \star & R_1 \end{bmatrix} \succeq 0, \;\; \Xi^{\perp^\top} \Phi \Xi^{\perp} \prec 0, \tag{6.23}$$

$$\Sigma = \begin{bmatrix} Q & K^\top W - Z^\top \\ \star & 2W\sigma - \mu \left(\frac{\sigma}{\bar{u}}\right)^2 \end{bmatrix} \succeq 0, \tag{6.24}$$

$$\mu - \delta > 0, \tag{6.25}$$

with $\Xi^{\perp} = \begin{bmatrix} \mathbb{A} & 0 & 0 & \mathbb{A}_d & -B & B_q \\ & & & I_{4n+2} & & \end{bmatrix}$ and

$$\Phi = \begin{bmatrix} & \begin{bmatrix} 0 & 0 \\ Z^\top & 0 \\ 0 & 0 \\ 0 & 0 \\ K_d{}^\top W & 0 \end{bmatrix} \\ \Upsilon & \\ & \\ \star & \begin{bmatrix} -2W & 0 \\ \star & -I \end{bmatrix} \end{bmatrix},$$

where Υ has been given in Theorem 6.1. Then

1. For any $q \in \mathcal{Q}$ and all $\phi_k \in \mathbb{D}_\phi = \{\phi_k \in \mathbb{R}^{(d_M+1)\times n}; \phi_k^\top \mathbb{P} \phi_k \leq \beta\}$, $\beta = \mu - \delta$, the trajectories of (6.22) do not leave the ellipsoid given by $\mathbb{D}_{\bar{x}} = \{\bar{x}_k \in \mathbb{R}^{(d_M+1)\times n}; \bar{x}_k^\top \mathbb{P} \bar{x}_k \leq \mu\}$, for all $k > 0$.
2. For $q_k = 0$, the set $\mathbb{D}_{\bar{x}}$ is a region of asymptotic stability of (6.22).

Proof. First, consider an auxiliary matrix $G \in \mathbb{R}^{1\times n}$ and application of Lemma 6.4 with $v = Kx_k + K_d x_{k-d_k}$, $\theta = Gx_k + K_d x_{k-d_k}$. If x_k belongs to the resulting set

$$\mathscr{L}(|K-G|, \bar{u}) = \{x \in \mathbb{R}^n; -\bar{u} \leq (K-G)x \leq \bar{u}\}, \tag{6.26}$$

then the inequality:

$$-2\varphi^{\top}(v_k)\mathrm{W}\left[\varphi(v_k)-\mathrm{G}x_k-\mathrm{K_d}x_{k-d_k}\right]\geq 0 \tag{6.27}$$

is satisfied for some W in $\mathbb{S}_1^+$.

Consider also relation (6.24). Use the fact that

$$\left(\frac{\mu\sigma}{\bar{u}^2}-\mathrm{W}\right)^{\top}\frac{\mu^{-1}\bar{u}^2}{\sigma}\left(\frac{\mu\sigma}{\bar{u}^2}-\mathrm{W}\right)\succeq 0$$

to replace $2\mathrm{W}\sigma-\mu\left(\frac{\sigma}{\bar{u}}\right)^2$ by $\mathrm{W}^{\top}\mu^{-1}\bar{u}^2\mathrm{W}$ in (6.24). Then, pre- and post-multiply the obtained inequality by $\mathrm{diag}\left(\mathrm{I},\mathrm{W}^{-1}\right)^{\top}$ to obtain relation:

$$\begin{bmatrix}\mathrm{Q} & (\mathrm{K}-\mathrm{G})^{\top}\\ \star & \mu^{-1}\bar{u}^2\end{bmatrix}\succeq 0$$

which ensures the inclusion of the ellipsoid $\varepsilon(\mathrm{Q},\mu)=\{x_k\in\mathbb{R}^n;x_k^{\top}\mathrm{Q}x_k\leq\mu\}$ in the polyhedral set $\mathscr{L}$. Since $x_k^{\top}\mathrm{Q}x_k\leq\bar{x}_k^{\top}\mathbb{P}\bar{x}_k\leq\mu$, if $\phi_k\in\mathbb{D}_{\phi}$, then $x_k\in\varepsilon(\mathrm{Q},\mu)\subset\mathscr{L}$, $\forall k>0$, and the sector condition is effectively validated.

Now, consider relation (6.23). Replace $\mathrm{Z}^{\top}$ by $\mathrm{G}^{\top}\mathrm{W}$ in Φ and note that left and right multiplication of the resulting matrix by $\xi_k^{\top}$ and $\xi_k=\begin{bmatrix}\gamma_k^{\top} & \varphi(v_k)^{\top} & q_k^{\top}\end{bmatrix}^{\top}$, respectively, leads to the expression

$$\xi_k^{\top}\Phi\xi_k=\gamma_k^{\top}\Upsilon\gamma_k-q_k^{\top}q_k-2\varphi^{\top}(v_k)\mathrm{W}\left[\varphi(v_k)-\mathrm{G}x_k-\mathrm{K_d}x_{k-d_k}\right], \tag{6.28}$$

where the vector $\gamma_k=\begin{bmatrix}x_{k+1}^{\top} & x_k^{\top} & x_{k-d_m}^{\top} & x_{k-d_\mathrm{M}}^{\top} & x_{k-d_k}^{\top}\end{bmatrix}^{\top}$ was first given in the proof of Theorem 6.1. From the proof of Theorem 6.1 and relation (6.21), we have that $\gamma_k^{\top}\Upsilon\gamma_k\geq\Delta\mathrm{V}_k$ and $-2\varphi^{\top}(v_k)\mathrm{W}\left[\varphi(v_k)-\mathrm{G}x_k-\mathrm{K_d}x_{k-d_k}\right]>0$, respectively, leading to

$$\xi_k^{\top}\Phi\xi_k\geq\gamma_k^{\top}\Upsilon\gamma_k-q_k^{\top}q_k\geq\Delta\mathrm{V}_k-q_k^{\top}q_k. \tag{6.29}$$

Therefore, by guaranteeing that $\xi_k^{\top}\Phi\xi_k<0$ we guarantee that $\Delta\mathrm{V}_k-q_k^{\top}q_k<0$ for all $\bar{x}_k\in\mathbb{D}_{\bar{x}}$, provided that $x_k\in\mathscr{L}$. Then by computing $\sum_{i=0}^{k}\left(\Delta\mathrm{V}_i-q_i^{\top}q_i\right)<0$ it follows $\mathrm{V}_k-\mathrm{V}_0-\sum_{i=0}^{k}q_i^{\top}q_i<0$, $\forall k\geq 0$. In other words, this implies that

- $\mathrm{V}_k<\mathrm{V}_0+\|q_k\|^2\leq\beta+\delta=\mu$, for all $k\geq 0$, thus the trajectories of (6.22) remain bounded by the ellipsoid given by $\mathbb{D}_{\bar{x}}=\{\bar{x}_k\in\mathbb{R}^{(d_\mathrm{M}+1)\times n};\bar{x}_k^{\top}\mathbb{P}\bar{x}_k\leq\mu\}$.

- If $q_k = 0$, $\forall k \geq \bar{k} \geq 0$, then $\Delta V_k \leq 0$, ensuring that $x_k \to 0$, without leaving $\mathbb{D}_{\bar{x}}$, as $k \to \infty$.

From Finsler's Lemma, satisfaction of $\xi_k^\top \Phi \xi_k < 0$, $\forall \xi$ such that $\Xi\xi = 0$, $\xi \neq 0$, with $\Xi = \begin{bmatrix} -I & \mathbb{A} & 0 & 0 & \mathbb{A}_d & -B & B_q \end{bmatrix}$ (and therefore of $\Delta V_k - q_k^\top q_k < 0$) along the trajectories of (6.22) is equivalent to the satisfaction of ${\Xi^\perp}^\top \Phi \Xi^\perp \prec 0$, where $\Xi^\perp$ is a basis for the null space of Ξ, thus leading to (6.23). This completes the proof of all the items in Theorem 6.2. □

Remark 6.4

Although the dimension of the matrix $\mathbb{P}$ can be high, specially for long delays, it does not lead to some numerical burden of the optimization schemes since the matrix $\mathbb{P}$ is not a decision variable in Theorem 6.2. In fact, the matrix $\mathbb{P}$ is assembled with the LKF matrices $\{Q,R,R_1,U,U_1\}$, which are the decision variables in the theorem. Furthermore, as introduced in Section 2.3, all the works dealing with the LKF approach to stability of saturated discrete-time delayed systems characterize the region of attraction by bounding some norm of the sequence of initial condition (see for example Chen and Fei (2014)). In this case, conservative operations are involved to find the scalar bound on the norm. No such conservatism is present in the case we utilise the matrix $\mathbb{P}$ since it is an augmentation of the LKF, which does not require any extra bounding.

Additionally, for open-loop stable systems, one may look for a condition ensuring the global stability of the closed-loop system.

Corollary 6.1

Assume the existence of matrices Q, R, U, R_1, U_1 in $\mathbb{S}_n^+$, matrices U_{12} in $\mathbb{R}^{n\times n}$ and W in $\mathbb{S}_1^+$ such that $T \succeq 0$, ${\Xi^\perp}^\top \Phi \Xi^\perp \prec 0$ with T, Ξ, and Φ defined in Theorem 6.2 and $Z^\top = K^\top W$, then

1. For $q_k = 0$, the whole state-space is a region of asymptotic stability of (6.22).
2. For any $q \in \mathcal{Q}$, and any initial condition $\phi \in \mathbb{R}^{(d_M+1)\times n}$, the trajectories of (6.22) remain bounded as follows:

$$V_k \leq V_0 + \delta, \forall k \geq 0.$$

Proof. Proof is straightforward by noting that (6.27) is satisfied for all $x_k \in \mathbb{R}^n$ when G = K. In this case, both relations (6.24) and (6.25) become pointless. □

6.4.3 Computational Issues

Theorem 6.2 provides conditions to prove regional stability results for the closed-loop system along with a characterization of the ellipsoidal region of stability and the energy-bounded disturbance that affects the system. By application of the presented convex conditions, different analysis results can be exploited. In the following, we present two particular cases of interest. First, we would like to find out the maximum energy bound (δ) on the external disturbance belonging to the set $\mathcal{Q}$ when the system is at equilibrium ($\bar{x}_0 = 0$). Secondly, we are interested in maximizing, in some sense, the estimate of the region of attraction.

6.4.3.1 Disturbance tolerance maximization

In the case of $\bar{x}_0 = 0$, it follows that $\beta = 0$ and $\mu = \delta$, and we seek to maximize the system tolerance to disturbances, that is, we aim at maximizing the energy bound on the set $\mathcal{Q}$. For given positive scalar σ, the following optimization procedure should be applied:

$$\begin{cases} \max\limits_{\{\mathrm{Q,R,U,R_1,U_1,U_{12},Z,W},\mu\}} \quad \mu \\ \quad \text{subject to (6.23), (6.24)} \end{cases} \tag{6.30}$$

6.4.3.2 Maximization of the plant initial conditions set

Consider system (6.7) affected by a fixed level of disturbance, that is a fixed δ. In this case, one is interested in maximizing the estimate on the region of attraction, that is the ellipsoid $\mathbb{D}_{\bar{x}}$. Many different criteria can be adopted, such as volume maximization and maximization of the ellipsoid semi-minor axis. In this work, we adopt the later criteria, which is equivalent to the minimization of the biggest eigenvalue of the matrix $\mathbb{P}\mu^{-1}$. The length of the semi-minor axis of the ellipsoid is equal to the radius of the maximum ball inside the ellipsoidal region of stability, and can be a useful qualitative measurement of the region in order to relate it to both the DTC tuning parameter ρ and the size of the delay. A convex optimization procedure to indirectly achieve this goal is to run the following optimization problem

$$\begin{cases} \min\limits_{\{\mathrm{Q,R,U,R_1,U_1,U_{12},Z,W},\mu\}} \quad \kappa_1\lambda - \kappa_2\mu \\ \quad \text{subject to (6.23), (6.24), (6.25)}, \mathbb{P} \prec \lambda \mathrm{I}_{(d_\mathrm{M}+1)\times n} \end{cases} \tag{6.31}$$

with κ_1 and κ_2 tuning weighting on λ and μ. The length of the semi-minor axis can then be computed by $\omega_b = \lambda_{max}^{-1/2}$, where λ_{max} is the maximum eigenvalue of the matrix $\mathbb{P}\mu^{-1}$. In the

case that no perturbation affects system (6.7), we have $\delta = 0$. Since, we can remove the last column as well as the last line of ${\Xi^{\perp}}^{\top}\Phi\Xi^{\perp}$ in (6.23) while running optimization problem (6.31).

Remark 6.5

Note that the initial condition for the open-loop plant (6.1) is characterized only by x_{p_0}. Although for the time-delay closed-loop system (6.7) we could choose to consider the past states as zero and consider the initial condition as the special case $\phi_k = \begin{bmatrix} x_0^\top & 0 & \cdots & 0 \end{bmatrix}^\top$, $x_0 = \begin{bmatrix} x_{p0}^\top & x_{s_0}^\top & x_{f_0}^\top \end{bmatrix}^\top$, we chose to consider the more general case in this work with the sequence ϕ_k so that the initial condition can be anything as long as it is inside the set $\mathbb{D}_\phi = \{\phi_k \in \mathbb{R}^{(d_\mathrm{M}+1)\times n}; \phi_k^\top \mathbb{P}\phi_k \leq \beta\}$.

6.5 Numerical Examples

6.5.1 Case study 1

This first example is dedicated to understanding how the DTC tuning parameter ρ relates to the system robustness. Simulations are performed for the open-loop unstable process $G(s) = \frac{1}{4s-1}$, studied in Normey-Rico *et al.* (2012). This model represents the linearized dynamical behaviour of the output concentration of some chemical reactors around the unstable operation point.

As in Normey-Rico *et al.* (2012), it is assumed that there exists a measurement delay due to the time needed by the concentration transducer to give the output variable, which can vary between 0.5 and 0.7 seconds. By considering a sampling time of 0.1 seconds we obtain the discrete-time process model (6.1) with $\mathrm{A}_p = 1.0253$, $\mathrm{B}_p = 0.1250$ and $\mathrm{C}_p = 0.2025$ and time-varying delay $5 \leq d_k \leq 7$.

Initially, we consider the DTC design from Torrico *et al.* (2018), in Chapter 4, with $d_n = 6$, $\rho = 0.90$, and desired closed-loop pole $\{0.92\}$, so that fast set-point regulation is achieved in the ideal case (no saturation and no time-varying delay).

To illustrate the closed-loop system time-response, Fig. 28 shows simulation results for an initial condition $\phi_k = 0\ \forall k \in [-d_\mathrm{M}, 0]$, and disturbance signal of energy $\delta = 27.3053$. Stability is guaranteed by means of Theorem 6.2 with $\sigma = 0.01$, using optimization problem (6.30). In this case $\mu = \delta$. Three cases are plotted:

- Ideal case, that is constant delay $d_k = d_n$ and no saturation $\bar{u} = \infty$.

- System with time-varying delay $5 \leq d_k \leq 7$ and no saturation, $\bar{u} = \infty$.
- System with both time-varying delay and saturation. In this case, for analysis purposes we consider $\bar{u} = 1.5$.

Figure 28 – Case study 1 simulation results.

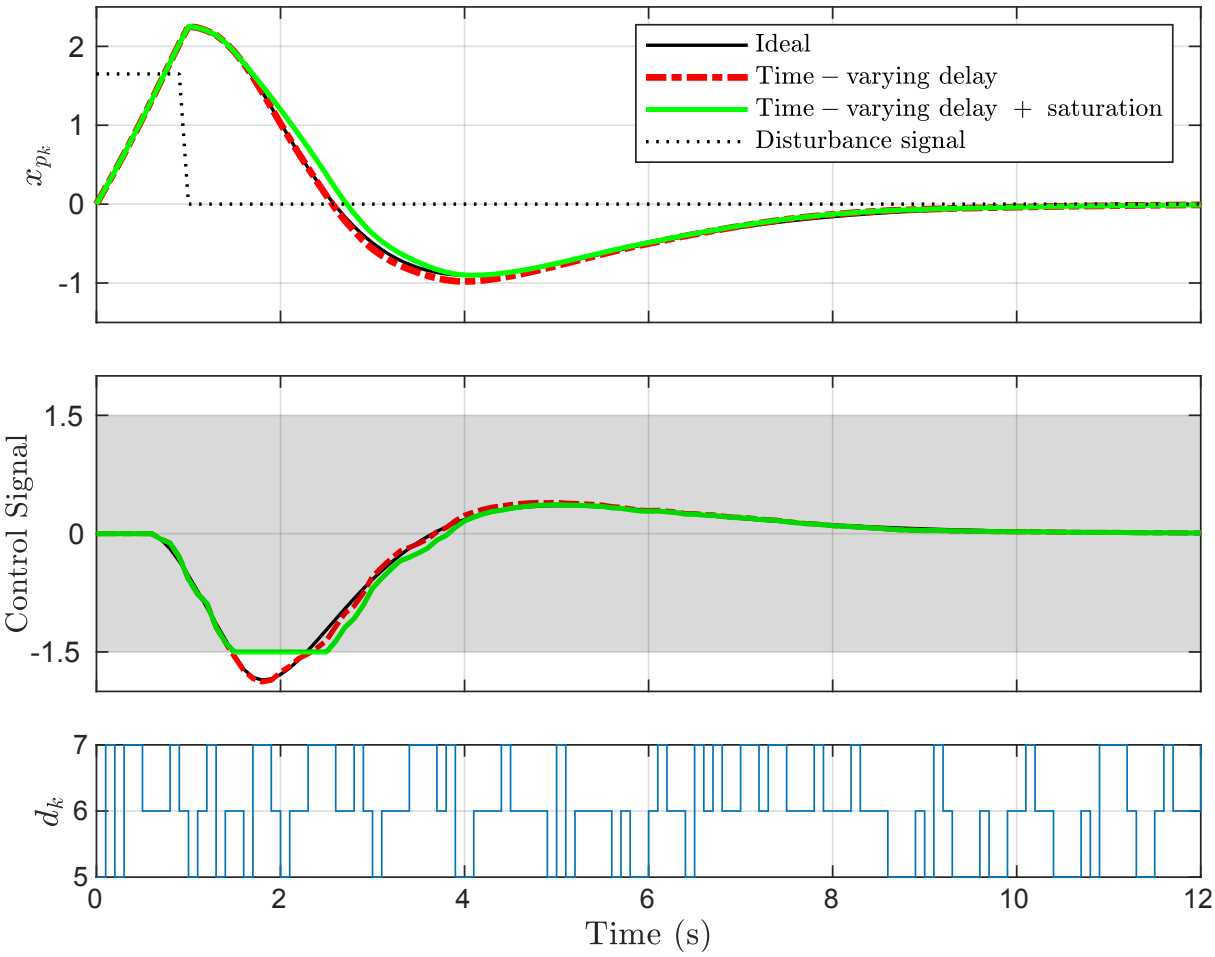

Source: The author.

In the following subsections, with the help from Theorems 6.1 and 6.2, and optimization procedures (6.30), (6.31), we will give more comments on the simulations and how the values of ρ and $\bar{u}$ affect the system robustness and effectiveness.

6.5.1.1 The unsaturated case

From Fig. 28, it can be noted that the DTC controller is robust to the uncertainty introduced by the time-varying delay since the response is very close to the response of the ideal case. For an extended analysis, by means of Theorem 6.1, Table 3 provides the admissible upper

bound d_{M} for various values of ρ with fixed lower bound $d_m = 5$.

From the DTC literature, it is well known that higher values of the robustness filter parameter ρ introduce more robustness to the system regarding uncertainties in the delay (in the constant case). This was also confirmed in the case of time-varying delays in Normey-Rico *et al.* (2012). As expected, Table 3 also illustrates this fact by showing that higher values of ρ allow for an increase in the admissible upper bound d_{M} on the delay. However, it is well-known in the DTC literature that higher values of ρ can also cause slower rejection of disturbances, which illustrates the trade-off between performance and robustness.

Table 3 – Case study 1- Admissible upper bound d_{M} for various values of ρ with $d_m = 5$ (unsaturated case).

ρ	0.89	0.91	0.93	0.95	0.97
d_{M}	9	10	12	15	18

Source: The author.

6.5.1.2 The saturated case

From Fig. 28 note that although the control signal saturates at the beginning of the simulation, the controller is capable of bringing the system back to equilibrium in a nice manner.

In order to better understand the relation between tuning parameter ρ, the bound on the control signal $\bar{u}$, the plant delay and robustness of the DTC strategy, Figures 29 and 30 show multiple 3-dimensional surfaces for different values of the maximum delay d_{M} built by interpolating a data grid of $(\rho, \bar{u})$ values, in which the $z-axis$ represent δ and ω_b (the radius of the maximum ball inside $\mathbb{D}_{\bar{x}}$), respectively. Such results are obtained by means of optimization problems (6.30) and (6.31) (in this case, with $\delta = 0$). One can observe that as ρ increases, the values of both ω_b and δ for which stability is guaranteed are increased. This nicely illustrates that, as in the unsaturated LTI case, higher values of ρ improve the system overall robustness for systems with both time-varying delays and input saturation. Of course, as the control bound $\bar{u}$ is increased, the system also becomes suitable to deal with bigger initial conditions and disturbances of higher energy. Additionally, as the maximum delay d_{M} is increased, both the values of δ and ω_b decrease. This illustrates the bad impact of the time delay in the stability region, and also in the disturbance tolerance of the closed loop.

Finally, a special case worth of comment is that of known constant delay $d_m = d_{\mathrm{M}} = d_n = 5$. Using optimization problems (6.30) and (6.31) with $\rho = 0.93, \bar{u} = 2$, we find significant

Figure 29 – Relation between DTC tuning parameter ρ, saturation limit $\bar{u}$, the maximum delay d_{M} (with $d_m = 5$), and the energy bound of the disturbance δ.

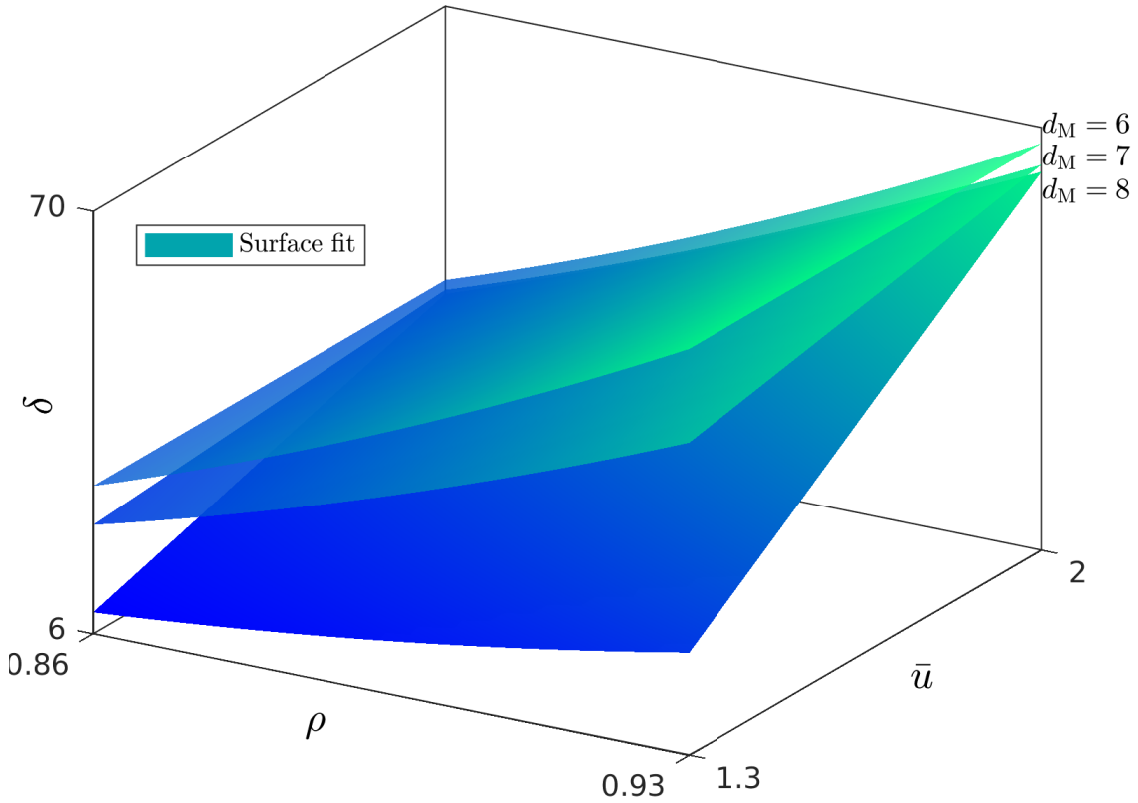

Source: The author.

Figure 30 – Relation between DTC tuning parameter ρ, saturation limit $\bar{u}$, the maximum delay d_{M} (with $d_m = 5$), and the radius ω_b of the maximum ball inside $\mathbb{D}_{\bar{x}}$.

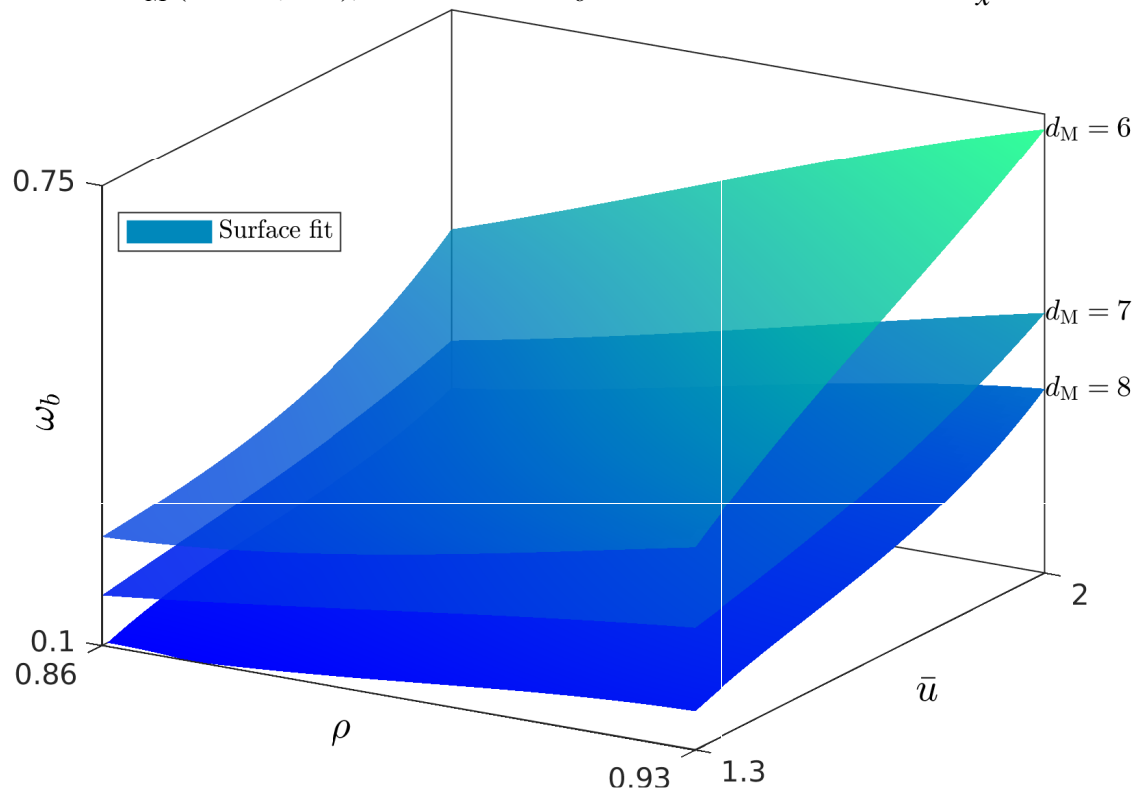

Source: The author.

increases in both ω_b and δ, being 1.0276 and 71.8202, respectively. This is due to the perfect delay compensation obtained by the predictor in this case. Let us remark that, for consistency of the results, the desired closed-loop pole for the DTC design and the Theorem 6.2 parameter σ were kept as $\{0.95\}$ and 0.05, respectively, throughout the simulations.

6.5.2 Case study 2

Consider the NCS studied in Hu *et al.* (2007):

$$\dot{x}_p = \begin{bmatrix} -0.80 & -0.01 \\ 1.00 & 0.10 \end{bmatrix} x_p + \begin{bmatrix} 0.4 \\ 0.1 \end{bmatrix} u$$

By considering a sampling time of 0.5 seconds, an induced network time delay, and choosing the second state as output for the DTC design, we obtain the discrete-time model (6.1) with $\mathrm{A}_p = \begin{bmatrix} 0.6693 & -0.0042 \\ 0.4231 & 1.0501 \end{bmatrix}$, $\mathrm{B}_p = \begin{bmatrix} 0.1647 \\ 0.0960 \end{bmatrix}$, and $\mathrm{C}_p = \begin{bmatrix} 0 & 1 \end{bmatrix}$. In Hu *et al.* (2007), the control law is given by $v_k = -\begin{bmatrix} 1.2625 & 1.2679 \end{bmatrix} x_{p_{k-d_k}}$, which guarantees closed-loop stability for a maximum induced delay of 1 second (or two samples), according to Theorem 4 of Hu *et al.* (2007). By using Theorem 6.1 of the work herein with $\mathbb{A} = \mathrm{A}_p$, $\mathbb{A}_\mathrm{d} = -\mathrm{B}_p \begin{bmatrix} 1.2625 & 1.2679 \end{bmatrix}$, we obtain that stability using the control law from Hu *et al.* (2007) is guaranteed for a maximum delay in the range $1 \leq d_k \leq 3$. In the case of no delay, the control law from Hu *et al.* (2007) would yield closed-loop poles $\{0.6950 + 0.0990i, 0.6950 - 0.0990i\}$. To design the DTC controller for this example, the desired closed-loop poles are chosen as $\{0.6950 + 0.0990i, 0.6950 - 0.0990i, 0.7\}$, and we initially set $\rho = 0.7$, which guarantees stability for the system by means of Theorem 6.1.

To illustrate the closed-loop system time-response, Fig. 31 shows simulation results for an initial condition given by $x_{p_0} = \begin{bmatrix} 0.4919 & 0.4919 \end{bmatrix}^\top$ and 0 in all other positions of ϕ_k. Even though the original example in Hu *et al.* (2007) does not deal with saturation, the response of the saturated DTC closed loop is also plotted, for illustration purposes, considering $\bar{u} = 1$. Stability in this case is guaranteed by means of Theorem 6.2 with $\sigma = 0.05$, using optimization problem (6.31) with $\delta = 0, \kappa_1 = \kappa_2 = 1$, obtaining $\mu = 0.070866$. To enlarge the region of stability in the directions of the plant states a small modification in (6.31) was used with substitution of $\mathbb{P} \prec \lambda \mathrm{I}_{(d_\mathrm{M}+1)\times n}$ by $\begin{bmatrix} \mathrm{I}_{n_p} & 0 \end{bmatrix} \mathbb{P} \begin{bmatrix} \mathrm{I}_{n_p} & 0 \end{bmatrix}^\top \preceq \lambda \mathrm{I}_{n_p}$. Although both strategies present similar performance, the control signal of the DTC strategy is less aggressive. Moreover, opposed to the compared control law, the DTC obtained the results by feedback of only one of the states.

Figure 31 – Case study 2 simulation results.

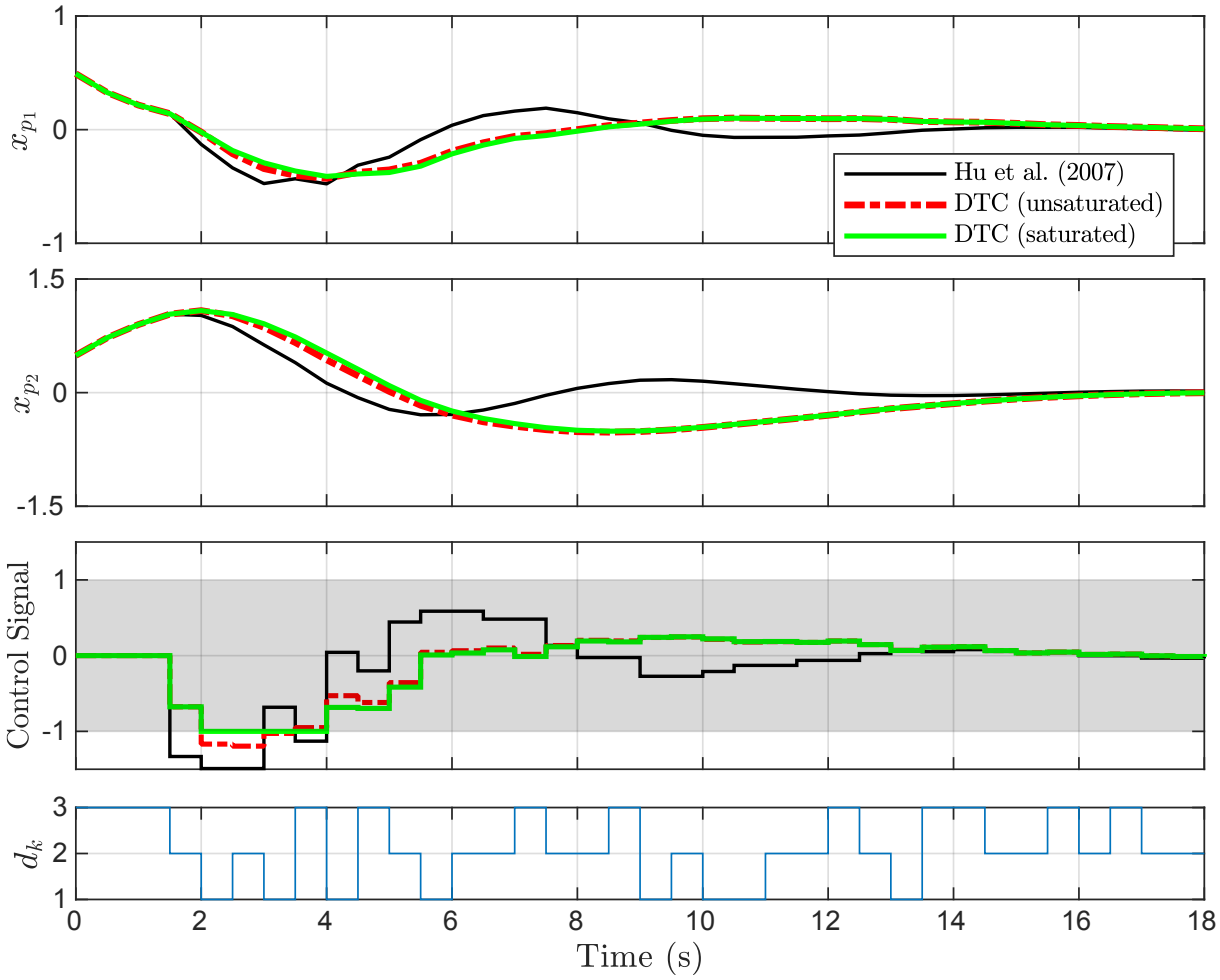

Source: The author.

The main advantage of the DTC strategy is yet the possibility to deal with much bigger delays by simply increasing the value of the robustness filter ($\mathcal{F}_r$) tuning parameter ρ. To illustrate this, Table 4 shows the relation between the maximum delay d_{M} and ρ for this example, obtained by means of Theorem 6.1. As shown in the table, with the DTC it is possible to guarantee stability for the system even for a time-varying delay in the range $1 \leq d_k \leq 7$.

Table 4 – Case study 2- Admissible upper bound d_{M} for various values of ρ with $d_m = 1$.

ρ	0.75	0.80	0.86	0.9
d_{M}	4	5	6	7

Source: The author.

In conclusion, the use of the DTC is advantageous when there is no access to the measurement of the full state since the DTC is able to stabilize the system with only measurement

of the output, and when it is desired to stabilize the system for long delays in the network. On the other hand, the advantage with the classical state feedback law is its implementation simplicity, with closed-loop order $n = n_p = 2$, while the closed-loop order using the DTC is $n = 3n_p + d_n + 2 = 10$.

6.6 Experimental Results

This section shows practical results of the DTC structure, applied for temperature control of an in-house neonatal intensive care unit (NICU) prototype, depicted in Fig. 32 (PEREIRA *et al.*, 2017). The physical structure of the NICU prototype consists of two main parts: an acrylic dome in which the temperature should be controlled; and a reservoir right below the acrylic dome containing a heating resistor, and a fan with constant speed. These two environments are connected by two openings so that the heated air can circulate through the acrylic dome. The control variable is the electrical voltage applied, by means of a driving circuitry, to the terminals of the heating resistor, and is constrained in the range from 0 to 2 Volts.

Figure 32 – Picture of the NICU prototype.

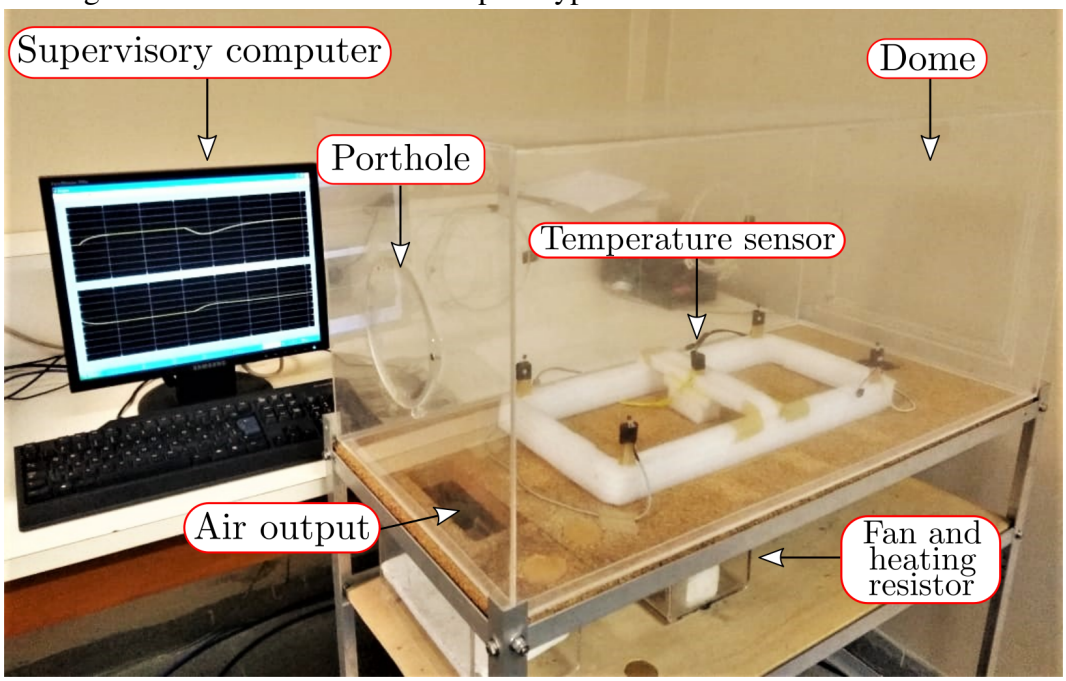

Source: The author.

The driving circuitry is commanded by a supervisory computer through the digital-to-analog converter (DAC) channel of a data acquisition card. In order to close the control loop, the temperature sensor inside the acrylic dome provides actual measurement to the supervisory

computer by using a microcontroller (μC), which implements the communication protocols of the sensor and converts the digital data from the sensor to analogue voltage values, combined with the analog-to-digital converter (ADC) channel of the same data acquisition card. The data acquisition card communicates with the supervisory computer through a USB cable.

In front of the acrylic dome, two portholes for manipulation of newborns are present which, when opened, disturb the temperature inside the dome due to the interaction with the external environment, which could be in much higher or lower temperature.

Using a step-test identification procedure (NORMEY-RICO; CAMACHO, 2007), the plant model has been identified around an equilibrium point designated by the pair

$$\left(x_{p_{eq}} = 28.3^{o}\text{C}, u_{eq} = 1 \text{ Volt}\right)$$

and is given by $P_n(s) = \frac{1.572e^{-1.17s}}{17.35s+1}$, where the time constant is given in minutes. Using a sampling time of 0.2 minutes, the discrete-time model is obtained as $P_n(z) = \frac{0.018017}{z-0.9885} z^{-6}$.

In order to experimentally validate the DTC ability to deal with both saturation and time-varying delays, we introduce an additional artificial measurement delay (d_{A_k}) which can vary between 0 and 4 samples and has been induced by software using a random number generator. Therefore, we obtain the discrete-time process model (6.1) with $\text{A}_p = 0.9885$, $\text{B}_p = 0.0180$, $\text{C}_p = 1$, time-varying delay $6 \leq d_k \leq 10$ and saturation level $\bar{u} = 1$. A detailed diagram depicting the incubator and the experimental setting is shown in Fig. 33.

For the design of the DTC, the desired closed-loop pole is set as $\{0.94\}$, and the robustness filter $\mathcal{F}_r$ is tuned with $\rho = 0.93$ to achieve a good trade-off between system robustness and disturbance rejection speed. Global stability has been guaranteed by means of Corollary 6.1.

Experimental results are shown in Fig. 34 for an initial temperature of $27.3^{o}C$ (one degree below the equilibrium temperature). It is important to note that even though the plant input became saturated during the first 12 minutes, the controller did not present windup issues and was able to go back to the equilibrium temperature of $28.3^{o}C$. In order to further assess controller robustness, front portholes of the NICU were opened between $t = 31.4$ min and $t = 38.4$ min. The room temperature was at $19.9^{o}C$ during the experiment, which introduces a high level of disturbance. Even though the control signal saturates again, such a disturbance was properly rejected and equilibrium was restored some time later.

Figure 33 – Experimental setup diagram of the NICU. Dashed lines refer to digital signals while solid ones refer to analogue signals.

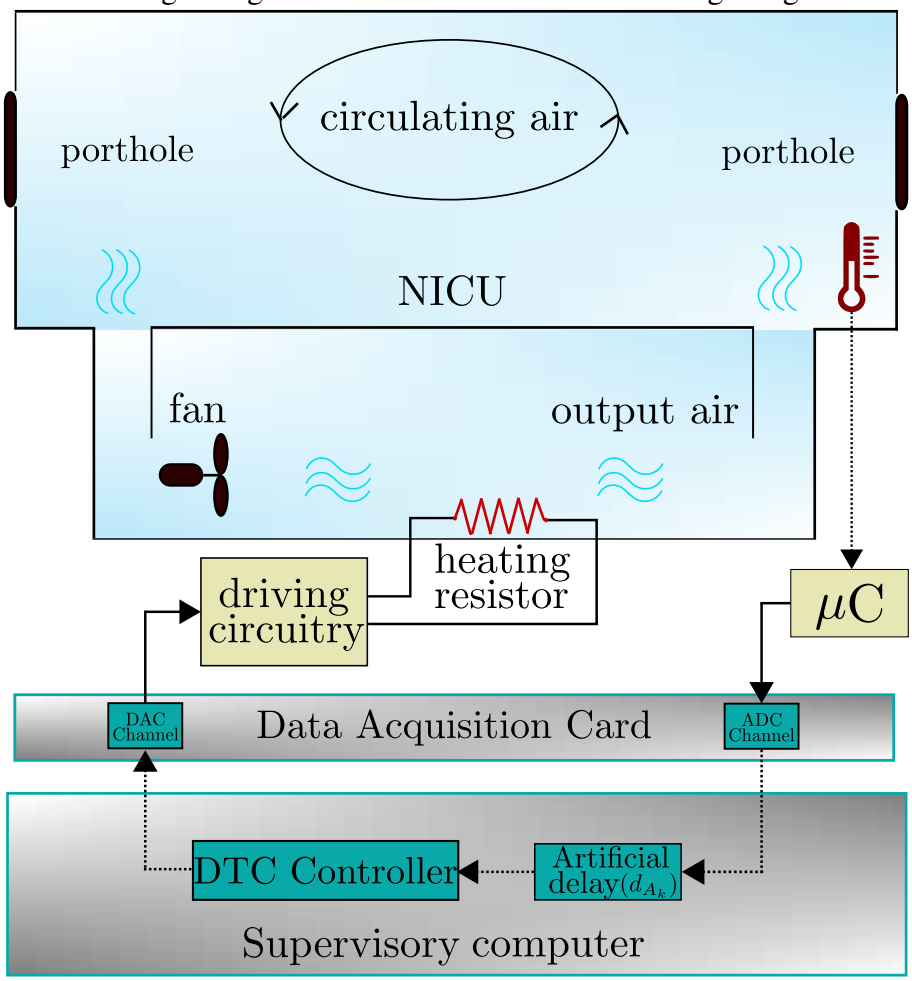

Source: The author.

Remark 6.6

The YALMIP toolbox (LÖFBERG, 2004) was used for solving the LMIs and optimization problems throughout the chapter. The obtained matrices $\{Q, R, U, R_1, U_1, U_{12}, Z, W\}$ for the two numerical examples and the experimental application can be consulted in the supplementary material for Alves Lima *et al.* (2021a) at <https://hal.archives-ouvertes.fr/hal-02965943>.

6.7 Discussion

This work presented, for the first time, stability analysis of a dead-time compensator structure for input-saturated processes with output time-varying delays. The simulation case studies and the experiment for the control of temperature in a neonatal incubator effectively showed the good qualities of DTC structures dealing with the addressed type of process. The

Figure 34 – Experimental results: Temperature control of a NICU.

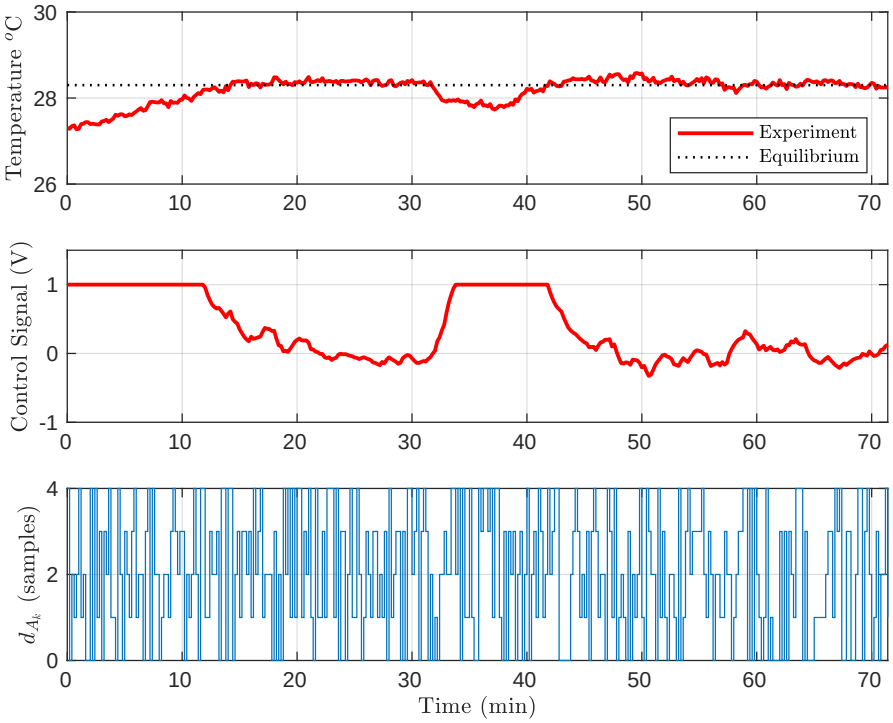

Source: The author.

numerical examples were useful to show that the DTC tuning parameter ρ may adjust the classical trade-off between robustness and disturbance rejection performance. Since DTCs are a class of controller frequently used in practical applications, the developed analysis is of importance for the control of industrial dead-time processes.

On the theoretical side, the developed conditions were effective to properly analyse stability of the closed loop, and a potentially less conservative methodology for the definition of the set of initial conditions has been proposed, which can be used in works employing the LKF approach for stability analysis of discrete-time systems. Future work will address the stabilization problem by developing a full state-space approach for the DTC which will allow LMI-based design of all the controller parameters or part of them. Also, we aim at using more elaborated LKFs in conjunction with less conservative inequalities. In this work, we studied the disturbance tolerance of the DTC, characterized by the bound on its energy given by γ. However, the analysis of other performance indexes as the $\mathcal{L}_2$ gain between the disturbance and the regulated output is also desired to be included.

Part III

Control Allocation

In this part, we change our focus from time delays and dead-time compensator strategies in the presence of saturating inputs to the problem of constrained control allocation. Although this part is much shorter than the previous one, it will hopefully be equally exciting. We initially make an effort to present a general introduction to the control allocation problem by making use of a simple example to illustrate the challenges related to this subject. Then, our contributions in this part, which are related to the development of theoretical conditions for the co-design of dynamic allocation functions and anti-windup are presented. The developments will take place in the continuous-time domain, as opposed to the previous part.

7 DYNAMIC ALLOCATION AND ANTI-WINDUP

This chapter addresses the design of dynamic allocation functions for systems with saturating actuators. The allocator can redistribute the desired control effort within the multiple actuators by penalizing each actuator to be more or less used, while also taking into account a criterium for minimization of their total energy consumption over time. Anti-windup gains are added to both the controller and the dynamic allocator to deal with the saturation condition. Convex conditions for the co-design of both the dynamic allocator and anti-windup gains are expressed in the form of linear matrix inequalities (LMIs). Such conditions allow dealing with the multiple objective problems of enlarging the estimates of the basin of attraction and minimizing the total energy consumption of the actuators. Two examples borrowed from the literature illustrate the proposed technique and show its effectiveness. However, we first introduce the concept of general control allocation and make use of a illustrative example to motivate the framework of control allocation.

7.1 Introduction to Allocation

Control allocation is widely used in over-actuated systems and consists of applying some algorithm to distribute the computed control effort throughout multiple redundant actuators. Control allocation arises, in general, when the regulated plant is modelled by using torques and/or forces as inputs, which in turn are generated by a set of multiple actuators (for example microthrusters in space applications) that jointly produce the desired control effort. The main goal of control allocation is then to distribute the computed controller output (often called the virtual input) among the multiple actuators in a manner such that the plant actual input (u_p) equals the desired effort computed by the controller (y_c) at all times. However, due to the constraints present in all real actuators, such as amplitude and rate saturation, not all virtual controls are achievable and the control allocator problem becomes that of minimizing the so-called allocation error $e = u_p - y_c$.

The control allocation problem is found in numerous applications and has been primarily studied in fields related to aeronautical applications. For example, Durham *et al.* (2016) dedicates an entire book to the allocation problem in aircraft control. On the other hand, it seems that a book reuniting general techniques in the theoretical context for control allocation is yet to be published. Nonetheless, a general overview of the problem can be found in the survey paper

by Johansen and Fossen (2013).

Let us take a look into the overview of the control allocation problem provided in Figure 35, where the block $\mathcal{C}$ represents the controller, and the block $\mathcal{P}$ stands for the plant. The control allocation sublevel, highlight in grey, is composed of the blocks $\mathcal{F}$, Φ, and M, where $\mathcal{F}$ is the control allocator, the function $\Phi(\cdot)$ represents some dynamics or nonlinearity in the actuators, and M is an influence map that translates how the multiple actuators combine to generate the plant input. Signals $r \in \mathbb{R}^q$, $y_c \in \mathbb{R}^{m_c}$, $y_f \in \mathbb{R}^{m_a}$, $\Phi(y_f) \in \mathbb{R}^{m_a}$, $u_p \in \mathbb{R}^{m_c}$, and $y_p \in \mathbb{R}^q$ are, respectively, the reference signal, the control command (or virtual input), the control allocator command, the actual value of the actuators signal, the plant actual input, and the plant output. The control allocator subsystem $\mathcal{F}$ is a degree of freedom for the designer and is responsible for distribution of the computed control effort among the multiple actuators. The function $\Phi(\cdot)$ could be, for example, a saturation or deadzone nonlinearity. The map $\mathrm{M} : \mathbb{R}^{m_a} \mapsto \mathbb{R}^{m_c}$ could be either a dynamic system or a static gain. Now that we have defined the signals and systems involved, we will make use of a simple example to better illustrate the treated allocation problem.

Figure 35 – Control allocation overview.

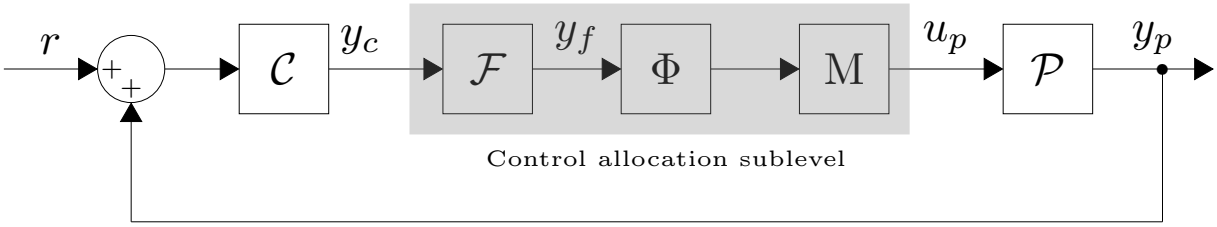

Source: The author.

7.1.1 Motivating example

In order to better illustrate the allocation problem, let us consider a simple example. Consider a plant described by the following equation

$$\dot{x} = \begin{bmatrix} -1 \end{bmatrix} x + \begin{bmatrix} 1 \end{bmatrix} u_p.$$

Suppose that $u_p \in \mathbb{R}$ represents a force acting on the system, which is generated by the sum of the forces produced by two actuators. In this case, we have the following relation $u_p = \mathrm{M}\Phi(y_f)$ with $\mathrm{M} = \begin{bmatrix} 1 & 1 \end{bmatrix}$. Suppose that $\Phi(\cdot)$ is a non-symmetric decentralized saturation and that each actuator can produce a force between 0 and 0.5 Newtons. The controller $\mathcal{C}$ produces the value of

the control command, which should be injected in the plant in ideal conditions. The question that arises, then, is:

Problem 7.1

Given the plant model $\mathcal{P}$, the controller $\mathcal{C}$, the mapping M and the actuator model $\Phi(\cdot)$, how to design an allocator $\mathcal{F} : \mathbb{R}^{m_c} \mapsto \mathbb{R}^{m_a}$ that is, in some sense, optimal, and preserves stability of the closed loop?

The answer to problem 7.1 is not a simple one. In fact, the problem could be much more complicated than the one illustrated by the motivating example. The influence map M could be a dynamical system and contain schedule parameters. The function $\Phi(\cdot)$, representing actuators, could be much more evolved than a deadzone or saturation function. In case the number of actuators is much greater than the number of plant inputs ($m_a \gg m_c$), the redundancy could be *stronger* and harder to deal with. Also, the plant model could be non-linear, which is by itself a problem much complicated than that of linear plants. Finally, in case of saturation, the multiple actuators could have been designed with different dimensions, thus owning different saturation levels. This last situation is not so uncommon in practical system as one might think.

Coming back to our simple example, suppose, for example, that the controller computes, at time t, the signal $y_c(t) = 0$. Naturally, to guarantee null allocation error, one needs to compute the allocator command y_f such that $\mathrm{M}\Phi(y_f) = y_c$, which implies null allocation error, i.e. $e = u_p - y_c = 0$. Since it is not possible to impose a value directly to $\Phi(y_f)$, one alternative is to compute y_f such that $\mathrm{M}y_f = y_c$, that is $\begin{bmatrix} 1 & 1 \end{bmatrix} y_f = 0$. However, note that this equation possesses infinitely many solutions. This introduces degrees of freedom that allows to compute the allocator command y_f by taking into account secondary optimization criterium. Such selection may not be straightforward and care must be taken to avoid some possible "dumb" selections. For example, $y_f = \begin{bmatrix} 1 & -1 \end{bmatrix}^\top$ is a valid solution. However, two evident problems arise with this selection. First of all, this choice is not wise in terms of energy consumption, since the solution $y_f = \begin{bmatrix} 0 & 0 \end{bmatrix}^\top$ could have been picked to avoid waste of energy. Secondly, due to the saturation, the actual plant input would be given by $u_p = \begin{bmatrix} 1 & 1 \end{bmatrix} \Phi \left(\begin{bmatrix} 1 \\ -1 \end{bmatrix} \right) = \begin{bmatrix} 1 & 1 \end{bmatrix} \begin{bmatrix} 0.5 \\ 0 \end{bmatrix} = 0.5$. Therefore, an allocation error between the desired control input y_c and the actual plant input u_p, given by $e = u_p - y_c = 0.5$, would occur, which is likely to cause bad behaviour or even instability of the

closed loop. The minimization of such an error is, therefore, the primary objective of a control allocator algorithm. Additionally, secondary objectives, such as the minimization of the total energy consumed by the actuators, can be taken into account when designing $\mathcal{F}$.

Different approaches in the literature exist to deal with the allocation problem, ranging from the use of quadratic programming that periodically minimizes some cost function of the allocation error by taking into account the constraints imposed by $\Phi(\cdot)$ to the design of $\mathcal{F}$ as a dynamical system that can be viewed as an augmentation to the controller $\mathcal{C}$. As pointed out in Johansen and Fossen (2013), Tjønnås and Johansen (2008), the advantages with the use of the control allocation approach are, therefore, modularity and ability to handle constraints as the redundancy of actuators allows multiple optimal criteria to be taken into account.

Hopefully, this short introduction served as an initial step to understanding the general view of the often not so evident control allocation problem. A review of the literature along with commonly used approaches will be realized within the next section, while later in the chapter we propose the co-design of a dynamic allocation function in conjunction with anti-windup to solve the allocation problem in the case that M is a static influence matrix and $\Phi(\cdot)$ is the standard symmetric saturation nonlinearity.

7.2 Literature review and this work

The control allocation problem is a subject treated in several papers dealing with specific applications, in particular in the aeronautical or spatial contexts: see, for example, the works of Jin (2005), Oppenheimer *et al.* (2006), Boada *et al.* (2013), Durham *et al.* (2016). It has also been treated, very recently, by Kreiss *et al.* (2021), in the context of power electronic devices, where the voltage on a resistive load is regulated by a centralized controller that computes the total necessary current to be inserted in the load circuit, while an allocator subsystem is used to distribute the total effort among multiple buck converters that deliver suitable currents, via a common DC bus, to generate, as much as possible, the total desired control effort.

Besides application-focused papers, technical solutions are also proposed in the literature from a theoretical point of view. Both the works in Galeani *et al.* (2015) and Serrani (2012) consider the output regulation problem of over-actuated systems in the presence of full information regarding the system states and exogenous inputs. More specifically, Galeani *et al.* (2015) proposes an allocation mechanism that takes the form of a hybrid system and accounts for input constraints. In Petersen and Bodson (2006), optimization-based algorithms, as interior

point method, are detailed to compute optimal allocation given the actuators constraints. The online implementation of this kind of technique can be, however, computationally expensive, while stability analysis of the closed loop is not straightforward. The presence of constraints inherently causes errors between the desired control effort and the actual plant input, which can lead to poor response and even instability. In this context, Lyapunov-based approaches with guarantees of stability for the constrained closed-loop system have also been searched, for example in de Castro and Brembeck (2019), Benosman *et al.* (2009), Liao *et al.* (2007), Johansen (2004). In this vein, the work in Alves Lima *et al.* (2021c) proposed the use of an allocation function and anti-windup designed with an optimization procedure that envisaged the minimization of this error while guaranteeing closed-loop stability. Nonetheless, the proposed allocation format and design procedure did not take into account other important issues as the ability to penalize the use of the different actuators and energy consumption minimization.

The work in Zaccarian (2009) formally defines the concepts of weak and strong redundancy, in which the former implies that multiple actuators can induce the same steady-state value for the plant output while the latter implies that they can also impose equal trajectories. The use of a dynamic allocator system between the controller and the plant is then proposed with the goal to distribute the control effort by penalizing the use of the multiple actuators. The paper also deals with the cases of input and rate saturation of the actuators. The use of dynamic allocation functions was shown to be a good alternative in terms of both computational effort and robustness. Nonetheless, some important issues regarding the strategy can be shortlisted: i) Zaccarian (2009) does not consider the co-design problem of the anti-windup loop and allocation. ii) The parameters of the allocator in Zaccarian (2009) are manually selected. iii) The formulation in Zaccarian (2009) is focused on the specific case where the size of the plant input (noted m_c here) is equal to the size of allocator output (noted m_a here) and the influence matrix (noted M here) is the identity matrix (i.e., $\mathrm{M} = \mathrm{I}$). In the current work, we can deal with a broader range of systems since we consider the case of $m_a \geq m_c$. iv) In the regulatory case (null external references) with actuator saturation, the states of the allocator are not guaranteed to asymptotically converge to the origin, which causes waste of energy in the actuators.

Indeed, this work aims at proposing a more general allocator function format and design method that solve the above-described problems. By considering a Lyapunov-based approach, theoretical conditions are derived in terms of linear matrix inequalities (LMIs) in order to solve the co-design of the allocator and anti-windup loop. Furthermore, an optimization scheme

consisting of the minimization of the energy consumption in the actuators and maximization of the closed-loop region of attraction is proposed. As in Zaccarian (2009), the use of the actuators can also be penalized according to the user desire. Some ideas from Alves Lima *et al.* (2021c) are also recovered to show that the allocator is somehow effective concerning the allocation error between the computed control effort and the actual plant input.

The chapter is organized as follows. Section 7.3 is dedicated to present the general view of the control allocation, and to specify the class of the plant, controller and allocation function under consideration. Section 7.4 presents the main theoretical conditions, together with the associated optimization scheme. In Section 7.5, two examples borrowed from the literature emphasize the interest of the proposed approach. Finally, in Section 7.6, discussion and forthcoming issues end the chapter.

7.3 Problem formulation

7.3.1 General view

Figure 36 – General view of control allocation problem with anti-windup.

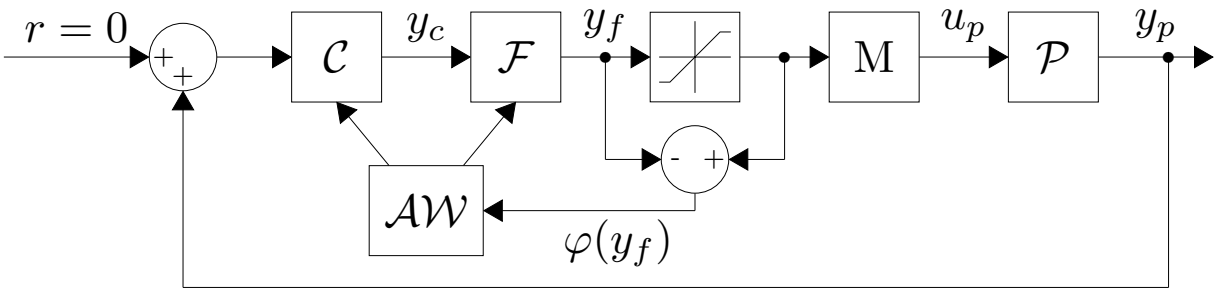

Source: The author.

Consider the general view of the control allocation problem with anti-windup shown in Fig. 36. Subsystems $\mathcal{C}$, $\mathcal{F}$, and $\mathcal{P}$ are the controller, the control allocator, and the plant, respectively, while M is the influence matrix and $\mathcal{AW}$ represents some anti-windup strategy. The plant is driven by u_p in $\mathbb{R}^{m_c}$ inputs. The controller computes a set of desired y_c in $\mathbb{R}^{m_c}$ efforts that must be injected in the plant in ideal conditions. The plant input is generated by a set of $m_a \geq m_c$ actuators, represented by the signal y_f in $\mathbb{R}^{m_a}$. The plant input is given by $u_p = \mathrm{M}sat(y_f)$ with the decentralized saturation function being defined as

$$sat(y_{f(i)}) = sign(y_{f(i)}) \min\{|y_{f(i)}|, \bar{u}_{(i)}\}, \bar{u}_{(i)} > 0, \tag{7.1}$$

for $i = 1, \ldots, m_a$, where $\bar{u}_{(i)}$ denotes the magnitude bound in each actuator, and the so-called influence matrix M in $\mathbb{R}^{m_c \times m_a}$ maps how each individual effort of the m_a actuators combines to generate the inputs acting on the plant. Furthermore, in this work we consider the regulatory case, i.e., $r = 0$.

The simplest allocation function often considered in the literature is given by the right pseudo-inverse of M, that is, $\mathcal{F} = \mathrm{M}^{\dagger}$, with $\mathrm{M}\mathrm{M}^{\dagger} = \mathrm{I}$. In the case the actuator is not subject to saturation or other nonlinearities, this allocator is able to guarantee stability of the closed loop since the interconnection is given by $u_p = \mathrm{M}\mathrm{M}^{\dagger} y_c = y_c$, and therefore no error between u_p and y_c is produced. However:

i. This popular static allocator is not able to take advantage of the multi-actuated nature of the system to redistribute the effort among desired actuators. This is important, for example, in case of actuator failures and/or operational constraints that demand certain actuators to be more or less used than others to produce the desired control effort.
ii. In the presence of nonlinearities as the actuator saturation, guarantees of stability of the closed loop, as well as estimation of regions of safe operation, need to be assured. In this context, more complex allocation functions with the ability to handle redundancy and constraints should be applied.

7.3.2 Plant and controller description

Consider the plant $\mathcal{P}$ described by the following equations

$$\mathcal{P} \sim \begin{cases} \dot{x}_p = \mathrm{A}_p x_p + \mathrm{B}_p u_p, \\ y_p = \mathrm{C}_p x_p, \end{cases} \tag{7.2}$$

where x_p in $\mathbb{R}^{n_p}$ is the plant state vector, u_p in $\mathbb{R}^{m_c}$ is the plant input, y_p in $\mathbb{R}^{q}$ is the measured output. A_p, B_p, and C_p are all constant and known matrices of appropriate dimensions. Furthermore, the pairs $(\mathrm{A}_p, \mathrm{B}_p)$ and $(\mathrm{C}_p, \mathrm{A}_p)$ are supposed to be controllable and observable.

Let us assume that the plant (7.2) is stabilized by a dynamic output controller $\mathcal{C}$ linearly designed via the connection $u_p = y_c$, that is without taking into account the saturation and with $\mathcal{F} = \mathrm{M}^{\dagger}$. The controller $\mathcal{C}$ is defined by the following equations

$$\mathcal{C} \sim \begin{cases} \dot{x}_c = \mathrm{A}_c x_c + \mathrm{B}_c y_p + \mathrm{E}_c \varphi(y_f), \\ y_c = \mathrm{C}_c x_c + \mathrm{D}_c y_p, \end{cases} \tag{7.3}$$

where x_c in $\mathbb{R}^{n_c}$ is the controller state vector and y_c in $\mathbb{R}^{m_c}$ is the controller output. A_c, B_c, C_c and D_c are supposed known. In this work, we consider the anti-windup signal $v_{aw} = \mathrm{E}_c\varphi(y_f)$, E_c in $\mathbb{R}^{n_c \times m_a}$, with the deadzone $\varphi(y_f)$ defined as

$$\varphi(y_f) = sat(y_f) - y_f, \tag{7.4}$$

where the saturation map is defined from (7.1) and y_f is the output of the allocation function. Such an anti-windup compensation is added in order to mitigate the undesired effects of saturation (see, for example, Tarbouriech *et al.* (2011), Zaccarian and Teel (2011)).

Remark 7.1

By construction, the linear connection plant-controller is supposed to be stable. In other words, the controller (7.3) (with $v_{aw} = 0$) stabilizes the plant (7.2) through the linear interconnection $u_p = y_c$ and therefore the matrix A_0, defined below, is Hurwitz.

$$\mathrm{A}_0 = \begin{bmatrix} \mathrm{A}_p + \mathrm{B}_p\mathrm{D}_c\mathrm{C}_p & \mathrm{B}_p\mathrm{C}_c \\ \mathrm{B}_c\mathrm{C}_p & \mathrm{A}_c \end{bmatrix} \text{ in } \mathbb{R}^{(n_p+n_c)\times(n_p+n_c)} \tag{7.5}$$

7.3.3 Dynamic allocation function description

Consider the influence matrix M in $\mathbb{R}^{m_c \times m_a}$ in the case $m_a > m_c$, supposedly full row rank. Let N in $\mathbb{R}^{m_a \times n_f}$, $n_f = m_a - m_c$, be a basis for the Kernel of M, i.e. $\mathrm{MN} = 0$. We then propose the following dynamic allocation function

$$\mathcal{F} \sim \begin{cases} \dot{x}_f = \mathrm{K}_f\mathrm{N}^\top\mathrm{W}\mathrm{N}x_f + \mathrm{K}_f\mathrm{N}^\top\mathrm{W}\mathrm{M}^\dagger y_c + \mathrm{E}_f\varphi(y_f), \\ y_f = \mathrm{N}x_f + \mathrm{M}^\dagger y_c, \end{cases} \tag{7.6}$$

where x_f in $\mathbb{R}^{n_f}$ is the allocator state vector, and y_f in $\mathbb{R}^{m_a}$ is the allocator output. Matrix W defined by W=diag$(w_1, w_2, \ldots, w_{m_a})$ in $\mathbb{S}^+_{m_a}$ is a matrix which receives the weightings that penalizes the use of each actuator. Matrices K_f in $\mathbb{R}^{n_f \times n_f}$ and E_f in $\mathbb{R}^{n_f \times m_a}$ must be designed to achieve desired behavior of the allocator by taking into account the presence of saturation. This allocation format is particularly interesting since it is in some sense optimal in terms of both the allocation error and actuators usage, as explained in the next two remarks.

Remark 7.2

Consider the general expression $y_f = \mathrm{C}_f x_f + \mathrm{D}_f y_c$, and let us define the allocator error as $e = u_p - y_c$. Then using the definition of $\varphi(y_f)$ in (7.4), the expression $e = \left(\mathrm{MD}_f - \mathrm{I}\right) y_c + \mathrm{MC}_f x_f + \mathrm{M}\varphi(y_f)$ is easily obtained. It is straightforward to see that the choice $\mathrm{D}_f = \mathrm{M}^\dagger$, $\mathrm{C}_f = \mathrm{N}$ leads to $e = \mathrm{M}\varphi(y_f)$, therefore the error is null in absence of saturation. Furthermore, by guaranteeing convergence of the extended vector $x = \begin{bmatrix} x_p^\top & x_c^\top & x_f^\top \end{bmatrix}^\top$ to the origin, we always obtain $e^* = 0$, where e^* is the steady-state value of e.

Remark 7.3

Consider the cost function

$$\min_{x_f} \mathrm{T}(y_f) = y_f^\top \mathrm{W} y_f \text{ subject to } y_f = \mathrm{N}x_f + \mathrm{M}^\dagger y_c^*, \tag{7.7}$$

where y_c^* is any controller output. The optimal solution to (7.7) is given by $x_f = -(\mathrm{N}^\top \mathrm{W}^\top \mathrm{N})^{-1} \mathrm{N}^\top \mathrm{W} \mathrm{M}^\dagger y_c^*$, which corresponds to the steady-state value of x_f in (7.6).

Remark 7.4: Case when $m_a = m_c$ and $\mathrm{M} = \mathrm{I}$

In some papers, like the one in Zaccarian (2009), the influence matrix M enters the plant model. In this case, $m_a = m_c$, the system has more inputs than states ($m_c > n_p$) and the input-redundancy nature of the plant is explicit. All the results in this work can straightforwardly be applied in this case by making $\mathrm{M} = \mathrm{I}$ and choosing N as a base for the null space of B_p, that is, $\mathrm{B}_p\mathrm{N} = 0$. Although in this case $\mathrm{MN} \neq 0$, convergence of the allocator error to zero takes place due to the fact that the allocator states x_f converges to zero at steady-state, thus the allocator recovers the property $u_p = y_c$ after some time.

7.3.4 Closed-loop system and problem formulation

By taking into account the definitions of $\mathcal{P}$, $\mathcal{C}$, $\mathcal{F}$, the definition of $\varphi(y_f)$ in (7.4) and the connection $u_p = \mathrm{M}sat(y_f)$, the complete closed-loop system with $x = \begin{bmatrix} x_p^\top & x_c^\top & x_f^\top \end{bmatrix}^\top$ in $\mathbb{R}^n$, $n = n_p + n_c + n_f$, can be written as

$$\begin{cases} \dot{x} = (\mathrm{A} + \mathrm{L}_f \mathrm{K}_f \bar{\mathrm{C}})x + (\mathrm{B} + \mathrm{LE})\varphi(y_f) \\ y_f = \mathrm{C}x \end{cases} \tag{7.8}$$

where $\mathrm{L}_f = \begin{bmatrix} 0_{n_f \times n_p} & 0_{n_f \times n_c} & \mathrm{I}_{n_f} \end{bmatrix}^\top$, $\bar{\mathrm{C}} = \mathrm{N}^\top \mathrm{W}\mathrm{C}$, and:

$$\mathrm{A} = \begin{bmatrix} \mathrm{A}_0 & 0 \\ 0 & 0 \end{bmatrix}, \mathrm{B} = \begin{bmatrix} \mathrm{B}_p \mathrm{M} \\ 0 \end{bmatrix}, \mathrm{E} = \begin{bmatrix} \mathrm{E}_c \\ \mathrm{E}_f \end{bmatrix}, \mathrm{L} = \begin{bmatrix} \mathrm{L}_c & \mathrm{L}_f \end{bmatrix},$$

$$\mathrm{L}_c = \begin{bmatrix} 0_{n_c \times n_p} & \mathrm{I}_{n_c} & 0_{n_c \times n_f} \end{bmatrix}^\top, \mathrm{C} = \begin{bmatrix} \mathrm{M}^\dagger \mathrm{D}_c \mathrm{C}_p & \mathrm{M}^\dagger \mathrm{C}_c & \mathrm{N} \end{bmatrix}$$

with A_0 defined in (7.5). The presence of the deadzone in the closed-loop dynamics (7.8) implies to characterize a suitable region of the state space in which the stability is ensured (see, for example, Tarbouriech *et al.* (2011)). In general, the global asymptotic stability of the origin (that is for any initial condition $x(0)$ in $\mathbb{R}^n$) does not hold except if the open loop has suitable properties of stability (SONTAG, 1984). Hence, regional stability (that is, only for initial conditions in a neighborhood of the origin) has to be studied. Since the exact characterization of the basin of attraction of the origin remains an open problem, a challenging problem consists in providing an estimate of the basin of attraction as accurate as possible.

Furthermore, we want to ensure some level of performance to the allocator in terms of the total energy consumption of the actuators, which can be done by imposing conditions that limit the energy of the signal $sat(y_f)$. With respect to (7.3) and (7.6), the main objective of this chapter is to propose the co-design of the dynamic allocation function, that is K_f, and E_f, along with the controller anti-windup gain E_c. Then the problem we intend to solve can be summarized as follows.

Problem 7.2

Given the controller matrices A_c, B_c, C_c, D_c, and the weighting matrix W, design matrices K_f, E_f and E_c, such that

i. the regional asymptotic stability of the closed-loop system (7.8) is ensured and the estimate of the region of attraction is maximized.

ii. the total energy consumption of the actuators over time is minimized.

7.4 Main results

7.4.1 Theoretical preliminaries

Consider a matrix $\mathrm{G} \in \mathbb{R}^{m_a \times n}$, and define the set

$$\mathscr{L}(\bar{u}) = \{x \in \mathbb{R}^n; |\mathrm{G}_{(i)} x| \leq \bar{u}_{(i)}, i = 1, ..., m_a\}, \tag{7.9}$$

Then, nonlinearity $\varphi(y_f)$, with y_f in (7.8), satisfies the following Lemma directly derived from Lemma 1.6 p.43 in Tarbouriech *et al.* (2011).

Lemma 7.1: Generalized sector condition

If x belongs to set $\mathscr{L}(\bar{u})$, defined in (7.9), then the deadzone nonlinearity $\varphi(y_f)$ satisfies the following inequality for any diagonal matrix S in $\mathbb{S}^+_{m_a}$

$$\varphi^\top(y_f)\mathrm{S}^{-1}[\varphi(y_f)+\mathrm{C}x-\mathrm{G}x]\leq 0. \tag{7.10}$$

Another important result widely known in the literature is re-enunciated next (see, for example, de Oliveira and Skelton (2001)).

Lemma 7.2: Finsler's Lemma

Consider ζ in $\mathbb{R}^n$, $\Upsilon=\Upsilon^\top$ in $\mathbb{R}^{n\times n}$, and Γ in $\mathbb{R}^{m\times n}$. The following facts are equivalent:

i. $\zeta^\top\Upsilon\zeta<0$, $\forall\zeta$ such that $\Gamma\zeta=0$, $\zeta\neq 0$.

ii. $\exists\mathfrak{I}$ in $\mathbb{R}^{n\times m}$ such that $\Upsilon+\mathfrak{I}\Gamma+\Gamma^\top\mathfrak{I}^\top\prec 0$.

7.4.2 Design of the allocator and anti-windup

The following theorem provides a solution to Problem 7.3.4.

Theorem 7.1

Assume the existence of matrices $\bar{\mathrm{P}}$ in $\mathbb{S}^+_n$, J_o in $\mathbb{R}^{(n_p+n_c)\times(n_p+n_c)}$, J_f in $\mathbb{R}^{n_f\times n}$, $\bar{\mathrm{K}}_f$ in $\mathbb{R}^{n_f\times n_f}$, K_e in $\mathbb{R}^{(n_c+n_f)\times m_a}$, $\bar{\mathrm{G}}$ in $\mathbb{R}^{m_a\times n}$, diagonal matrix $\mathrm{S}=\mathrm{S}^\top$ in $\mathbb{S}^+_{m_a}$ and positive scalar γ such that

$$\Psi=\left[\begin{array}{c|c}\Psi_a&\Psi_b\\\hline\star&\Psi_c\end{array}\right]=\left[\begin{array}{cc|cc}-\bar{\mathrm{J}}-\bar{\mathrm{J}}^\top&\Psi_{12}&\Psi_{13}&0\\\star&\Psi_{22}&\Psi_{23}&\bar{\mathrm{J}}\mathrm{C}^\top\mathrm{W}^{\frac{1}{2}}\\\hline\star&\star&-2\mathrm{S}&\mathrm{S}\mathrm{W}^{\frac{1}{2}}\\\star&\star&\star&-\gamma\mathrm{I}\end{array}\right]\prec 0 \tag{7.11}$$

$$\left[\begin{array}{cc}\bar{\mathrm{P}}&\bar{\mathrm{G}}_{(i)}^\top\\\star&\bar{u}^2_{(i)}\end{array}\right]\succeq 0,\ \text{for } i=1,\ldots,m_a, \tag{7.12}$$

hold with $\Psi_{12} = \bar{P} + A\dot{J}^\top + Z - \dot{J}$, $Z = \text{diag}(0_{n_p+n_c}, \bar{K}_f)$, $\Psi_{13} = BS + LK_e$, $\Psi_{22} = He\{A\dot{J}^\top + Z\}$, $\Psi_{23} = \Psi_{13} + \bar{G}^\top - \dot{J}C^\top$, and where $\dot{J} = \begin{bmatrix} \bar{C}^\perp J_o^\top & J_f^\top \end{bmatrix}^\top$ in $\mathbb{R}^{n\times n}$, $\bar{C}^\perp$ in $\mathbb{R}^{n\times(n_p+n_c)}$ is a matrix such that $\bar{C}\bar{C}^\perp = 0$. Then, matrices $E = \begin{bmatrix} E_c^\top & E_f^\top \end{bmatrix}^\top = K_e S^{-1}$, $K_f = \bar{K}_f \left(\bar{C} J_f^\top\right)^{-1}$ are solution to Problem 7.3.4. In other words:

i. the closed-loop system (7.8) is asymptotically stable in the ellipsoid $\varepsilon(P,1) = \{x \text{ in } \mathbb{R}^n; x^\top P x \leq 1\}$, with $P = J\bar{P}J^\top$ and $J = \dot{J}^{-1}$;

ii. the energy of the actuators usage signal is limited and given by $\int_0^\infty sat(y_f(\tau))^\top W sat(y_f(\tau)) d\tau \leq \gamma$.

Proof. Note first that the satisfaction of inequality (7.11) means that matrix $\dot{J}$ is non-singular. Consider then a quadratic Lyapunov function $V(x) = x^\top P x$, with $P \succ 0$ in $\mathbb{S}_n^+$. The satisfaction of relation (7.12) ensures the inclusion of the ellipsoid $\varepsilon(P,1) = \{x \text{ in } \mathbb{R}^n; x^\top P x \leq 1\}$ in the set $\mathscr{L}(\bar{u})$ as defined in (7.9) by using the changes of variables $\bar{G} = G\dot{J}^\top$, $P = J\bar{P}J^\top$ and $J = \dot{J}^{-1}$. Therefore, the satisfaction of relation (7.12) means that Lemma 7.1 applies and one gets $-2\varphi^\top(y_f)S^{-1}[\varphi(y_f) + Cx - Gx] \geq 0$, for any x in $\varepsilon(P,1) \subseteq \mathscr{L}(\bar{u})$. Then for $x \in \varepsilon(P,1) \subseteq \mathscr{L}(\bar{u})$, one gets $\dot{V}(x) \leq \dot{V}(x) - 2\varphi^\top(y_f)S^{-1}[\varphi(y_f) + Cx - Gx] \leq \dot{V}(x) - 2\varphi^\top(y_f)S^{-1}[\varphi(y_f) + Cx - Gx] + \gamma^{-1} sat(y_f)^\top W sat(y_f)$. Hence to obtain $\dot{V}(x) < 0$. it suffices that

$$\dot{V}(x) - 2\varphi^\top(y_f)S^{-1}[\varphi(y_f) + (C-G)x] + \gamma^{-1} sat(y_f)^\top W sat(y_f) < 0, \tag{7.13}$$

with $S \succ 0$. Consequently, $\dot{V}(x) + \gamma^{-1} sat(y_f)^\top W sat(y_f) < 0$ is also satisfied, which can be integrated resulting in

$$\gamma^{-1} \int_0^\infty sat(y_f(\tau))^\top W sat(y_f(\tau)) d\tau < V(x(0)) \leq 1, \tag{7.14}$$

which leads to item ii) of Theorem 7.1. By using (7.4) and defining the augmented vector $\zeta = \begin{bmatrix} \dot{x}^\top & x^\top & \varphi(y_f)^\top \end{bmatrix}^\top$, we can rewrite inequality (7.13) as $\zeta^\top \Upsilon \zeta < 0$, with the matrix Υ given by:

$$\begin{bmatrix} 0 & P & 0 \\ \star & C^\top W^{\frac{1}{2}} \gamma^{-1} W^{\frac{1}{2}} C & (G-C)^\top S^{-1} + C^\top W^{\frac{1}{2}} \gamma^{-1} W^{\frac{1}{2}} \\ \star & \star & W^{\frac{1}{2}} \gamma^{-1} W^{\frac{1}{2}} - 2S^{-1} \end{bmatrix}.$$

We also have that the relation $\Gamma\zeta = 0$ holds for

$$\Gamma = \begin{bmatrix} -I & A + L_f K_f \bar{C} & B + LE \end{bmatrix}. \tag{7.15}$$

From Lemma 7.2, by considering $\mathfrak{I} = \begin{bmatrix} \mathrm{J}^\top & \mathrm{J}^\top & 0 \end{bmatrix}^\top$, we obtain the new condition $\overline{\Psi} = \Upsilon + \mathfrak{I}\Gamma + \Gamma^\top \mathfrak{I}^\top \prec 0$. By applying a Schur complement to $\overline{\Psi}$, followed by pre- and post-multiplying by $\mathrm{diag}(\mathrm{J}^{-1}, \mathrm{J}^{-1}, \mathrm{S}, \mathrm{I})$ and its transpose, respectively, and making changes of variable $\bar{\mathrm{J}} = \mathrm{J}^{-1}$, $\bar{\mathrm{P}} = \bar{\mathrm{J}}\mathrm{P}\bar{\mathrm{J}}^\top$, $\bar{\mathrm{G}} = \mathrm{G}\bar{\mathrm{J}}^\top$, $\mathrm{K}_e = \mathrm{ES}$ we obtain the equivalent condition

$$\begin{bmatrix} -\bar{\mathrm{J}} - \bar{\mathrm{J}}^\top & \bar{\mathrm{P}} + (\mathrm{A} + \mathrm{L}_f \mathrm{K}_f \bar{\mathrm{C}})\bar{\mathrm{J}}^\top - \bar{\mathrm{J}} & \Psi_{13} & 0 \\ \star & \mathrm{He}\{(\mathrm{A} + \mathrm{L}_f \mathrm{K}_f \bar{\mathrm{C}})\bar{\mathrm{J}}^\top\} & \Psi_{23} & \bar{\mathrm{J}}\mathrm{C}^\top \mathrm{W}^{\frac{1}{2}} \\ \star & \star & -2\mathrm{S} & \mathrm{S}\mathrm{W}^{\frac{1}{2}} \\ \star & \star & \star & -\gamma \mathrm{I} \end{bmatrix} \prec 0,$$

Note that $\bar{\mathrm{C}}^\perp$ in $\mathbb{R}^{n \times (n_p + n_c)}$ is the orthogonal complement of $\bar{\mathrm{C}}^\top$ (i.e. $\bar{\mathrm{C}}\bar{\mathrm{C}}^\perp = 0$ with $rank(\bar{\mathrm{C}}) = n_f$) such that $\begin{bmatrix} \bar{\mathrm{C}}^\perp & \bar{\mathrm{C}}^\top \end{bmatrix}$ is square and nonsingular. Thanks to this, the specific structure $\bar{\mathrm{J}} = \begin{bmatrix} \bar{\mathrm{C}}^\perp \mathrm{J}_o^\top & \mathrm{J}_f^\top \end{bmatrix}^\top$, with J_o in $\mathbb{R}^{(n_p + n_c) \times (n_p + n_c)}$, J_f in $\mathbb{R}^{n_f \times n}$ does not prevent the existence of J_o and J_f making $\bar{\mathrm{J}}$ non singular. Hence, such a structure for $\bar{\mathrm{J}}$ allows to have $\mathrm{Z} = \mathrm{L}_f \begin{bmatrix} \bar{\mathrm{C}}\bar{\mathrm{C}}^\perp \mathrm{J}_o{}^\top & \mathrm{K}_f \bar{\mathrm{C}} \mathrm{J}_f^\top \end{bmatrix} = diag(0_{n_p + n_c}, \bar{\mathrm{K}}_f)$ in the term Ψ_{22}, where the satisfaction of inequality (7.11) implies that $\bar{\mathrm{C}}\mathrm{J}_f^\top$ is non-singular with a full row rank matrix J_f (i.e. $rank(\mathrm{J}_f) = n_f$), allowing the computation of K_f. Hence, it follows that if relations (7.11) and (7.12) are satisfied then (7.13) is also satisfied, or equivalently $\dot{\mathrm{V}}(x) < 0$, for any x in $\varepsilon(\mathrm{P}, 1)$. Then the two items of Theorem 7.1 are proven and the proof is completed. □

The following proposition can be stated about Theorem 7.1.

Proposition 7.1

LMI (7.11) in Theorem 7.1 is always feasible.

Proof. Matrix Ψ can be written as $\Psi = \Psi_0 + \mathrm{He}\{\begin{bmatrix} \mathrm{L}^\top & \mathrm{L}^\top & 0 & 0 \end{bmatrix}^\top \mathrm{K}_e \begin{bmatrix} 0 & 0 & \mathrm{I} & 0 \end{bmatrix}\}$. Hence by using the elimination lemma (DE OLIVEIRA; SKELTON, 2001), it follows that there are always values of K_e (consequently of $\mathrm{E} = \begin{bmatrix} \mathrm{E}_c^\top & \mathrm{E}_f^\top \end{bmatrix}^\top$) such that $\Psi \prec 0$ is feasible if and only if the two conditions $\mathcal{N}_1^\top \Psi_0 \mathcal{N}_1 \prec 0$ and $\mathcal{N}_2^\top \Psi_0 \mathcal{N}_2 \prec 0$ hold where matrices

$$\mathcal{N}_1 = \begin{bmatrix} \mathrm{I}_n & 0 & 0 & 0 \\ 0 & \mathrm{I}_n & 0 & 0 \\ 0 & 0 & 0 & \mathrm{I}_{m_a} \end{bmatrix}^\top \text{ and } \mathcal{N}_2 = \begin{bmatrix} \mathrm{I}_n & -\mathrm{I}_n & 0 & 0 \\ 0 & 0 & \mathrm{I}_{m_a} & 0 \\ 0 & 0 & 0 & \mathrm{I}_{m_a} \end{bmatrix}^\top$$

are the Kernel basis of $\begin{bmatrix} 0 & 0 & \mathrm{I} & 0 \end{bmatrix}$ and $\begin{bmatrix} \mathrm{L}^\top & \mathrm{L}^\top & 0 & 0 \end{bmatrix}$. Define without loss of generality $\bar{\mathrm{C}}^\perp = \begin{bmatrix} \mathrm{I}_{n_p+n_c} & \Theta^\top \end{bmatrix}^\top$ with $\Theta = -\left(\mathrm{N}^\top \mathrm{W} \mathrm{N}\right)^{-1} \begin{bmatrix} \mathrm{N}^\top \mathrm{W} \mathrm{M}^\dagger \mathrm{D}_c \mathrm{C}_p & \mathrm{N}^\top \mathrm{W} \mathrm{M}^\dagger \mathrm{C}_c \end{bmatrix}$, and the partition $\mathrm{J}_f = \begin{bmatrix} \mathrm{J}_{fo} & \mathrm{J}_{ff} \end{bmatrix}$ with J_{fo} in $\mathbb{R}^{n_f \times (n_p+n_c)}$ and J_{ff} in $\mathbb{R}^{n_f \times n_f}$, which leads to $\bar{\mathrm{J}} = \begin{bmatrix} \mathrm{J}_o & \mathrm{J}_o \Theta^\top \\ \mathrm{J}_{fo} & \mathrm{J}_{ff} \end{bmatrix}$. Then we can rewrite Ψ_a as

$$\begin{bmatrix} \begin{bmatrix} -\mathrm{He}\{\mathrm{J}_o\} & -\mathrm{J}_o \Theta^\top - \mathrm{J}_{fo}^\top \\ \star & -\mathrm{He}\{\mathrm{J}_{ff}\} \end{bmatrix} & \begin{bmatrix} \mathrm{A}_0 \mathrm{J}_o^\top - \mathrm{J}_o & \mathrm{A}_0 \mathrm{J}_{fo}^\top - \mathrm{J}_o \Theta^\top \\ \mathrm{J}_{fo} & \bar{\mathrm{K}}_f - \mathrm{J}_{ff} \end{bmatrix} + \bar{\mathrm{P}} \\ \star & \begin{bmatrix} \mathrm{He}\{\mathrm{A}_0 \mathrm{J}_o^\top\} & \mathrm{A}_0 \mathrm{J}_{fo}^\top \\ \star & \mathrm{He}\{\bar{\mathrm{K}}_f\} \end{bmatrix} \end{bmatrix}.$$

The feasibility of $\mathcal{N}_1^\top \Psi_0 \mathcal{N}_1 \prec 0$ is related to ensure $\Psi_a \prec 0$. Since A_0 is Hurwitz by construction, there always exist full rank matrix J_o such that $\mathrm{He}\{\mathrm{A}_0 \mathrm{J}_o^\top\} \prec 0$ and $-\mathrm{He}\{\mathrm{J}_o\} \prec 0$, full rank matrices J_{ff},J_{fo} and $\bar{\mathrm{K}}_f$ can be computed to ensure $\Psi_a \prec 0$. Similarly the feasibility of $\mathcal{N}_2^\top \Psi_0 \mathcal{N}_2 \prec 0$ is directly related to $-2\bar{\mathrm{P}} \prec 0$. Finally, Schur complement can be used to show that $\mathcal{N}_1^\top \Psi_0 \mathcal{N}_1 \prec 0$, $\mathcal{N}_2^\top \Psi_0 \mathcal{N}_2 \prec 0$ for large enough values of γ and S. □

Remark 7.5: On the choice of matrix W

From Remark 3 and item ii) of Theorem 1, the entries of the matrix W are inversely proportional to the level of usage of each actuator. Although the user can specify any desired value $w_i > 0$, one promising choice in the case the level of saturation of the actuators is different is to make $w_i = \bar{u}_{(i)}^{-2}$. Many other criteria, such as the operation cost of different actuators could also be taken into account.

Remark 7.6

In case the plant state matrix A_p is Hurwitz stable, global stability of the closed loop can be achieved and the design of K_f, E_f, E_c can also be realized by solving LMI (7.11) with $\bar{\mathrm{G}} = 0$.

7.4.3 Optimization issues

From (7.14), it becomes clear that minimization of γ leads to minimization of the energy of $sat(y_f(t))$. Therefore, while solving the LMIs in Theorem 7.1 (or in Remark 7.6), we

can accomplish better results for the allocator by minimizing γ. In case of Theorem 7.1, the maximization of the ellipsoid $\varepsilon(\mathrm{P},1)$ is also of interest. Therefore, a multi-objective optimization procedure applies. Consider a positive definite matrix P_0 and the following matrix inequality

$$\begin{bmatrix} \mathrm{P}_0 & \mathrm{I} \\ \star & \bar{\mathrm{J}}+\bar{\mathrm{J}}^{\top} - \bar{\mathrm{P}} \end{bmatrix} \succeq 0. \tag{7.16}$$

Then, minimization of the trace of P_0 indirectly leads to minimization of the trace of P and, therefore, to maximization of the ellipsoid $\varepsilon(\mathrm{P},1)$. Consider weighting parameters κ_1, κ_2. Then the following optimization procedure takes place in case of Theorem 7.1

$$\min\ (\kappa_1\lambda + \kappa_2\gamma)\ \text{subject to (7.11), (7.12), (7.16)}, \mathrm{P}_0 \preceq \lambda \mathrm{I} \tag{7.17}$$

In case global asymptotic stability is sought (Remark 7.6), the following optimization procedure applies

$$\min \gamma \text{ subject to (7.11) with } \bar{\mathrm{G}} = 0 \tag{7.18}$$

7.5 Simulation results

7.5.1 Example 1

Consider the satellite formation flying control problem from Boada *et al.* (2013), where the controlled output y_p represents the relative position between two satellites in a vertical axis. Given two satellites, the objective is to cancel the lateral position error between them in the $z-axis$. The process can be represented by the following model

$$\left[\begin{array}{c|c} \mathrm{A}_p & \mathrm{B}_p \\ \hline \mathrm{C}_p & \mathrm{D}_p \end{array}\right] = \left[\begin{array}{cc|cc} 0 & 1 & 0 & 0 \\ 0 & 0 & m_1^{-1} & -m_2^{-1} \\ \hline 1 & 0 & 0 & 0 \end{array}\right],$$

where m_1^{-1} and m_2^{-1} are the masses of the two satellites. The plant input is given by $u_p = \begin{bmatrix} u_{p_1} \\ u_{p_2} \end{bmatrix} = \begin{bmatrix} F_1 \\ F_2 \end{bmatrix}$, where F_1 and F_2 are forces that act individually in each satellite. Each satellite possesses 4 thrusters that jointly produce the force applied in each of them. The influence matrix is given by $\mathrm{M} = \begin{bmatrix} \mathrm{M}_1 & 0 \\ 0 & \mathrm{M}_2 \end{bmatrix}$, with $\mathrm{M}_1 = \mathrm{M}_2 = \begin{bmatrix} 1 & -1 & -1 & 1 \end{bmatrix}$. We assume that each thruster can produce a force between 0 mN and 100 mN, therefore the saturation

limits are not symmetric. In order to apply the developed conditions, the same symmetrizing technique of Boada *et al.* (2013) takes place, consisting of substituting the asymmetric saturation by a symmetric one with limits $\bar{u}_i = 50\ mN, i = 1,\ldots,8$, followed by addition of the kernel symmetrizing vector $\xi = \bar{u}$. Although Boada *et al.* (2013) explored the combination of the static allocator ($\mathcal{F} = \mathrm{M}^{\dagger}$) with three different anti-windup strategies, here we focalize on the co-design of the dynamic allocator ($\mathcal{F}$ given by (7.6)) and the anti-windup gain E_c. After choosing $m_1 = m_2 = 1000\ kg$, a stabilizing LQG controller is designed using identity matrices for all the weights. The resulting controller is given by

$$\left[\begin{array}{c|c} \mathrm{A}_c & \mathrm{B}_c \\ \hline \mathrm{C}_c & \mathrm{D}_c \end{array}\right] = \left[\begin{array}{cc|c} -1.7321 & 1.0000 & 1.7321 \\ -1.0014 & -0.0532 & 1.0000 \\ \hline -0.7071 & -26.6009 & 0 \\ 0.7071 & 26.6009 & 0 \end{array}\right].$$

We then compute $\mathrm{M}^{\dagger}$=0.25diag$(\mathrm{M}_1^{\top}, \mathrm{M}_2^{\top})$, $\mathrm{N} = \mathrm{diag}(\mathrm{N}_1, \mathrm{N}_2)$, with N_1=N_2=$\begin{bmatrix} 1 & 1 & -1 \\ & \mathrm{I}_3 & \end{bmatrix}$. We choose W=diag$(100, 1, \ldots, 1)$ to illustrate the allocator ability, which means that we want to penalize the use of the first actuator. We use optimization procedure (7.17) with weights $\kappa_1 = 1, \kappa_2 = 0.15$, so that regional asymptotic stability can be guaranteed by means of Theorem 7.1. To enlarge the region of stability in the direction of the first plant state, representing the distance between the satellites, we used a small modification in (7.17) by substitution of $\mathrm{P}_0 \preceq \lambda \mathrm{I}$ by $\begin{bmatrix} 1 & 0_{1\times(n-1)} \end{bmatrix} \mathrm{P}_0 \begin{bmatrix} 1 & 0_{1\times(n-1)} \end{bmatrix}^{\top} \preceq \lambda$. The obtained anti-windup and allocator matrices for this example are given by

$$\left[\begin{array}{c} \mathrm{E}_c \\ \hline \mathrm{E}_f \end{array}\right] = \left[\begin{array}{cccccccc} 0.0019 & -0.0000 & 0.0394 & -0.0193 & 0.0325 & -0.0411 & -0.0411 & 0.0411 \\ -0.0002 & -0.0047 & 0.0142 & -0.0043 & 0.0118 & -0.0160 & -0.0160 & 0.0160 \\ \hline 1.2781 & 0.0144 & 0.1663 & -0.0741 & 0.1006 & 0.1297 & 0.1297 & -0.1297 \\ -0.6243 & -0.0044 & -0.0738 & 0.3141 & 0.2881 & -0.0918 & -0.0918 & 0.0918 \\ 0.7725 & 0.0088 & 0.0736 & 0.2114 & 0.3749 & 0.0720 & 0.0720 & -0.0720 \\ -0.9763 & -0.0119 & 0.0949 & -0.0674 & 0.0721 & 0.9519 & -0.3357 & 0.3357 \\ -0.9763 & -0.0119 & 0.0949 & -0.0674 & 0.0721 & -0.3357 & 0.9519 & 0.3357 \\ 0.9763 & 0.0119 & -0.0949 & 0.0674 & -0.0721 & 0.3357 & 0.3357 & 0.9519 \end{array}\right],$$

$$\mathrm{K}_f = \begin{bmatrix} -1.1684 & 0.6813 & -0.4766 & 0.0034 & 0.0034 & -0.0034 \\ 0.7282 & -1.0438 & -0.3054 & 0.0249 & 0.0249 & -0.0249 \\ -0.4528 & -0.3418 & -0.8017 & 0.0284 & 0.0284 & -0.0284 \\ -0.0200 & 0.0792 & 0.0584 & -0.8628 & 0.1381 & -0.1381 \\ -0.0200 & 0.0792 & 0.0584 & 0.1381 & -0.8628 & -0.1381 \\ 0.0200 & -0.0792 & -0.0584 & -0.1381 & -0.1381 & -0.8628 \end{bmatrix}.$$

We simulate the system response for an initial condition of $x_p(0) = \begin{bmatrix} -0.25 & 0 \end{bmatrix}^\top$, with $x_c(0) = 0$ and $x_f(0) = 0$. Figure 37 shows the obtained results. To better illustrate the ability of the dynamic allocator, two cases are plotted: dynamic allocator ($\mathcal{F}$ defined in (7.6)) plus anti-windup gain (E_c) and static allocator ($\mathcal{F} = \mathrm{M}^\dagger$) plus anti-windup gain (E_c). Both strategies are able to stabilize the system, however it can be observed that the dynamic allocation successfully reduces the usage of the penalized actuator.

Figure 37 – Example 1: Output and actuators .

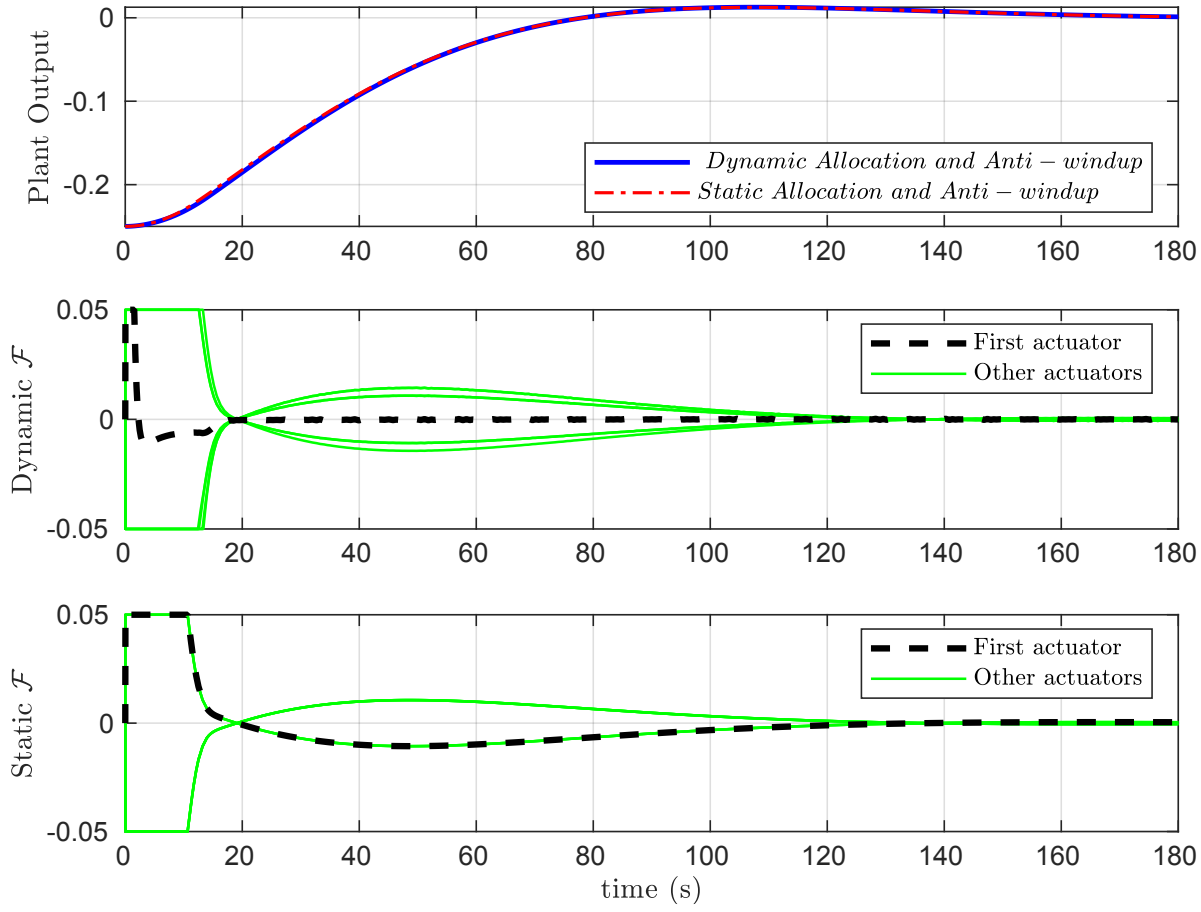

Source: The author.

For better assessment of the results, the value of $\int_0^{180} sat(y_f(\tau))^\top \mathrm{W} sat(y_f(\tau)) d\tau$ for the simulation in Figure 37 was computed to serve as a measure of performance, being equal to 0.781 in the case of the dynamic allocator and 3.634 for the static allocator, thus further illustrating the ability of the proposed strategy to minimize the energy of the usage of the actuators.

7.5.2 Example 2

In this example we consider the exponentially stable plant from Zaccarian (2009), where the saturation limits are given by $\bar{u} = \begin{bmatrix} 1 & 0.01 & 0.02 \end{bmatrix}^\top$. The plant is defined by the following data:

$$\left[\begin{array}{c|c} \mathrm{A}_p & \mathrm{B}_p \\ \hline \mathrm{C}_p & \mathrm{D}_p \end{array}\right] = \left[\begin{array}{cc|ccc} -0.157 & -0.094 & 0.87 & 0.253 & 0.743 \\ -0.416 & -0.45 & 0.39 & 0.354 & 0.65 \\ \hline 0 & 1 & 0 & 0 & 0 \end{array}\right].$$

There is no loss of generality in considering this example since $\mathrm{D}_p = 0$. To control the system and guarantee asymptotic tracking of constant references in the absence of saturation, Zaccarian (2009) inserts an integrator and designs a stabilizing LQG controller[1] which purposefully only uses the first two input channels. The resulting controller is given by

$$\left[\begin{array}{c|c} \mathrm{A}_c & \mathrm{B}_c \\ \hline \mathrm{C}_c & \mathrm{D}_c \end{array}\right] = \left[\begin{array}{cccc|c} -1.57 & 0.5767 & 0.822 & -0.65 & 0 \\ -0.9 & -0.501 & -0.94 & 0.802 & 0 \\ 0 & 1 & -1.61 & 1.614 & 0 \\ 0 & 0 & 0 & 0 & -1 \\ \hline 1.81 & -1.2 & -0.46 & 0 & 0 \\ -0.62 & 1.47 & 0.89 & 0 & 0 \\ 0 & 0 & 0 & 0 & 0 \end{array}\right].$$

For this example, $m_a = m_c$ and $\mathrm{M} = \mathrm{I}$. We select then N as the Kernel of B_p, resulting in $\mathrm{N} = \begin{bmatrix} -0.4726 & -1.3143 & 1 \end{bmatrix}^\top$. The entries of matrix W are chosen as $w_i = \bar{u}_{(i)}^{-2}$. In this case, we utilize optimization procedure (7.18) which allows to establish global asymptotic stability

[1] Although LQG controllers allow to penalize the desired control effort y_c in their design phase this does not imply a penalization of the use of the actuators y_f.

results (Remark 7.6). We obtain, thus $\mathrm{K}_f = -0.2006$ and matrices E_c, E_f given by

$$\left[\begin{array}{c} \mathrm{E}_c \\ \hline \mathrm{E}_f \end{array}\right] = \left[\begin{array}{ccc} -0.9453 & -0.4282 & -0.7295 \\ -0.2943 & -0.2793 & -0.6308 \\ -0.3130 & 0.9045 & 0.1361 \\ -0.4013 & 0.4583 & 0.2161 \\ \hline -0.1567 & 0.9386 & -0.3464 \end{array}\right].$$

The parameters of the strategy from Zaccarian (2009) can be found therein. We simulate the system response for an initial condition $x_p(0) = \left[\begin{array}{cc} 0 & 1 \end{array}\right]^\top$, with $x_c(0) = 0$ and $x_f(0) = 0$. Figure 38 shows the output response, the computed control signal and the plant input for both the proposed strategy and the one from Zaccarian (2009). The fundamental difference in the results relies in the fact that for the proposed strategy the plant input signals (u_p) converge to the origin, thus avoiding waste of energy in the actuators.

Figure 38 – Example 2: Plant output, controller output and plant input signals.

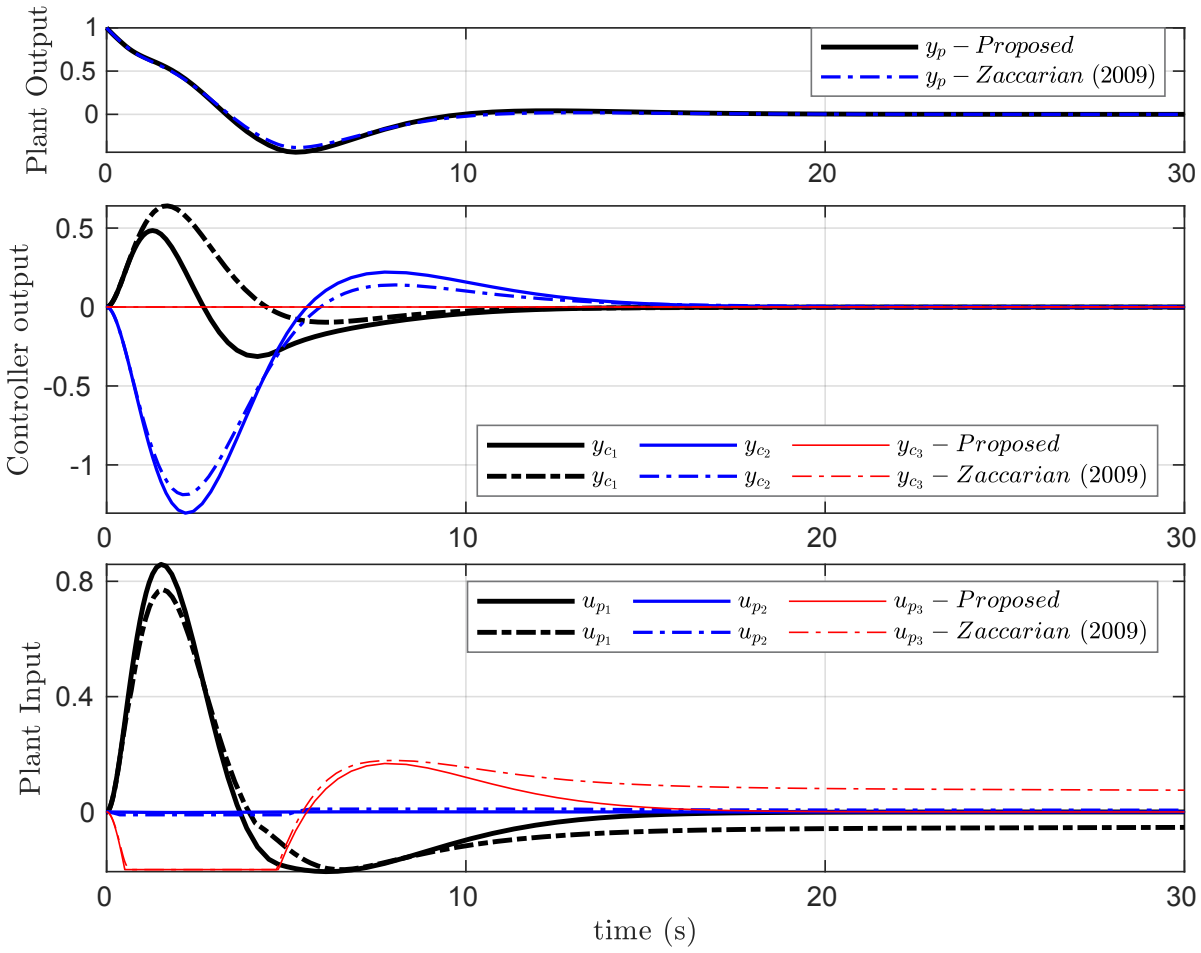

Source: The author.

7.6 Discussion

In this chapter, we proposed the co-design of dynamic allocation functions along with anti-windup gains to deal with over actuated/input redundant systems with saturating actuators. The novelty of the work relied upon the extension of the ideas in Zaccarian (2009) to a more general scenario, including the ability to deal with a much broader spectrum of cases and inserting optimization criteria that allow both to minimize energy consumption in the actuators and to maximize estimations on the region of attraction. The application of the developed conditions in the examples effectively showed the advantages of the proposed scheme. Future work could deal with many other cases, as the consideration of other nonlinearities affecting the actuator and the event-triggered control.

GENERAL CONCLUSIONS

In this thesis, we dealt with the control of input saturated systems in conjunction with the problems of time delays and control allocation. The main novelties were presented throughout Parts II and III, more specifically in Chapters 5, 6 and 7. Herein, we will make an effort to draw some general conclusions and perspectives from this work.

In Part II of the thesis, we focused on the analysis, control and anti-windup problems related to systems with input and output time delays controlled by DTC structures. The core contributions of this part were split among two chapters.

- In Chapter 5, we developed a model-based controller and anti-windup strategy for input-saturated linear systems with constant input delays. Differently from most strategies regarding this type of system, we dealt with practical aspects, such that set-point tracking, disturbance rejection and modelling uncertainties were taken into account. The consideration of these practical aspects was made easier by employing a decoupled structure that split the system into linear and nonlinear loops. It was shown that the simplified tuning of the linear loop could take into account aspects that are important to the control engineer in the industry. On the other hand, modern mathematical tools were used for developing conditions that aid relief the undesired aspects of the saturation nonlinearity by means of the LMI-based design of an anti-windup filter. Moreover, one big novelty from this chapter was the possibility to deal with both time-delayed and delay-free systems in a unified manner, which was made possible by means of simple modifications in the structure of the base DTC controller. In order to provide more degrees of freedom for the designer, the concept of $\mathbb{D}$-stability was used so that the poles of the anti-windup conditioning filter were allocated within a desired region of the complex plane, thus adjusting system response to saturation events.
- In Chapter 6, we went back to the original structure of the Simplified Dead-time Compensator (SDTC) in order to solve some of the problems left open by the previous chapter. The model of the saturation is added to the predictor path in its implementation structure so that prediction is correctly updated. In order that the system could be analysed as a whole and no longer split into two loops, we rewrote the closed loop as a system augmented of the plant and predictor states, resulting in a state-delayed equivalent system. In this case, we considered stability of the closed loop in the presence of output time-varying measurement delays, input saturation, and input disturbances of limited energy. Due to

the state-delayed representation, we were able to use a Lyapunov-Krasovskii functional along with generalized sector conditions to provide stability analysis and relate the tuning of DTC controllers to upper bounds on the time-varying delay, the bound on the energy of input disturbances, and the sizes of estimations on the region of attraction. Since DTCs are model-based controllers, care was taken in order to find conditions expressed in the form of LMIs that did not numerically suffer from the high dimensionality of the closed loop. Furthermore, it was shown that, similarly to the linear case, the DTC can also be tuned to improve system robustness with respect to time-varying delays and the saturation condition. Additionally, we proposed a new strategy for the characterization of the region of attraction by means of the augmented LKF that can be applied in any work dealing with state-delayed discrete-time systems and therefore is a contribution not necessarily linked with DTCs.

Since we explored regional stability of the saturated closed loops, the developed strategies in Part II are suitable to deal with open-loop stable, integrative and unstable SISO processes. Due to their simplified tuning and discrete-time nature, implementation of the proposed schemes is supposed to be straight forward and should present great potential if applied to commercial applications.

In the much shorter Part III, we addressed the design problem of allocation functions and anti-windup for over-actuated systems. Following a general introduction on the subject of control allocation, the contributions reported in Chapter 7 are related to the proposal of convex conditions for the co-design of a dynamic allocation function and static anti-windup gains that act both on the controller and in the allocator. The proposed solution presented many advantages compared with previous ones in the control allocation literature:

- The co-design of the dynamic allocator and anti-windup is realized by means of convex optimization procedures expressed in the form of LMIs, which are computationally easy to solve.
- The proposed strategy allows the designer to choose how much to individually penalize the use of each actuator. This allows, for example, to establish a rule that forces actuators with a larger capacity to be more employed than others.
- The allocator is optimal in terms of energy usage of the actuators since the allocator states are guaranteed to converge to the origin.
- The proposal is more general and can deal with a broader range of cases than previous

formulations dealing with dynamic allocation.

- The design conditions are always feasible under the assumption that the controller stabilizes the linear plant-controller interconnection.

Furthermore, the proposal is suitable to deal with unstable plants, since we provide conditions for regional stabilization with estimations on the region of attraction. Unlike the contributions in the time-delay part of the thesis, the allocation strategy is useful for dealing with multiple-input multiple-output (MIMO) plants.

Therefore, the contributions reported in this thesis are mainly concerned with the presence of actuator saturation in control loops. Nonetheless, the specific situations considered were those of time-delayed and over-actuated systems. The results in the time-delay part were developed in the discrete-time domain since they deal with the so-called DTCs, which are model-based controllers that require digital implementation. Their discrete-time nature should provide control engineers with safe implementation and operation in commercial applications. It is also important to remark that although the chapters in Part II were mainly focused on the so-called SDTC, all the proposed methods could be easily extended to other members of the classical family of DTC controllers. Regarding control allocation, we decided to explore formulations in the continuous-time domain, since the developed strategies did not involve prediction and therefore do not require digital implementation. Thus, we have dealt with both discrete-time and continuous-time strategies, which enlarges the possible range of applications for the studies presented in the thesis. Finally, it is worth to remind that all the proposals were effectively validated through either simulation case studies or experimental results, in which the application to the temperature control of neonatal incubators deserves to be mentioned.

Perspectives

The results reported in this thesis leave room for many possible future extensions, which are shortlisted below:

- Although the design of the anti-windup conditioning filter $M(z)$ in Chapter 5 was shown to be effective by considering the nominal nonlinear loop, LMIs for the uncertain case deserve to be investigated and should be developed as well. Regarding this, perhaps a straightforward manner to obtain convex design conditions would be to consider the plant matrices to contain polytopic uncertainties, thus leading to polytopic LMIs.
- Other $\mathbb{D}$-stability regions, as disk and conic regions could be explored for pole placement

of the conditioning filter $M(z)$ in Chapter 5. Moreover, a deeper study on the relation between the anti-windup performance and location of the poles would be of interest.

- Regarding Chapter 6, a straightforward continuation would be the development of a DTC strategy that could be stabilized via LMIs synthesis conditions. Nonetheless, translation of all the steps for their design into LMIs is not an easy task due to the nonlinearities that arise when one tries to respect all the characteristics of the SDTC controller, especially the ability to design the robustness filter to cancel the unstable poles of the plant model. As an alternative, the LMI synthesis of observer-predictive structures, which do not need pole cancellation to guarantee a stable implementation, could be a much more interesting step going forward. In fact, a work consisting of this idea is already in developments. Another possibility concerning Chapter 6 is to include an anti-windup strategy to further improve the closed-loop characteristics of the DTC in the presence of the saturation. Additionally, the development of works in the sampled-data framework where the discretization of the plant is avoided and the sample and hold effects are modelled by a time-varying delay would be a very interesting step going forward with the SDTC strategy.
- Finally, concerning Chapter 7, the control allocation technique can potentially be extended in several directions. For example, other nonlinearities such as rate saturation and cone-bounded ones could be considered in the actuator model. Also, we could deal with the case of event-trigger, which is a recent trend in control. The case of allocation in systems with delays is also a direction of great interest.

BIBLIOGRAPHY

ALBERTOS, P.; GARCÍA, P. Robust control design for long time-delay systems. *J Process Control*, v. 19, n. 10, p. 1640–1648, 2009.

ALVES LIMA, T.; PRUDÊNCIO DE ALMEIDA FILHO, M.; TORRICO, B. C.; NOGUEIRA, F. G.; CORREIA, W. B. A practical solution for the control of time-delayed and delay-free systems with saturating actuators. *European Journal of Control*, v. 51, p. 53 – 64, 2020. ISSN 0947-3580.

ALVES LIMA, T.; TARBOURIECH, S.; GOUAISBAUT, F.; PRUDÊNCIO DE ALMEIDA FILHO, M.; GARCÍA, P.; TORRICO, B. C.; NOGUEIRA, F. G. Analysis and experimental application of a dead-time compensator for input saturated processes with output time-varying delays. *IET Control Theory & Applications*, v. 15, n. 4, p. 580–593, 2021.

ALVES LIMA, T.; TARBOURIECH, S.; NOGUEIRA, F. G.; TORRICO, B. C. Co-design of dynamic allocation functions and anti-windup. *IEEE Control Systems Letters*, v. 5, n. 6, p. 2198–2203, 2021.

ALVES LIMA, T.; TARBOURIECH, S.; NOGUEIRA, F. G.; TORRICO, B. C. Energy-based design of dynamic allocation in the presence of saturating actuators. In: . [S.l.: s.n.], 2021. p. to appear. ISSN 2405-8963. 24th International Symposium on Mathematical Theory of Networks and Systems.

ALVES LIMA, T.; TORRICO, B. C.; PRUDÊNCIO DE ALMEIDA FILHO, M.; FORTE, M. D. N.; PEREIRA, R. D. O.; NOGUEIRA, F. G. First-order dead-time compensation with feedforward action. In: *2019 18th European Control Conference (ECC)*. [S.l.: s.n.], 2019. p. 3638–3643.

ASTROM, K. J.; HANG, C. C.; LIM, B. C. A new Smith predictor for controlling a process with a integrator and long dead-time. *IEEE Trans Autom Control*, v. 39, n. 2, p. 343–345, 1994.

BENOSMAN, M.; LIAO, F.; LUM, K.; WANG, J. L. Nonlinear control allocation for non-minimum phase systems. *IEEE Transactions on Control Systems Technology*, v. 17, n. 2, p. 394–404, 2009.

BOADA, J.; PRIEUR, C.; TARBOURIECH, S.; PITTET, C.; CHARBONNEL, C. Formation flying control for satellites: Anti-windup based approach. In: FASANO, G.; PINTÉR, J. D. (Ed.). *Modeling and Optimization in Space Engineering*. New York, NY: Springer New York, 2013. p. 61–83. ISBN 978-1-4614-4469-5.

BOUOUDEN, S.; CHADLI, M.; ZHANG, L.; YANG, T. Constrained model predictive control for time-varying delay systems: Application to an active car suspension. *International Journal of Control, Automation and Systems*, Springer Science and Business Media LLC, v. 14, n. 1, p. 51–58, fev. 2016.

BOYD, S.; GHAOUI, L. E.; FERON, E.; BALAKRISHNAN, V. *Linear Matrix Inequalities in System and Control Theory*. Philadelphia, PA: SIAM, 1994. v. 15. (Studies in Applied Mathematics, v. 15). ISBN 0-89871-334-X.

BRIAT, C. *Linear Parameter-Varying and Time-Delay Systems*. [S.l.]: Springer Berlin Heidelberg, 2015.

CAMACHO, E. F.; BORDONS, C. *Model Predictive Control*. [S.l.]: Springer-Verlag London, 2007.

CASTILLO, A.; GARCÍA, P. Predicting the future state of disturbed LTI systems: A solution based on high-order observers. *Automatica*, v. 124, p. 109365, 2021. ISSN 0005-1098.

CASTRO, M. F.; SEURET, A.; LEITE, V. J.; SILVA, L. F. Robust local stabilization of discrete time-varying delayed state systems under saturating actuators. *Automatica*, v. 122, p. 109266, 2020. ISSN 0005-1098.

CHEN, Y.; FEI, S. Exponential stabilization for discrete-time time-delay systems with actuator saturation. In: *Proceedings of the 33rd Chinese Control Conference*. [S.l.: s.n.], 2014. p. 6130–6135.

CHEN, Y.; FEI, S.; LI, Y. Stabilization of neutral time-delay systems with actuator saturation via auxiliary time-delay feedback. *Automatica*, v. 52, p. 242 – 247, 2015. ISSN 0005-1098.

CHEN, Y.; FEI, S.; LI, Y. Robust stabilization for uncertain saturated time-delay systems: A distributed-delay-dependent polytopic approach. *IEEE Transactions on Automatic Control*, v. 62, n. 7, p. 3455–3460, 2017.

CHILALI, M.; GAHINET, P. H∞ design with pole placement constraints: an LMI approach. *IEEE Transactions on Automatic Control*, v. 41, n. 3, p. 358–367, Mar 1996. ISSN 0018-9286.

DE CASTRO, R.; BREMBECK, J. Lyapunov-based control allocation for over-actuated nonlinear systems. In: *2019 American Control Conference (ACC)*. [S.l.: s.n.], 2019. p. 5033–5038.

DE OLIVEIRA, F. S.; SOUZA, F. O.; PALHARES, R. M. PID tuning for time-varying delay systems based on modified Smith predictor. *IFAC-PapersOnLine*, v. 50, n. 1, p. 1269 – 1274, 2017. ISSN 2405-8963. 20th IFAC World Congress.

DE OLIVEIRA, M. C.; SKELTON, R. E. Stability tests for constrained linear systems. In: MOHEIMANI, S. R. (Ed.). *Perspectives in robust control*. London: Springer London, 2001. p. 241–257.

DE SOUZA, C.; LEITE, V. J. S.; SILVA, L. F. P.; CASTELAN, E. B. ISS robust stabilization of state-delayed discrete-time systems with bounded delay variation and saturating actuators. *IEEE Transactions on Automatic Control*, v. 64, n. 9, p. 3913–3919, 2019.

DUAN, G.; YU, H. *LMIs in Control Systems: Analysis, Design and Applications*. [S.l.]: Taylor & Francis, 2013. ISBN 9781466582996.

DUCARD, G. J. Control allocation. In: ____. *Fault-tolerant Flight Control and Guidance Systems*. [S.l.]: Springer London, 2009. cap. 5, p. 89–106.

DURHAM, W.; BORDIGNON, K. A.; BECK, R. *Aircraft Control Allocation*. [S.l.]: John Wiley & Sons, Ltd, 2016.

FLESCH, R. C. C.; NORMEY-RICO, J. E.; FLESCH, C. A. A unified anti-windup strategy for siso discrete dead-time compensators. *Control Engineering Practice*, v. 69, p. 50–60, 2017.

FRIDMAN, E. A new Lyapunov technique for robust control of systems with uncertain non-small delays. *IMA Journal of Mathematical Control and Information*, v. 23, n. 2, p. 165–179, 2006.

FRIDMAN, E. *Introduction to Time-Delay Systems*. [S.l.]: Springer International Publishing, 2014. 68, 83, 247-251 p.

FRIDMAN, E.; PILA, A.; SHAKED, U. Regional stabilization and H∞ control of time-delay systems with saturating actuators. *International Journal of Robust and Nonlinear Control*, v. 13, n. 9, p. 885–907, 2003.

GALEANI, S.; SERRANI, A.; VARANO, G.; ZACCARIAN, L. On input allocation-based regulation for linear over-actuated systems. *Automatica*, v. 52, p. 346 – 354, 2015. ISSN 0005-1098.

GALEANI, S.; TARBOURIECH, S.; TURNER, M.; ZACCARIAN, L. A tutorial on modern anti-windup design. *European Journal of Control*, v. 15, n. 34, p. 418–440, 2009.

GALEANI, S.; TEEL, A. R.; ZACCARIAN, L. Constructive nonlinear anti-windup design for exponentially unstable linear plants. *Systems & Control Letters*, v. 56, n. 5, p. 357 – 365, 2007. ISSN 0167-6911.

GARCÍA, P.; ALBERTOS, P. A new dead-time compensator to control stable and integrating processes with long dead-time. *Automatica*, v. 44, n. 4, p. 1062–1071, 2008.

GARCÍA, P.; ALBERTOS, P. Robust tuning of a generalized predictor-based controller for integrating and unstable systems with long time-delay. *Journal of Process Control*, v. 23, n. 8, p. 1205 – 1216, 2013.

GARCÍA, P.; ALBERTOS, P.; HAGGLUND, T. Control of unstable non-minimum-phase delayed systems. *J Process Control*, v. 16, n. 10, p. 1099–1111, 2006.

GENG, X.; HAO, S.; LIU, T.; ZHONG, C. Generalized predictor based active disturbance rejection control for non-minimum phase systems. *ISA Transactions*, v. 87, p. 34 – 45, 2019. ISSN 0019-0578.

GOMES DA SILVA JR., J. M.; GHIGGI, I.; TARBOURIECH, S. Non-rational dynamic output feedback for time-delay systems with saturating inputs. *International Journal of Control*, Taylor & Francis, v. 81, n. 4, p. 557–570, 2008.

GOMES DA SILVA JR., J. M.; TARBOURIECH, S. Antiwindup design with guaranteed regions of stability: an LMI-based approach. *IEEE Transactions on Automatic Control*, v. 50, n. 1, p. 106–111, Jan 2005. ISSN 0018-9286.

GOMES DA SILVA JR., J. M.; TARBOURIECH, S.; GARCIA, G. Anti-windup design for time-delay systems subject to input saturation an LMI-based approach. *European Journal of Control*, v. 12, n. 6, p. 622 – 634, 2006. ISSN 0947-3580.

GONZALEZ, A.; BALAGUER, V.; GARCÍA, P.; CUENCA, A. Gain-scheduled predictive extended state observer for time-varying delays systems with mismatched disturbances. *ISA Transactions*, v. 84, p. 206 – 213, 2019. ISSN 0019-0578.

GUPTA, R. A.; CHOW, M. Networked control system: Overview and research trends. *IEEE Transactions on Industrial Electronics*, v. 57, n. 7, p. 2527–2535, July 2010. ISSN 0278-0046.

HE, Y.; WU, M.; LIU, G.; SHE, J. Output feedback stabilization for a discrete-time system with a time-varying delay. *IEEE Transactions on Automatic Control*, v. 53, n. 10, p. 2372–2377, 2008.

HERRMANN, G.; TURNER, M. C.; POSTLETHWAITE, I. Discrete-time and sampled-data anti-windup synthesis: stability and performance. *International Journal of Systems Science*, Taylor & Francis, v. 37, n. 2, p. 91–113, 2006.

HESPANHA, J. P.; NAGHSHTABRIZI, P.; XU, Y. A survey of recent results in networked control systems. *Proceedings of the IEEE*, v. 95, n. 1, p. 138–162, Jan 2007. ISSN 0018-9219.

HETEL, L.; DAAFOUZ, J.; IUNG, C. Equivalence between the Lyapunov–Krasovskii functionals approach for discrete delay systems and that of the stability conditions for switched systems. *Nonlinear Analysis: Hybrid Systems*, v. 2, n. 3, p. 697 – 705, 2008. ISSN 1751-570X. Special Issue Section: Analysis and Design of Hybrid Systems.

HIEN, L. V.; TRINH, H. New finite-sum inequalities with applications to stability of discrete time-delay systems. *Automatica*, v. 71, n. Supplement C, p. 197 – 201, 2016. ISSN 0005-1098.

HU, J.; YANG, Y.; LIU, H.; CHEN, D.; DU, J. Non-fragile set-membership estimation for sensor-saturated memristive neural networks via weighted try-once-discard protocol. *IET Control Theory & Applications*, Institution of Engineering and Technology, v. 14, p. 1671–1680(9), September 2020. ISSN 1751-8644.

HU, L.-S.; BAI, T.; SHI, P.; WU, Z. Sampled-data control of networked linear control systems. *Automatica*, v. 43, n. 5, p. 903 – 911, 2007. ISSN 0005-1098.

HUBA, M. Comparing 2DOF PI and predictive disturbance observer based filtered PI control. *J Process Control*, v. 23, p. 1379–1400, 2013.

JIN, J. Modified pseudoinverse redistribution methods for redundant controls allocation. *Journal of Guidance, Control, and Dynamics*, American Institute of Aeronautics and Astronautics (AIAA), v. 28, n. 5, p. 1076–1079, set. 2005.

JOHANSEN, T. A. Optimizing nonlinear control allocation. In: *43rd IEEE Conference on Decision and Control (CDC)*. [S.l.: s.n.], 2004. p. 3435–3440 Vol.4.

JOHANSEN, T. A.; FOSSEN, T. I. Control allocation—A survey. *Automatica*, v. 49, n. 5, p. 1087 – 1103, 2013. ISSN 0005-1098.

KAYA, I. A new Smith predictor and controller for control of processes with long dead time. *ISA Trans*, v. 42, p. 101–110, 2003.

KHALIL, H. K. *Nonlinear Systems*. [S.l.]: Prentice Hall, 2002.

KIRTANIA, K.; CHOUDHURY, M. A. A. S. Set point weighted modified Smith predictor for integrating and double integrating processes with time delay. *J Process Control*, v. 22, n. 3, p. 612–625, 2012.

KOTHARE, M. V.; CAMPO, P. J.; MORARI, M.; NETT, C. N. A unified frame-work for the study of anti-windup designs. *Automatica*, v. 30, n. 12, p. 1869–1883, 1994.

KREISS, J.; BODSON, M.; DELPOUX, R.; GAUTHIER, J.-Y.; TRÉGOUËT, J.-F.; LINSHI, X. Optimal control allocation for the parallel interconnection of buck converters. *Control Engineering Practice*, v. 109, p. 104727, 2021. ISSN 0967-0661.

KRSTIC, M. *Delay Compensation for Nonlinear, Adaptive, and PDE Systems*. [S.l.]: Birkhäuser Boston, 2009.

KWON, O.; PARK, M.; PARK, J. H.; LEE, S.; CHA, E. Stability and stabilization for discrete-time systems with time-varying delays via augmented Lyapunov–Krasovskii functional. *Journal of the Franklin Institute*, v. 350, n. 3, p. 521 – 540, 2013. ISSN 0016-0032.

LAMNABHI-LAGARRIGUE, F.; ANNASWAMY, A.; ENGELL, S.; ISAKSSON, A.; KHARGONEKAR, P.; MURRAY, R. M.; NIJMEIJER, H.; SAMAD, T.; TILBURY, D.; HOF, P. V. den. Systems & control for the future of humanity, research agenda: Current and future roles, impact and grand challenges. *Annual Reviews in Control*, v. 43, n. Supplement C, p. 1 – 64, 2017. ISSN 1367-5788.

LASSERRE, J. B. Reachable, controllable sets and stabilizing control of constrained linear systems. *Automatica*, v. 29, n. 2, p. 531–536, 1993.

LÉCHAPPÉ, V.; MOULAY, E.; PLESTAN, F.; GLUMINEAU, A.; CHRIETTE, A. New predictive scheme for the control of LTI systems with input delay and unknown disturbances. *Automatica*, v. 52, p. 179 – 184, 2015. ISSN 0005-1098.

LI, Z.-S.; MO, X.-Q.; GUO, S.-J.; LAN, W.-Y.; HUANG, C.-Q. 4-Degree-of-freedom anti-windup scheme for plants with actuator saturation. *Journal of Process Control*, v. 47, p. 111 – 120, 2016. ISSN 0959-1524.

LIAO, F.; LUM, K.; WANG, J. L.; BENOSMAN, M. Constrained nonlinear finite-time control allocation. In: *2007 American Control Conference*. [S.l.: s.n.], 2007. p. 3801–3806.

LIOU, C.-T.; YU-SHU, C. The effect of nonideal mixing on input multiplicity in a CSTR. *Chemical Engineering Science*, v. 46, n. 8, p. 2113 – 2116, 1991. ISSN 0009-2509.

LIU, J.; ZHANG, J. Note on stability of discrete-time time-varying delay systems. *IET Control Theory & Applications*, v. 6, n. 2, p. 335–339, January 2012. ISSN 1751-8644.

LIU, K.; SEURET, A.; XIA, Y. Stability analysis of systems with time-varying delays via the second-order Bessel–Legendre inequality. *Automatica*, v. 76, p. 138 – 142, 2017. ISSN 0005-1098.

LIU, T.; GARCÍA, P.; CHEN, Y.; REN, X.; ALBERTOS, P.; SANZ, R. New predictor and 2DOF control scheme for industrial processes with long time delay. *IEEE Transactions on Industrial Electronics*, v. 65, n. 5, p. 4247–4256, May 2018.

LÖFBERG, J. Yalmip : A toolbox for modeling and optimization in MATLAB. In: *In Proceedings of the CACSD Conference*. Taipei, Taiwan: [s.n.], 2004. p. 284–289.

LOUISELL, J. Delay diferential systems with time-varying delay: New directions for stability theory. *Kybernetika*, v. 37, n. 3, p. 239 – 251, 2001.

MATAUSEK, M. R.; MICIC, A. D. A modified Smith predictor for controlling a process with a integrator and long dead-time. *IEEE Trans Autom Control*, v. 41, n. 8, p. 1199–1203, 1996.

MATAUSEK, M. R.; MICIC, A. D. On the modified Smith predictor for controlling a process with a integrator and long dead-time. *IEEE Trans on Autom Control*, v. 44, n. 8, p. 1603–1606, 1999.

MATAUSEK, M. R.; RIBIC, A. I. Control of stable, integrating and unstable processes by the modified Smith predictor. *J Process Control*, v. 22, n. 1, p. 338–343, 2012.

MEGRETSKI, A. $\mathcal{L}_2$ BIBO output feedback stabilization with saturated control. *IFAC Proceedings Volumes*, v. 29, n. 1, p. 1872 – 1877, 1996. ISSN 1474-6670. 13th World Congress of IFAC, 1996, San Francisco USA, 30 June - 5 July.

MORARI, M.; ZAFIRIOU, E. *Robust Process Control*. [S.l.]: Prentice-Hall, 1989.

NAAMANE, K.; CHAIBI, R.; TISSIR, E. H.; HMAMED, A. Stabilization of discrete-time T-S fuzzy systems with saturating actuators. In: *2017 International Conference on Advanced Technologies for Signal and Image Processing (ATSIP)*. [S.l.: s.n.], 2017. p. 1–5.

NAM, P. T.; PATHIRANA, P. N.; TRINH, H. Discrete Wirtinger-based inequality and its application. *Journal of the Franklin Institute*, v. 352, n. 5, p. 1893 – 1905, 2015. ISSN 0016-0032.

NORMEY-RICO, J.; BORDONS, C.; CAMACHO, E. Improving the robustness of dead-time compensating pi controllers. *Control Engineering Practice*, v. 5, n. 6, p. 801 – 810, 1997. ISSN 0967-0661.

NORMEY-RICO, J. E.; CAMACHO, E. F. *Control of Dead-time Processes*. Berlin: Springer, 2007.

NORMEY-RICO, J. E.; CAMACHO, E. F. Dead-time compensators: A survey. *Control Engineering Practice*, v. 16, n. 4, p. 407 – 428, 2008. Special Section on Manoeuvering and Control of Marine Craft.

NORMEY-RICO, J. E.; CAMACHO, E. F. Simple robust dead-time compensator for first-order plus dead-time unstable processes. *Ind Eng Chem Res*, v. 47, n. 14, p. 4784–4790, 2008.

NORMEY-RICO, J. E.; GARCÍA, P.; GONZALEZ, A. Robust stability analysis of filtered Smith predictor for time-varying delay processes. *Journal of Process Control*, v. 22, n. 10, p. 1975 – 1984, 2012. ISSN 0959-1524.

OPPENHEIMER, M. W.; DOMAN, D. B.; BOLENDER, M. A. Control allocation for over-actuated systems. In: *2006 14th Mediterranean Conference on Control and Automation*. [S.l.: s.n.], 2006. p. 1–6.

PANDEY, S.; DAS, B.; TADEPALLI, S. K. Comments on "New finite-sum inequalities with applications to stability of discrete time-delay systems". *Automatica*, v. 91, p. 320 – 321, 2018. ISSN 0005-1098.

PAPACHRISTODOULOU, A.; PEET, M. M.; NICULESCU, S. I. Stability analysis of linear systems with time-varying delays: Delay uncertainty and quenching. In: *2007 46th IEEE Conference on Decision and Control*. [S.l.: s.n.], 2007. p. 2117–2122. ISSN 0191-2216.

PARK, P.; KO, J. W.; JEONG, C. Reciprocally convex approach to stability of systems with time-varying delays. *Automatica*, v. 47, n. 1, p. 235 – 238, 2011. ISSN 0005-1098.

PEREIRA, R. D.; VERONESI, M.; VISIOLI, A.; NORMEY-RICO, J. E.; TORRICO, B. C. Implementation and test of a new autotuning method for PID controllers of TITO processes. *Control Engineering Practice*, v. 58, p. 171 – 185, 2017. ISSN 0967-0661.

PETERSEN, J. A. M.; BODSON, M. Constrained quadratic programming techniques for control allocation. *IEEE Transactions on Control Systems Technology*, v. 14, n. 1, p. 91–98, Jan 2006.

PRUDÊNCIO DE ALMEIDA FILHO, M. *Contributions on model-based controllers applied to dead-time systems*. Tese (Doutorado) — Universidade Federal do Ceará, 2020.

RAO, A. S.; CHIDAMBARAM, M. Enhanced Smith predictor for unstable processes with time delay. *Industrial & Engineering Chemistry Research*, v. 44, n. 22, p. 8291–8299, 2005.

RAO, A. S.; CHIDAMBARAM, M. Analytical design of modified Smith predictor in a two-degrees-of-freedom control scheme for second order unstable processes with time delay. *ISA Trans*, v. 47, n. 4, p. 407–419, 2008.

RAO, A. S.; RAO, V. S. R.; CHIDAMBARAM, M. Simple analytical design of modified Smith predictor with improved performance for unstable first-order plus time delay (FOPTD) processes. *Industrial & Engineering Chemistry Research*, v. 46, n. 13, p. 4561–4571, 2007.

RODRÍGUEZ, C.; ARANDA-ESCOLÁSTICO, E.; GUZMÁN, J. L.; BERENGUEL, M.; HÄGGLUND, T. Revisiting the simplified IMC tuning rules for low-order controllers: Novel 2DoF feedback controller. *IET Control Theory & Applications*, Institution of Engineering and Technology, v. 14, p. 1700–1710(10), September 2020. ISSN 1751-8644.

SANZ, R. *Robust control strategies for unstable systems with input/output delays*. Tese (Doutorado) — Universitat Politecnica de Valencia, 2018.

SANZ, R.; GARCÍA, P.; ALBERTOS, P. Enhanced disturbance rejection for a predictor-based control of LTI systems with input delay. *Automatica*, v. 72, p. 205 – 208, 2016. ISSN 0005-1098.

SANZ, R.; GARCÍA, P.; ALBERTOS, P. A generalized Smith predictor for unstable time-delay siso systems. *ISA Transactions*, v. 72, p. 197 – 204, 2018. ISSN 0019-0578.

SANZ, R.; GARCÍA, P.; FRIDMAN, E.; ALBERTOS, P. Rejection of mismatched disturbances for systems with input delay via a predictive extended state observer. *International Journal of Robust and Nonlinear Control*, v. 28, n. 6, p. 2457–2467, 2018.

SANZ, R.; GARCÍA, P.; FRIDMAN, E.; ALBERTOS, P. Robust predictive extended state observer for a class of nonlinear systems with time-varying input delay. *International Journal of Control*, Taylor & Francis, v. 93, n. 2, p. 217–225, 2020.

SANZ, R.; GARCÍA, P.; KRSTIC, M. Observation and stabilization of LTV systems with time-varying measurement delay. *Automatica*, v. 103, p. 573 – 579, 2019. ISSN 0005-1098.

SERRANI, A. Output regulation for over-actuated linear systems via inverse model allocation. In: *2012 IEEE 51st IEEE Conference on Decision and Control (CDC)*. [S.l.: s.n.], 2012. p. 4871–4876.

SEURET, A.; GOUAISBAUT, F. Wirtinger-based integral inequality: Application to time-delay systems. *Automatica*, v. 49, n. 9, p. 2860 – 2866, 2013. ISSN 0005-1098.

SEURET, A.; GOUAISBAUT, F. Hierarchy of LMI conditions for the stability analysis of time-delay systems. *Systems & Control Letters*, v. 81, p. 1 – 7, 2015. ISSN 0167-6911.

SEURET, A.; GOUAISBAUT, F. Stability of linear systems with time-varying delays using Bessel–Legendre inequalities. *IEEE Transactions on Automatic Control*, v. 63, n. 1, p. 225–232, Jan 2018. ISSN 2334-3303.

SEURET, A.; GOUAISBAUT, F.; FRIDMAN, E. Stability of discrete-time systems with time-varying delays via a novel summation inequality. *IEEE Transactions on Automatic Control*, v. 60, n. 10, p. 2740–2745, Oct 2015. ISSN 0018-9286.

SEURET, A.; MARX, S.; TARBOURIECH, S. Hierarchical estimation of the region of attraction for systems subject to a state delay and a saturated input. In: *2019 18th European Control Conference (ECC)*. [S.l.: s.n.], 2019. p. 2915–2920.

SHAO, H.; HAN, Q. L. New stability criteria for linear discrete-time systems with interval-like time-varying delays. *IEEE Transactions on Automatic Control*, v. 56, n. 3, p. 619–625, March 2011. ISSN 0018-9286.

SHEN, Y.; WANG, Z.; SHEN, B.; ALSAADI, F. E. H∞ filtering for multi-rate multi-sensor systems with randomly occurring sensor saturations under the p-persistent CSMA protocol. *IET Control Theory Applications*, v. 14, n. 10, p. 1255–1265, 2020.

SKOGESTAD, S.; POSTLETHWAITE, I. *Multivariable Feedback Control: Analysis and Design*. [S.l.]: Wiley, 2005. ISBN 047001167X.

SMITH, O. J. M. Closer control of loops with dead time. *Chemical Engineering Progress*, v. 53, n. 5, p. 217–219, 1957.

SONTAG, E. D. An algebraic approach to bounded controllability of linear systems. *Int. J. Control*, v. 39, n. 1, p. 181–188, 1984.

SUN, W.; FU, B. Adaptive control of time-varying uncertain non-linear systems with input delay: a Hamiltonian approach. *IET Control Theory & Applications*, v. 10, n. 15, p. 1844–1858, 2016.

SUN, X.-M.; LIU, G.-P.; REES, D.; WANG, W. Delay-dependent stability for discrete systems with large delay sequence based on switching techniques. *Automatica*, v. 44, n. 11, p. 2902 – 2908, 2008. ISSN 0005-1098.

TARBOURIECH, S.; GARCIA, G.; GOMES DA SILVA JR., J. M.; QUEINNEC, I. *Stability and Stabilization of Linear Systems with Saturating Actuators*. London: Springer, 2011. 19-20,43 p.

TARBOURIECH, S.; GOMES DA SILVA JR., J. M. Synthesis of controllers for continuous-time delay systems with saturating controls via LMIs. *IEEE Transactions on Automatic Control*, v. 45, n. 1, p. 105–111, Jan 2000. ISSN 0018-9286.

TARBOURIECH, S.; GOMES DA SILVA JR., J. M.; GARCIA, G. Delay-dependent anti-windup loops for enlarging the stability region of time delay systems with saturating inputs. *Journal of Dynamic Systems, Measurement, and Control*, ASME International, v. 125, n. 2, p. 265, 2003.

TARBOURIECH, S.; GOMES DA SILVA JR., J. M.; GARCIA, G. Delay-dependent anti-windup strategy for linear systems with saturating inputs and delayed outputs. *International Journal of Robust and Nonlinear Control*, Wiley, v. 14, n. 7, p. 665–682, may 2004.

TARBOURIECH, S.; TURNER, M. Anti-windup design: an overview of some recent advances and open problems. *IET Control Theory Applications*, v. 3, n. 1, p. 1–19, January 2009. ISSN 1751-8644.

TEEL, A. R. A nonlinear small gain theorem for the analysis of control systems with saturation. *IEEE Transactions on Automatic Control*, v. 41, n. 9, p. 1256–1270, Sept 1996. ISSN 0018-9286.

TEEL, A. R.; KAPOOR, N. The $\mathcal{L}_2$ anti-windup problem: Its definition and solution. In: *1997 European Control Conference (ECC)*. [S.l.: s.n.], 1997. p. 1897–1902.

TJØNNÅS, J.; JOHANSEN, T. A. Adaptive control allocation. *Automatica*, v. 44, n. 11, p. 2754 – 2765, 2008. ISSN 0005-1098.

TORRICO, B. C.; CAVALCANTE, M. U.; BRAGA, A. P. S.; ALBUQUERQUE, A. A. M.; NORMEY-RICO, J. E. Simple tuning rules for dead-time compensation of stable, integrative, and unstable first-order dead-time processes. *Ind Eng Chem Res*, v. 52, p. 11646–11654, 2013.

TORRICO, B. C.; CORREIA, W. B.; NOGUEIRA, F. G. Simplified dead-time compensator for multiple delay siso systems. *ISA Transactions*, v. 60, p. 254–261, 2016.

TORRICO, B. C.; PRUDÊNCIO DE ALMEIDA FILHO, M.; ALVES LIMA, T.; FORTE, M. D. do N.; SÁ, R. C.; NOGUEIRA, F. G. Tuning of a dead-time compensator focusing on industrial processes. *ISA Transactions*, v. 83, p. 189 – 198, 2018.

TORRICO, B. C.; PRUDÊNCIO DE ALMEIDA FILHO, M.; ALVES LIMA, T.; SANTOS, T. L.; NOGUEIRA, F. G. New simple approach for enhanced rejection of unknown disturbances in LTI systems with input delay. *ISA Transactions*, 2019. ISSN 0019-0578.

TURNER, G. H. M. C.; POSTLETHWAITE, I. Anti-windup compensation using a decoupling architecture. In: TARBOURIECH, G. G. S.; GLATTFELDER, A. H. (Ed.). *Advanced Strategies in Control Systems with Input and Output Constraints*. Berlin: [s.n.], 2007. p. 127–128,145,149.

TURNER, M. C.; HERRMANN, G.; POSTLETHWAITE, I. Accounting for uncertainty in anti-windup synthesis. In: *Proceedings of the 2004 American Control Conference*. [S.l.: s.n.], 2004. v. 6, p. 5292–5297 vol.6. ISSN 0743-1619.

TURNER, M. C.; HERRMANN, G.; POSTLETHWAITE, I. Incorporating robustness requirements into antiwindup design. *IEEE Transactions on Automatic Control*, v. 52, n. 10, p. 1842–1855, Oct 2007. ISSN 0018-9286.

TURNER, M. C.; KERR, M. A nonlinear modification for improving dynamic anti-windup compensation. *European Journal of Control*, v. 41, p. 44 – 52, 2018. ISSN 0947-3580.

TURNER, M. C.; POSTLETHWAITE, I. A new perspective on static and low order anti-windup synthesis. *International Journal of Control*, Taylor & Francis, v. 77, n. 1, p. 27–44, 2004.

WANG, S.; GAO, Y.; LIU, J.; WU, L. Saturated sliding mode control with limited magnitude and rate. *IET Control Theory & Applications*, Institution of Engineering and Technology, v. 12, p. 1075–1085(10), May 2018. ISSN 1751-8644.

WANG, Y.; JI, H. Input-to-state stability-based adaptive control for spacecraft fly-around with input saturation. *IET Control Theory & Applications*, Institution of Engineering and Technology, v. 14, p. 1365–1374(9), July 2020. ISSN 1751-8644.

WESTON, P. F.; POSTLETHWAITE, I. Linear conditioning for systems containing saturating actuators. *Automatica*, v. 36, n. 9, p. 1347 – 1354, 2000. ISSN 0005-1098.

YANG, R.; SUN, L. Finite-time robust control of a class of nonlinear time-delay systems via Lyapunov functional method. *Journal of the Franklin Institute*, v. 356, n. 3, p. 1155 – 1176, 2019. ISSN 0016-0032.

YANG, T. C. Networked control system: a brief survey. *IEE Proceedings - Control Theory and Applications*, v. 153, n. 4, p. 403–412, July 2006. ISSN 1350-2379.

ZACCARIAN, L. Dynamic allocation for input redundant control systems. *Automatica*, v. 45, n. 6, p. 1431 – 1438, 2009. ISSN 0005-1098.

ZACCARIAN, L.; TEEL, A. R. *Modern Anti-windup Synthesis: Control Augmentation for Actuator Saturation (Princeton Series in Applied Mathematics)*. [S.l.]: Princeton University Press, 2011.

ZHANG, B.; XU, S.; ZOU, Y. Improved stability criterion and its applications in delayed controller design for discrete-time systems. *Automatica*, v. 44, n. 11, p. 2963 – 2967, 2008. ISSN 0005-1098.

ZHANG, D.; SHI, P.; WANG, Q.-G.; YU, L. Analysis and synthesis of networked control systems: A survey of recent advances and challenges. *ISA Transactions*, v. 66, p. 376 – 392, 2017.

ZHANG, M.; JIANG, C. Problem and its solution for actuator saturation of integrating process with dead time. *ISA Trans.*, v. 47, p. 80–84, 2008.

ZHANG, W.-A.; YU, L. Stability analysis for discrete-time switched time-delay systems. *Automatica*, v. 45, n. 10, p. 2265 – 2271, 2009. ISSN 0005-1098.

ZHANG, X.; ZHOU, Z. Integrated fault estimation and fault tolerant attitude control for rigid spacecraft with multiple actuator faults and saturation. *IET Control Theory & Applications*, Institution of Engineering and Technology, v. 13, p. 2365–2375(10), October 2019. ISSN 1751-8644.

ZHANG, X.-M.; HAN, Q.-L.; SEURET, A.; GOUAISBAUT, F. An improved reciprocally convex inequality and an augmented Lyapunov–Krasovskii functional for stability of linear systems with time-varying delay. *Automatica*, v. 84, p. 221 – 226, 2017. ISSN 0005-1098.

ZHU, X.-L.; YANG, G.-H. Jensen inequality approach to stability analysis of discrete-time systems with time-varying delay. In: *2008 American Control Conference*. [S.l.: s.n.], 2008. p. 1644–1649. ISSN 0743-1619.